



UCAM
UNIVERSIDAD CATÓLICA
DE MURCIA

ESCUELA INTERNACIONAL DE DOCTORADO

Programa de Doctorado en Ciencias de la Salud

Función de la telomerasa en envejecimiento y
rejuvenecimiento. Búsqueda de compuestos bioactivos
que regulen su actividad.

Autor:

David Hernández Silva

Directores:

Dra. Dña. Francisca Alcaraz Pérez

Dr. D. Horacio Emilio Pérez Sánchez

Dra. Dña. María Luisa Cayuela Fuentes

Murcia, 30 de Septiembre de 2022



UCAM

UNIVERSIDAD CATÓLICA
DE MURCIA

ESCUELA INTERNACIONAL DE DOCTORADO

Programa de Doctorado en Ciencias de la Salud

Función de la telomerasa en envejecimiento y
rejuvenecimiento. Búsqueda de compuestos bioactivos
que regulen su actividad.

Autor:

David Hernández Silva

Directores:

Dra. Dña. Francisca Alcaraz Pérez.

Dr. D. Horacio Emilio Pérez Sánchez.

Dra. Dña. María Luisa Cayuela Fuentes.

Murcia, 30 de Septiembre de 2022



AUTORIZACIÓN DEL DIRECTOR DE LA TESIS PARA SU PRESENTACIÓN

La Dra. Dña. Francisca Alcaraz Pérez, el Dr. D. Horacio Pérez Sánchez, la Dra. Dña. María Luisa Cayuela Fuentes, como Directores⁽¹⁾ de la Tesis Doctoral titulada “Función de la telomerasa en envejecimiento y rejuvenecimiento. Búsqueda de compuestos bioactivos que regulen su actividad”, realizada por D. David Hernández Silva en el Programa de Doctorado Ciencias de la Salud, **autoriza su presentación a trámite** dado que reúne las condiciones necesarias para su defensa.

LO QUE FIRMO, PARA DAR CUMPLIMIENTO AL REAL DECRETO 99/2011 DE 28 DE ENERO, EN MURCIA A 28 DE SEPTIEMBRE DE 2022.

Francisca Alcaraz Pérez

Horacio Pérez Sánchez

María Luisa Cayuela Fuentes

⁽¹⁾ Si la Tesis está dirigida por más de un Director tienen que constar y firmar ambos.

Resumen

El papel de la telomerasa en el envejecimiento y el rejuvenecimiento. Búsqueda de compuestos bioactivos que regulen su actividad.

El envejecimiento es un proceso biológico fundamental que ocurre de forma universal en el que se producen diferentes cambios tanto a nivel molecular como celular, dando lugar a la aparición de diferentes enfermedades como la diabetes, las enfermedades degenerativas, el síndrome metabólico, la inflamación crónica e incluso el cáncer. Por ello, en la actualidad existe un gran interés por ralentizar o retrasar el proceso de envejecimiento, así como las enfermedades relacionadas con el mismo.

En esta Tesis, hemos desarrollado modelos de envejecimiento prematuro, incluyendo los producidos por acortamiento telomérico o inflamación de bajo grado, para el cribado fenotípico de fármacos. Es importante destacar que la fisiología y la respuesta química se conservan en su mayoría entre el pez cebra y los mamíferos, incluyendo los procesos que conducen al envejecimiento. Hemos combinado estrategias de cribado de VS e in vivo para elegir los mejores compuestos. Se han aplicado métodos basados en la estructura (acoplamiento proteína-ligando) y en el ligando (mapeo farmacóforo) al resveratrol y al navitoclax como moléculas diana. Las técnicas de VS revelaron una lista de polifenoles y compuestos senolíticos que se probaron en modelos de pez cebra de envejecimiento prematuro.

Los resultados obtenidos permitieron identificar una novedosa e inesperada función antiinflamatoria para los senolíticos y funciones protectoras antienvjecimiento para las moléculas antioxidantes en nuestros modelos de envejecimiento prematuro. Se necesita mucha más investigación para aclarar el mecanismo de acción de ambos tipos de compuestos (senolíticos y polifenoles) que

esperamos puedan ayudar a mejorar las enfermedades asociadas al envejecimiento y a mejorar la esperanza de vida.

Palabras Clave: Envejecimiento, modelos de pez cebra, escrutinio *in silico* e *in vivo*.

Términos Tesauro: Biología Celular (24;07;00); Bioquímica (23;02;00).

Abstract

The role of telomerase in aging and rejuvenation. Search for bioactive compounds that regulate their activity.

Aging is a fundamental biological process that occurs universally in which different changes occur at both the molecular and cellular level, leading to the appearance of different diseases such as diabetes, degenerative diseases, metabolic syndrome, chronic inflammation, and even cancer. Therefore, there is currently a great interest in slowing down or delaying the aging process as well as the diseases that are related to aging.

In this Thesis, we have developed models of premature aging, including those produced by telomere shortening or low-grade inflammation, for phenotypic screening of drugs. It is important to note that the physiology and chemical response are mostly conserved between zebrafish and mammals, including the processes leading to aging. We have combined strategies of VS and *in vivo* screening to choose the best compounds. Structure-based (protein-ligand docking) and ligand-based (pharmacophore mapping) methods have been applied to resveratrol and navitoclax as target molecules. VS techniques revealed a list of polyphenols and senolytic compounds that were tested in zebrafish models of premature aging.

The results obtained allowed us to identify a novel and unexpected anti-inflammatory function for senolytics and protective anti-aging functions for antioxidant molecules in our models of premature aging. Much more research is needed to clarify the mechanism of action of both types of compounds (senolytics and polyphenols) that we hope can help to ameliorate diseases associated with aging and improve the healthspan.

Keywords: Aging, Zebrafish models, *in silico* and *in vivo* screening.

Términos Tesauro: Biología Celular (24;07;00); Bioquímica (23;02;00).

AGRADECIMIENTOS

En primer lugar, quiero dar las gracias a mis directores de Tesis Paqui, Horacio y María Luisa, ya que sin ellos este trabajo no hubiera sido posible. Siempre agradeceré la oportunidad que me brindaste al permitirme poder iniciar mi carrera científica en vuestro grupo.

Paqui, como todos te llamamos yo te conocí poco tiempo después de llegar al grupo, pero desde el primer momento que llegaste me acogiste super bien en el grupo y me hiciste estar super bien junto con el resto de mis compañeros, además no quiero dejar pasar esta oportunidad para darte una vez más las gracias por todo lo que has hecho por mí.

Horacio, desde el primer momento que te conocí me transmitiste tu amor por la química computacional, y supiste trasmitirme todos los conocimientos básicos necesarios para realizar la Tesis Doctoral con toda la paciencia del mundo, después de esas tardes interminables explicando lo que hacíamos en la pizarra que siempre acababa llena, estos momentos nunca se olvidarán. No dejar pasar esta oportunidad para darte las gracias por todo.

María Luisa, lo primero de todo, muchísimas gracias por darme la oportunidad de poder entrar en tu grupo para realizar la Tesis Doctoral con vosotros. Desde el primer momento que llegué me sentí super a gusto y me sentí arropado en una ciudad que no era la mía donde me encontraba solo, pero gracias a ti y tu grupo me he sentido como en casa.

También me has trasmitido el amor por el pez cebra, la telomerasa y a la ciencia en general, ya que eres una persona que quiere ayudar a todo el mundo, ya sea con la investigación o a nivel personal. Ya han pasado 5 años desde que yo tuve la gran oportunidad de entrar en tu grupo y, aunque siempre hay momentos buenos, otros no tan buenos, tan solo puedo decir que he aprendido mucho, he crecido muchísimo tanto a nivel personal como laboral y solo me queda poder las gracias una vez más por estos años de aprendizaje.

CITA

*Cada aprendizaje de la vida nos
hace más sabios,
y más capaces de afrontarla
(Anónimo).*

ÍNDICE GENERAL

AUTORIZACIÓN DE LOS DIRECTORES

RESUMEN

ABSTRACT

INDICE GENERAL

I.INTRODUCTION.....	31
I.1 Telomeres and telomerase.	33
I.2 Cellular senescence.....	37
I.3 Aging and rejuvenation.....	40
I.3.1 Strategies to achieve rejuvenation.	41
I.3.1.1 Overexpression of telomerase.	41
I.3.1.2 Anti-aging drugs.	42
I.3.1.3 Fasting and caloric restriction.	46
I.4 Zebrafish models to study aging.....	48
I.4.1 Telomeres and telomerase in zebrafish.	50
I.4.2 Immunosenescence in zebrafish.	53
I.4.3 Chronic inflammation and oxidative stress in zebrafish.	54
I.5 Virtual Screening (VS).....	57
I.5.1 Structure-Based Methods (SBVS)	58
I.5.2 Ligand-Based Methods (LBVS)	59
I.5.3 Pharmacophoric Methods	60
I.5.3.1 Combination OF SBVS and LBVS	63
I.6 Combination of virtual screening and zebrafish models.	64
I.6.1 Xenograft.	66
I.6.2 Infection models.	66
I.6.3 Drug toxicity testing.	67

II. JUSTIFICACIÓN	70
III. OBJETIVOS.....	74
IV. MATERIALS AND METHODS.....	78
IV.1 Maintenance of zebrafish.	80
IV.2 Gene expression analysis.	81
IV.3 Telomerase activity assay.	82
IV.4 Telomeric length measurement.....	82
IV.5 Senescence-associated β -galactosidase (SA β -gal) activity assay.	83
IV.6 Measurement of oxidative stress levels (H ₂ O ₂ analysis).	83
IV.7 Acridine Orange (AO) Staining Assay.	84
IV.8 Imaging of zebrafish larvae.....	84
IV.9 Survival curves.....	84
IV.10 Molecule File.....	85
IV.11 Ligand database.	85
IV.12 Virtual Screening.	85
IV.13 Ligand-Based Virtual Screening.	85
IV.14 Toxicity assay.	85
IV.15 Chemical treatment.....	85
IV.16 Diet Preparation and Feeding of Zebrafish Larvae.....	86
IV.17 Statistical analysis.....	86
V.1 <i>In vivo</i> models of premature aging in zebrafish.	89
V.1.1 Shortened telomere-induced premature aging, the ST2 model.	89
V.2 Premature aging induced by DNA damage caused by chemotherapy, the QiDD model.....	95
V.3 High-cholesterol diet-induced meta-inflammation zebrafish model, the HCD model.	98
V.4 Inflammaging zebrafish model, the Spint1a-deficient model.	101
V.5 Evaluation of the anti-aging potential of resveratrol and navitoclax in the ST2 model. A proof of concept.	103

V.6 In silico discovery of new drugs with anti-aging potential.....	108
V.6.1 Natural antioxidants derived from resveratrol.....	108
V.6.1.1 Structure-based virtual screening (SBVS) method: protein-ligand docking.	108
V.6.1.2 Ligand-based virtual screening (LBVS) method: pharmacophore mapping.	108
V.7 Drugs derived from senolytics.	113
V.7.1 Ligand-based virtual screening (LBVS) method: navitoclax pharmacophore mapping.....	113
V.7.2 Ligand-based virtual screening (LBVS) method: Dasatinib pharmacophore mapping.....	114
V.8 In vivo validation of candidates with anti-aging potential in different aging zebrafish models for repurposing.	117
V.8.1 Analyzed the toxicity assay.	117
V.8.2 Shortened telomere-induced premature aging, the ST2 model.	118
V.8.3 Premature aging induced by DNA damage caused by chemotherapy, the QiDD model.....	121
V.9 High-cholesterol diet-induced metainflammation zebrafish model, the HCD model.	125
V.10 Inflammaging zebrafish model, the Spint1a-deficient model.	130
VI. DISCUSSION	143
VI.1 In vivo zebrafish models of premature aging.	146
VI.2 Evaluation of the anti-aging potential of resveratrol and navitoclax in the ST2 model. A proof of concept.....	148
VI.3 In silico discovery of new drugs with anti-aging potential.....	149
VI.4 In vivo validation of candidates with anti-aging potential in different aging zebrafish models for repurposing.	150
VII. CONCLUSIONS.....	155
VIII. LIMITACIONES Y FUTURAS LINEAS DE INVESTIGACIÓN.....	159
IX. REFERENCES	164

X. ANEXOS	192
X.1 ANEXO: CALIDAD DE LAS PUBLICACIONES.....	194
X.1.1. Senescence-Independent Anti-Inflammatory Activity of the Senolytic Drugs Dasatinib, Navitoclax, and Venetoclax in Zebrafish Models of Chronic Inflammation.....	194
X.1.2 Virtual and zebrafish screening models in tandem, for drug discovery and development.....	195
X.2 ANEXO: PATENTES.....	195
X.3 ANEXO: OTRAS COMUNICACIONES	195

SIGLAS Y ABREVIATURAS

AD	Autodock 4
AK	Autodock Vina
ADMET	Administration, distribution, Metabolism and Excretion
AMPK	AMP-activated protein kinase
AVV	Adeno-associated virus
Bcl-2	B cell lymphoma 2
CHT	Caudal Hematopoietic Tissue
CR	Caloric Restriction
CPU	Central Processing Unit
CVD	Cardiovascular disease
DB	Drug Bank
DDRs	DNA damage responses
DMSO	Dimethyl sulfoxide
DNA	Deoxyribonucleic Acid
Dpf	Days post-fecundation
FDA	Food and Drug Administration
<i>F</i>	Forward, direct primer
gDNA	Genomic DNA
GSH	Glutation
HCC	Hepatocellular carcinoma
HCD	High Cholesterol diet
HGFA	Hepatocyte growth factor
Hpf	Hours post-fecundation
HTS	High-throughput screens
HSCs	Hematopoietic stem cells
H2AX	Phosphorylated Histone

IG	Immunoglobulin
iPSC	Pluripotent stem cells
IUPAC	International Union of Pure and Applied Chemistry
IGF	Insule Growth Factor
Kb	Kilobases
KDa	Kilodaltons
LBVS	Ligand-Based Methods
LF	LeadFinder
mTOR	Mammalian Target of Rapamycin
MMPs	Matrix Metalloproteinase
NAD	Nicotinamide phosphoribosyl
NAMPT	Nicotinamide phosphoribosyltransferase
NAFLD	Non-alcoholic fatty liver disease
NASH	Non-alcoholic steatohepatitis
ND	Normal Diet
NF- κ B	Nuclear proinflammatory factor κ B
NMR	Nuclear magnetic resonance spectroscopy
Nt	Nucleotides
OMIN	Online Mendelian Inheritance in Man
PARP1	Poly(ADP-ribose) polymerase 1
PCR	Polymerase Chain Reaction
PDB	Brookhaven Protein Data Bank
qPCR	Quantitative Polymerase Chain Reaction
Q-TRAP	Quantitative-TRAP Telomeric Repeat Amplification Protocol
QiDD	Chemotherapy-induced DNA damage
R	Reverse primer
RT	Room Temperatures
RNA	Ribonucleic Acid

RNP	Ribonucleoprotein
ROS	Species Reactive Oxygen
<i>rps11</i>	Ribosomal protein subunit 11 encoding gene
RTA	Relative Telomerase Activity
SASP	Phenotype secretor-associated senescence
SA β -gal	Senescence-associated beta-galactosidase
SB	Structure based
SBVS	Structure-Based Methods
SEM	Standard Error of Mean
SISPS	Stress-induced premature senescence
SIRT1	Sirtuin-1
ST2	Short telomeres 2 ^o generation
<i>TERC</i>	Telomerase RNA Component
TERT	Telomerase catalytic subunit
TGF- β	Transforming Growth factor β
TNF α	Tumor necrosis factor
VEGF	Vascular Endothelial Growth Factor
VS	Virtual Screening
Wt	Wild type
zf	Zebrafish
zfTert	Reverse transcriptase
zfTR	RNA component of telomerase
36b4	Acidic ribosomal phosphoprotein P0

ÍNDICE DE FIGURAS, DE TABLAS Y DE ANEXOS**ÍNDICE DE FIGURAS**

Figure 1. Telomeres and telomerase.....	34
Figure 2. Consequences of telomere shortening.	36
Figure 3. Different methods that induce senescence.....	38
Figure 4. Senescence as a central hallmark of aging.....	40
Figure 5. The nine hallmarks of aging.....	41
Figure 6. Telomerase gene therapy to promote health span in mice.....	43
Figure 7. Anti-aging drugs.....	47
Figure 8. Caloric restriction (CR)-related processes involved in improving health and longevity.....	48
Figure 9. Advantages of the zebrafish model.....	51
Figure 10. Telomerase-deficient premature aging zebrafish model.....	53
Figure 11. Rag1-deficient zebrafish immunosenescence model.....	55
Figure 12. Spint1a-deficient zebrafish inflammaging model.....	56
Figure 13. NAFLD/NASH zebrafish metainflammation model.....	57
Figure 14. Schematic representation of the different types of VS methods.....	59
Figure 15: Graphic representation of the different molecular descriptors.....	61
Figure 16: Ligand-protein interaction zone, the conformation of the ligand in the active center (yellow box).....	62

Figure 17: Pharmacophoric model of the ligand.....	63
Figure 18. Combination of virtual screening and <i>in vivo</i> target-based screening in zebrafish.....	66
Figure 19. Workflow for the generation of the ST2 model and phenotype.....	90
Figure 20. Telomeric characterization of the ST2 model.....	91
Figure 21. The ST2 larvae show increased cellular senescence.....	92
Figure 22. The ST2 larvae show increased oxidative stress levels.....	93
Figure 23. The ST2 larvae show increased cell death levels.....	94
Figure 24. The ST2 larvae show premature death.....	95
Figure 25: General workflow for the generation of the QiDD model.....	96
Figure 26. The QiDD larvae show a drastic attrition of telomere length.....	97
Figure 27. The QiDD larvae show a limited survival.....	98
Figure 28: General workflow for the generation of the zebrafish model of metainflammation produced by a 10% cholesterol diet.....	99
Figure 29. Characterization of the HCD-induced metainflammation zebrafish model.....	100
Figure 30. HCD-induced metainflammation larvae do not show telomere shortening.....	101
Figure 31. Spint1a-deficient zebrafish larvae do not show premature aging.....	102
Figure 32. The Spint1a-deficient larvae show increased cell death levels.....	103
Figure 33: General workflow for the treatment the ST2 zebrafish larvae.....	104

Figure 34. Resveratrol improves telomerase expression, activity, and telomere length in the ST2 model of premature aging.....	105
Figure 35. Navitoclax treatment decreases cellular senescence levels in the ST2 model of premature aging.....	106
Figure 36. Resveratrol treatment decreases cell death levels in the ST2 model of premature aging.....	107
Figure 37. Resveratrol treatment increases the ST2 larvae survival.....	108
Figure 38. Schematic representation of pharmacophoric features.....	110
Figure 39. Pharmacophoric method for resveratrol.....	111
Figure 40. 3D representation of the predicted interaction between resveratrol-derived candidates and the catalytic subunit of telomerase (TERT).....	113
Figure 41. Schematic representation of pharmacophoric features.....	114
Figure 42: Schematic representation of pharmacophoric features.....	116
Figure 43. Pharmacophoric method for dasatinib.....	117
Figure 44. Candidate toxicity assessment.....	118
Figure 45. General workflow for antioxidant treatment in the ST2 model of premature aging.....	119
Figure 46. Telomeric characterization of the ST2 model after antioxidant treatment.....	120
Figure 47. Effect of resveratrol-derived antioxidants on ST2 larvae survival.....	121

Figure 48: General workflow for the evaluation of antioxidants in the QiDD model.....	122
Figure 49. Effect of resveratrol-derived antioxidants on QiDD larvae survival.....	123
Figure 50. Effect of resveratrol-derived antioxidants on QiDD larvae survival.....	124
Figure 51. Effect of resveratrol-derived antioxidants on QiDD larvae survival.....	125
Figure 52. Effect of resveratrol-derived antioxidants on QiDD larvae survival.....	125
Figure 53. Effect of resveratrol-derived antioxidants on QiDD larvae survival.....	125
Figure 54. General workflow for the evaluation of antioxidants in the HCD-induced metainflammation model.....	126
Figure 55. Evaluation of selected antioxidant compounds in the HCD-induced metainflammation model.....	127
Figure 56. General workflow for the evaluation of navitoclax in the HCD-induced metainflammation model.....	128
Figure 57. Evaluation of selected antioxidant compounds in the HCD-induced metainflammation model.....	129
Figure 58. Navitoclax increased genes related to inflammation phenotype of HCD-fed larvae.....	130
Figure 59. General workflow for the evaluation of antioxidants in the Spint1a-deficient inflammaging model.....	131

Figure 60. Apigenin, genestein, naringenin, sakuranetin and tricetin ameliorate the skin inflammation phenotype of Spint1a-deficient larvae.....	132
Figure 61. Genestein, naringenin and sakuranetin, contrary to resveratrol, ameliorate the skin inflammation phenotype of Spint1a-deficient larvae.....	134
Figure 62. Apigenin and genestein ameliorate oxidative stress levels of Spint1a-deficient larvae.....	135
Figure 63. Apigenin, genestein, hesperetin, quercetin and sakuranetin ameliorate the cell death levels of Spint1a-deficient larvae.....	137
Figure 64. General workflow for the evaluation of senolytics in the <i>Spint1a</i>-deficient inflammaging model.....	138
Figure 65. Senolytics ameliorate the skin inflammation phenotype of Spint1a-deficient larvae.....	139
Figure 66. Senolytics ameliorate the skin inflammation phenotype of Spint1a-deficient larvae.....	141
Figure 67. Senolytics ameliorate genes related to inflammation phenotype of Spint1a-deficient larvae.....	142

ÍNDICE DE TABLAS

Table I: Primers used for gene expression.....	82
Table II: Primers used for telomere length.....	84
Table III: Interaction between resveratrol-derived candidates and the telomerase catalytic subunit (TERT).....	112
Table IV. Summary of the effect of the adjuvant treatment.....	125

I. INTRODUCTION

INTRODUCTION

I.1 Telomeres and telomerase.

Genomic stability is the key to preserve the genomic information and to ensure its pass to next generations, guaranteeing the survival of the species. In eukaryotic organisms, the edges of chromosomes are one of the most vulnerable parts of the genome. Together with a specific complex of proteins collectively known as shelterin, telomeres form specialized structures that ensure their integrity preventing chromosome shortening, chromosome fusion, or chromosome degradation if they are recognized as double-strand DNA breaks by the DNA repair machinery (Simon et al., 2015; Smith et al., 2020). Hence, structure and function of telomeres are highly conserved throughout evolution (review by Galati *et al.*, 2013).

Telomeres consist of long extensions of linear DNA made up of a guanine rich sequence motif (TTAGGG) repeated in tandem that vary in length according to the species (Srinivas et al., 2020). Exceptionally, the chromosome ends of a few insect species (*Drosophila* and some dipterans), instead of telomeric motifs, possess tandem arrays of retrotransposons (Abad et al., 2004).

Under normal conditions, because DNA synthesis requires an RNA template to initiate DNA replication and this template is eventually degraded, a short single stranded region would be left at the end of chromosomes. The 'end replication problem' is responsible for the shortening of telomeres in most somatic cells with each cell division because DNA synthesis is unidirectional ($5' \rightarrow 3'$) and requires an RNA sequence to prime DNA replication. On the leading strand, the synthesis is continuous; but, on the lagging strand, DNA synthesis is discontinuous, in fragments (called 'Okazaki fragments') that require RNA primers to provide the 5' starting point. Once the lagging strand is completed and the RNA primer removed, the lagging strand results shorter than the leading one (Lindqvist et al., 2015).

During ontogenesis, eukaryotic organisms solved this problem by recruiting the enzyme telomerase, a specialized and unique RNA-dependent DNA polymerase that synthesizes telomeric repeats in chromosomal ends, thus

maintaining them at a 'safe' telomeric length, since a reduced telomere length is an initial requirement for cell replication (Blackburn, 2005; Smith et al., 2020).

Telomerase complex is a ribonucleoprotein composed by the telomerase reverse transcriptase (TERT, the catalytic subunit), telomerase RNA (*TR*, which provides the template for the reverse transcription of new telomere DNA by TERT), and species-specific accessory proteins that regulate telomerase biogenesis, subcellular localization, and its function *in vivo* (Wyatt et al., 2010) (**Fig. 1**).

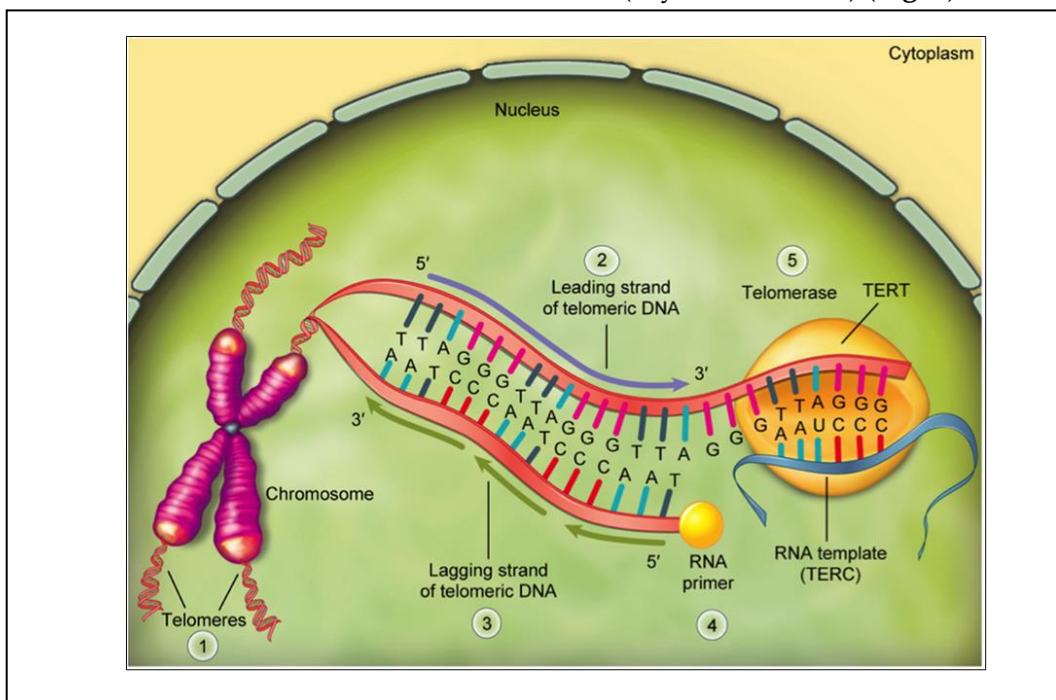


Figure 1. Telomeres and telomerase. Telomeres are located at the end of chromosomes and serve a chromosome protection function (1). While the synthesis of the leading strand of telomeric DNA is continuous (2), the lagging strand is discontinuous (3). Therefore, once the RNA primer (4) is removed, the lagging strand results shorter than the leading one with each cell division. To overcome this 'end replication problem', telomerase reverse transcriptase (TERT) adds telomere sequences along the leading strand (5) by using the RNA component (*TERC*) as a template. Adapted from Lindqvist et al., (2015).

Telomerase is generally active only during embryogenesis and development. In adults, its expression is restricted to rapidly dividing cells (Ulaner & Giudice, 1997). Consequently, in most adult cells, after a few cell divisions throughout life, telomeres reach a critical length and chromosomes become uncapped and are recognized as damaged DNA, leading to the DNA damage response (DDR). This is followed by activation of the tumor suppressor protein p53, which leads to cell cycle arrest, or also called replicative senescence, which leads to cellular senescence and apoptosis affecting cells that are dividing very rapidly, including cells that are dividing very rapidly, including cells that are dividing very rapidly, including cells that are dividing very rapidly, including cells that are dividing very rapidly that divides very rapidly, including blood cells (Sahin et al., 2011).

Both cell death and senescence can trigger stem cell dysfunction, leading to degenerative diseases and even tissue death. When *p53* activation does not occur, cells with critical telomere length can survive, leading to genomic instability that could result in cancer. Critically short telomeres also affect cells with a slower cell cycle, leading to decreased mitochondrial activity and lower energy production,

with an increased release of oxygen free radicals (ROS), leading to further damage to both telomeres and other cellular components (Tümpel & Rudolph, 2012) (Fig. 2).

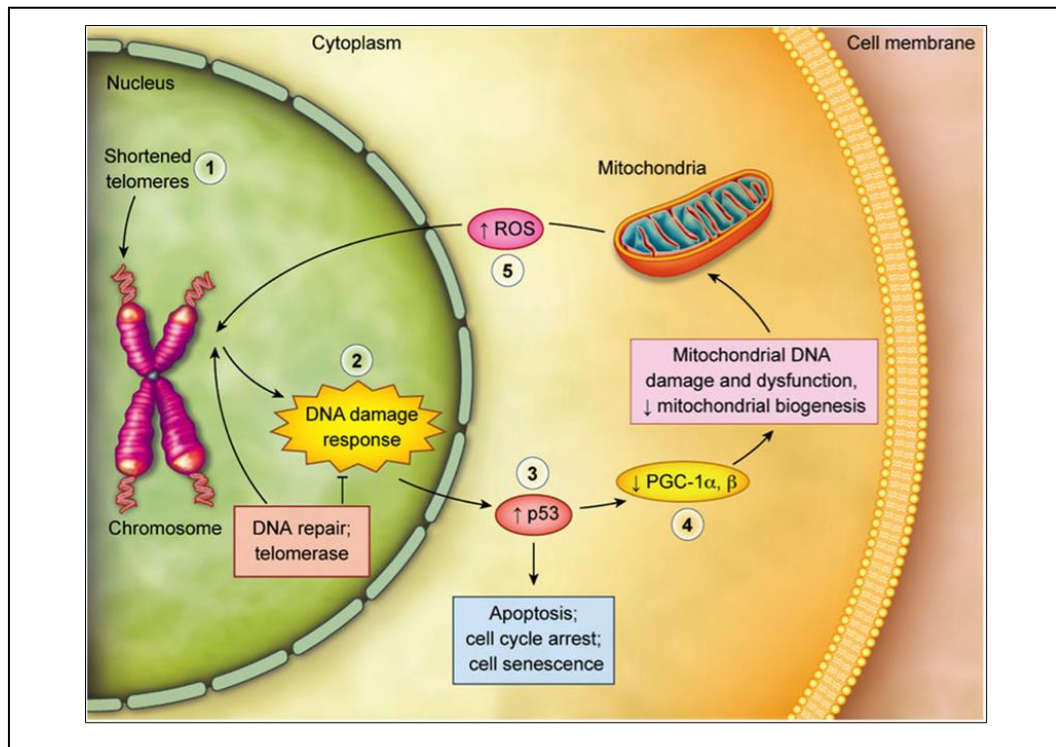


Figure 2. Consequences of telomere shortening. Critically short telomeres (1) initiate DNA damage responses (2) and activation of the tumor suppressor protein p53, which can lead to cell cycle arrest, cell senescence and apoptosis (3). Activation of p53 can also triggers mitochondrial DNA damage and dysfunction, reducing mitochondrial biogenesis (4). This results in releasing of excessive amounts of reactive oxygen species (ROS) (5) which, in turn, further damage telomeres and other cellular components. *Adapted from Lindqvist et al., (2015).*

I.2 Cellular senescence.

Cellular senescence consists of a state of permanent cell cycle arrest that can be induced in primary cells in response to a variety of stimuli. Originally identified as replicative senescence (Hayflick, 1965), it has been also described a different type of senescence induced by the activation of the *RAS* oncogene in a process known as 'oncogene-induced senescence' (OIS), showing the potential role of senescence as an anti-cancer mechanism designed to suppress proliferation of cells with oncogenic mutations (Serrano *et al.*, 1997).

Telomere shortening is the main molecular mechanism responsible for cellular senescence. In addition to replication stress, telomeres can be shortened and damaged by either exogenous or endogenous sources through a process called stress-induced premature senescence (SIPS) (de Magalhães & Passos, 2018). An example of an exogenous source is chemotherapy (Schmitt *et al.*, 2002). The genotoxic effects of chemotherapeutic agents are the main treatment in the fight against cancer, since they attack and destroy highly proliferative cells, but they are not specific to cancer cells, but also to healthy cells, causing a high cell toxicity with multiple powerful side effects. But chemotherapy toxic effects last much longer, even after the disease is overcome. It has been observed that cancer survivors show DNA damage-induced premature aging that causes shortened life expectancy (Ness & Wogksch, 2020).

Telomeres can also be damaged by different endogenous sources from the organism's own metabolism. For example, it is known that high oxidative stress levels, through the generation of reactive oxygen species (ROS), induce telomere shortening (Stillman *et al.*, 2005), predisposing cells to senescence or apoptosis (Blasco, 2005; López-Otín *et al.*, 2013). It has been observed that older organisms tend to develop a chronic pro-inflammatory status with low-grade inflammation, termed inflammaging. Inflammaging is characterized by high levels of pro-inflammatory markers in cells and tissues, and chronic activation of the innate immune system, even in the absence of risk factors and clinically active diseases (Franceschi *et al.*, 2000). One of the main stimuli that fuels inflammaging is nutrient excess through the so-called meta-inflammation process (Franceschi *et al.*, 2018). High nutrient intake is a critical contributor to the onset of insulin resistance and, specifically, excessive pro-inflammatory fatty acids result in an increased activation

of inflammatory responses that affect adipose tissue, liver, pancreas, muscle, and brain (Gregor & Hotamisligil, 2011).

In this context, senescence is a protective mechanism that prevents the proliferation of old, damaged, and potentially tumorigenic cells. The negative consequence is their accumulation and increased aging at the organismal level. However, there are also beneficial effects of senescence, for example in the context of embryonic development (Muñoz-Espín et al., 2013), tissue repair/regeneration (Demaria et al., 2014), and cellular reprogramming (Mosteiro et al., 2016; Wanner et al., 2021) (Fig. 3).

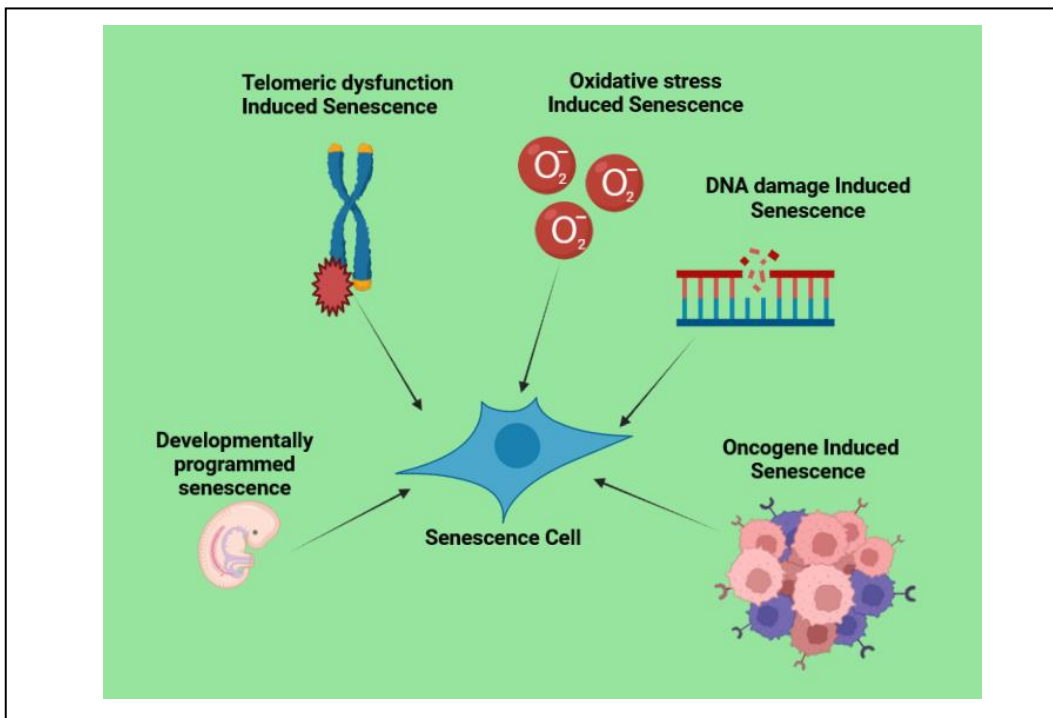


Figure 3. Different methods that induce senescence. Cells are subjected to a variety of stresses including oncogenes, oxidative damage, DNA damage, telomeric dysfunction and embryonic development that can cause cellular senescence. *Adapted from Wanner et al., 2021.*

Senescent cells are resistant to apoptosis and exhibit phenotypic changes and senescence markers that accumulate in aging tissues (Dimri, Leet, et al., 1995) such

as senescence-associated β -galactosidase (SA β -gal) activity, senescence-associated heterochromatin foci, sustained expression of cell cycle inhibitors (p21/CDKN1A and p16/CDKN2A), and a pronounced senescence associated secretory phenotype SASP (Kumari & Jat, 2021). SASP is composed mainly of pro-inflammatory cytokines, especially interleukin-1 (IL-1), interleukin-6 (IL-6), and interleukin-8 (IL-8), and chemokines such as MCP-1, as well as factors of growth, such as insulin growth factor (IGF), tumor necrosis factor-alpha (TNF- α), and metalloproteinases (Maduro et al., 2021). While in the short term the SASP helps promote recognition and clearance of senescent cells by phagocytosis, long term secretion has a variety of age-related deleterious effects (Xue et al., 2007). SASP reinforces several aspects of senescence including growth arrest and the SASP itself via an autocrine loop. Secretion of MMPs and factors such as VEGF can remodel the surrounding tissue, inducing angiogenesis and reducing fibrosis. Finally, secretion of molecules such as TGF- β can spread the senescence phenotype in a paracrine manner to surrounding cells (McHugh & Gil, 2018).

Under normal conditions, the immune system is responsible for detecting and eliminating senescent and apoptotic cells to prevent them from causing inflammation and to promote cell renewal. The immune system, which demands a high rate of cell proliferation and renewal, is one of the most affected by telomere shortening and undergoes its own aging process called immunosenescence that culminates in cessation of replication (Pawelec, 2012). This phenomenon is associated with lymphopenia, the progressive depletion of naïve T cells and the reduced proliferation ability of T cells (Goronzy et al., 2015; Wherry & Kurachi, 2015). The combination of immunosenescence and inflammaging results in a diminished capacity of the immune system to remove senescent cells (Antonangeli et al., 2019; Prata et al., 2018). This leads to an accumulation of senescent cells in tissues that amplifies the SASP signal and induces chronic inflammation, which negatively affects tissue regeneration and function, rendering the tissue more vulnerable to inflammation and aging-related diseases (Childs et al., 2015; Bernardes de Jesus & Blasco, 2012) (**Fig. 4**).

I.3 Aging and rejuvenation.

When senescence processes affect the entire organism, we call it aging. This biological process occurs in all eukaryotic organisms. Consist of a gradual and general decline in capacity because of the accumulation of damage in molecules, cells, and tissues over a lifetime, with an increased probability of many chronic diseases such as diabetes, cardiovascular and neurodegenerative diseases, and even cancer (Rodríguez-Rodero et al., 2011). A series of conserved hallmarks of aging has been proposed, including: i) telomere attrition; ii) genomic instability; iii) epigenetic alterations; iv) loss of proteostasis; v) deregulated nutrient sensing; vi) mitochondrial dysfunction; vii) cellular senescence; viii) stem cell exhaustion; and ix) altered intercellular communication (López-Otín et al., 2013) (Fig. 5).



Figure 5. The nine hallmarks of aging. Adapted from López-Otín et al., (2013).

Aging depends not only on the chronological age but also on the biological age, which is related to the physiological state of the cells, tissues, and organs. Therefore, the manner and rate of biological aging depends on everyone (Angarola & Anczuków, 2021; Melzer et al., 2020). In the last century, the great advances in both public health and medicine have allowed the increase in life expectancy globally. This implies that more than 2.1 billion people in 2050 will be over 60 years old, leading to a 5-fold increased risk in age-related diseases, which is a major public health problem from the social and economic point of view (Melzer et al., 2020).

Having a longer life expectancy but suffering from age-related diseases is not desirable. Geroscience is a new research field focused on understanding the basic mechanisms driving aging and the link between aging and age-related chronic diseases. Its goal is to provide novel preventive or diagnostic measures and treatments with the aim of rejuvenating, understanding rejuvenation as reducing the burden of age-related diseases and disabilities and delaying the onset of aging to increase healthy life expectancy (Kennedy et al., 2014).

I.3.1 Strategies to achieve rejuvenation.

Several approaches have been explored to slow down aging, including overexpression of telomerase (Cox & Mason, 2010), fasting (de Cabo & Mattson, 2019), caloric restriction (Pifferi & Aujard, 2019), exercise (Galloza et al., 2017), nutraceuticals (Jian-Guo Jiang et al., 2016) and senolytic drugs to selectively induce apoptosis in senescent cells (Kirkland & Tchkonja, 2020).

I.3.1.1 Overexpression of telomerase.

Telomere shortening is the main factor causing aging, so the overexpression of telomerase is a tempting strategy to achieve rejuvenation. However, it has been demonstrated in mice that transgenic overexpression of the catalytic subunit of telomerase, *mTERT*, increases cancer incidence, therefore masking the potential beneficial effects of constitutive telomerase activation (González-Suárez et al., 2005). This setback has been overcome by over-expressing *mTERT* in a cancer protective background with increased expression of tumor suppressor genes, which results in extension of the median lifespan (Tomás-Loba et al., 2008). The

combination of caloric restriction (CR), that partially mimics a tumor suppressive condition, attenuates telomere erosion associated to aging and synergizes with *mTERT* overexpression, resulting in increasing healthspan and extending mouse longevity (Vera et al., 2013). Another successful approach is the use of a gene therapy with non-integrative adeno-associated virus (AAV). In this way, overexpression of *mTERT* in old mice delays aging symptoms, improves memory and increases longevity but not cancer incidence (Bernardes de Jesus & Blasco, 2012) (Fig. 6).

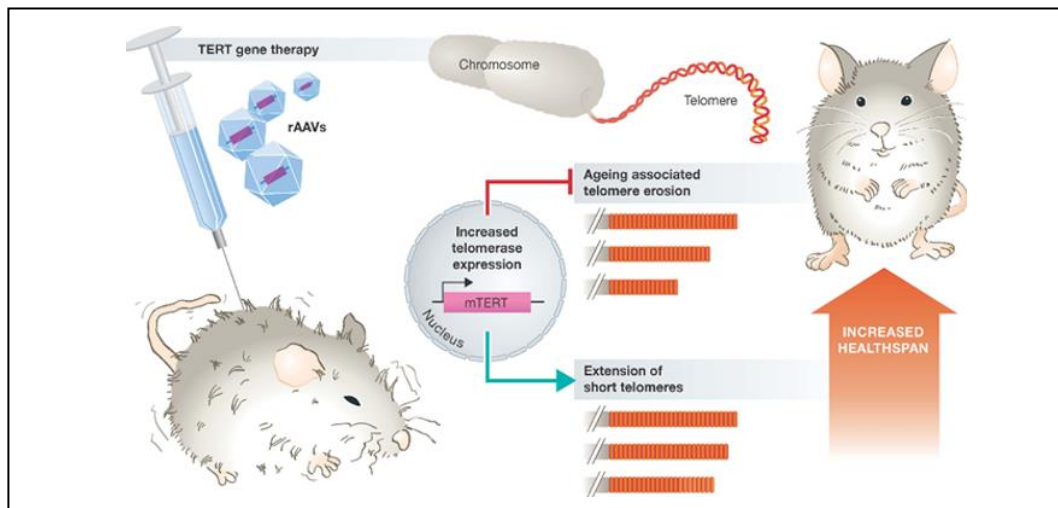


Figure 6. Telomerase gene therapy to promote healthspan in mice. Overexpression of the catalytic subunit of telomerase gene (*TERT*) by using a modified adenovirus vector (rAAV) corrects aging associated telomere erosion and extends short telomeres in a variety of tissues. Consequently, animals show improved healthspan and extended lifespan. *Adapted from Boccardi et al., (2012).*

I.3.1.2 Anti-aging drugs.

Some FDA approved drugs target one or more molecules to reduce cellular damage, slow down aging-associated diseases and prolong the healthspan, such as (summarized in Fig. 7):

- i) **Resveratrol.** A polyphenol that is abundant in grape skin and seeds, shows antioxidant, anti-inflammatory and anticancer properties (Galiniak et al., 2019). Resveratrol is involved in anti-aging as an activator of the sirtuin family and the Nrf2 pathway (Cao et al., 2018; Price et al., 2012; Wang et al., 2016). In addition, resveratrol can act directly on transcriptional regulators thus acting as an anti-inflammatory and antioxidant, ameliorating aging-related diseases such as inflammatory and cardiovascular diseases, and even Alzheimer's disease through various mechanisms (Park et al., 2012; Sawda et al., 2017; Tsai et al., 2014; Xia et al., 2017; Y. Zhu et al., 2019). It has been also reported the effect of resveratrol on telomerase activation, pointing to a great therapeutic potential of resveratrol for a wide variety of cardiovascular diseases (Gutlapalli et al., 2020). But, unlike in animal models, the effects of resveratrol in humans are controversial, so it is difficult to use resveratrol in large-scale clinical trials at this stage. Therefore, it would be very desirable to test whether other resveratrol-derived molecules give better results.
- ii) **TA-65.** A natural molecule containing *Astragalus membranaceus* extract induces telomerase activation both *in vitro* (Molgora et al., 2013; Tsoukalas et al., 2019) and *in vivo*. In murine models, TA-65 dietary supplementation results in the increasement of healthspan without increasing cancer incidence and in the amelioration of aging-induced deteriorations in the liver (Alshinnawy et al., 2021; de Jesus et al., 2011). In humans, several pilot studies have shown that oral administration of TA-65 improves the macular function in patients with early macular degeneration (Dow & Harley, 2016) and reduces cardiovascular disease risk by reducing inflammation in patients with metabolic syndrome.
- iii) **Metformin.** A hypoglycemic drug used to treat type 2 diabetes (Pryor & Cabreiro, 2015) has been shown to reduce the pathogenesis and mortality of cardiovascular diseases (Palmer et al., 2016; Schlender et al., 2017). In addition, it has been reported the positive effect of metformin on cancer, neurodegenerative diseases, dementia, and cognitive impairment (Barzilai et al., 2016; Ng et al., 2014). Metformin targets the major pathways of aging because it affects inflammatory, cellular stress and autophagy responses, etc. by acting both inside and outside the cell. Extracellularly, metformin

decreases insulin levels and IGF-1 signaling while influencing multiple cytokines to participate in anti-aging processes (Liu et al., 2011). Intracellularly, metformin reduces ROS production by inhibiting mitochondrial complex I in the electron transport chain generation and AMPK activation (Batandier et al., 2006; Cho et al., 2015). Metformin also reduces DNA damage (Algire et al., 2012; Cabreiro et al., 2013) and triggers a simultaneous increase in mechanistic target of rapamycin (mTOR) protein kinase signal inhibition and SIRT1 activation, which results in a longer lifespan (Nair et al., 2014; Pérez-Revuelta et al., 2014). In addition to glucose homeostasis, metformin also affects the tumor suppressor pathway, exerting excellent anti-cancer effects (DeCensi et al., 2010). However, it has been also reported that 745 proteins are regulated by metformin long-term treatment (Stynen et al., 2018) which could explain both the positive effects but also the side effects of metformin treatment throughout life. Therefore, before considering metformin as an anti-aging drug, more research is needed to determine its broader effects, the molecular mechanism of action, and its safety implications.

- iv) **Rapamycin.** A macrolide produced by *Streptomyces hygroscopicus* initially discovered as an antifungal agent, is currently the only known pharmacological substance to prolong lifespan in all studied model organisms and the only one in mammals (Weichhart, 2018) through the inhibition of mTOR signalling pathway. Short-term or intermittent administration of rapamycin specifically inhibits mTORC1, reducing protein and nucleotide synthesis, promoting autophagy responses, while also reducing cellular stress responses (Saxton & Sabatini, 2017) These effects of rapamycin may delay age-related diseases and promote longevity (Bitto et al., 2016; Carosi & Sargeant, 2019; C. L. Chung et al., 2019; Mannick et al., 2014; Neff et al., 2013). In contrast, long-term administration of rapamycin results in the inhibition of mTORC2, leading to metabolic dysfunction and reduced lifespan, through a still not clear mechanism (Arriola Apelo & Lamming, 2016). Therefore, further experiments are needed to determine the beneficial effects of rapamycin on aging and age-related diseases through mTORC1 inhibition while minimizing the side effects associated with mTORC2 inhibition.

v) **Senolytic.** Are drugs that selectively induce apoptosis in senescent cells, which are apoptosis-resistant cells (Zhu et al., 2018), being a promising strategy for extending both healthspan and lifespan. It has also been reported the effectiveness of senolytics for some age-related diseases, such as idiopathic pulmonary fibrosis, sarcopenia, osteoarthritis, and glomerulosclerosis (Kim & Kim, 2019). For example, navitoclax or ABT263 is a Bcl-2 family inhibitor, leading to apoptosis of senescent cells, regardless of cell type (Chang et al., 2016). Navitoclax is also used to treat lymphoid neoplasms and chronic lymphocytic leukaemia among others (Billard, 2013; Wendt, 2008). Dasatinib is another senolytic approved by the FDA for clinical use since 2006. Dasatinib is a potent inhibitor of tyrosine kinase BCR/ABL, promoting cell apoptosis through a series of receptors called dependence receptors such as ephrins (Kirkland & Tchkonja, 2020). Like the previous one, dasatinib is being used to treat different cancer including chronic myeloid leukaemia, Philadelphia chromosome-positive acute lymphoblastic leukaemia, advanced prostate cancer and thyroid cancer (Breccia & Alimena, 2011; Chan et al., 2012). Venetoclax or ABT-199 is a selective, oral BCL-2 inhibitor presenting antitumor activity against non-Hodgkin's lymphoma (Souers et al., 2013), chronic lymphocytic leukaemia (Vogler et al., 2013) and acute leukaemias (Khaw et al., 2014; R. Pan et al., 2014) *in vitro*. Several *in vivo* mouse xenograft studies also showed activity against aggressive (Myc+) lymphomas (Vandenberg & Cory, 2013) as well as acute leukaemia (Peirs et al., 2014). Although these exciting anti-aging effects of senolytics, their use has its own limitations. Navitoclax causes severe thrombocytopenia and neutropenia, which limits its application (Niedernhofer & Robbins, 2018). Another potential problem is tissue atrophy caused by massive senescent cell removal. Moreover, senolytics eliminate both the harmful and the beneficial effects of senescent cells. For example, senescent cells also play a positive role as an effective barrier against tumorigenesis in the early stages of cancer (Calcinotto et al., 2019). This dual function of senolytics should be considered and therefore, it is necessary to improve the targeting of senolytics to selectively inhibit their harmful effects on cells and tissues.

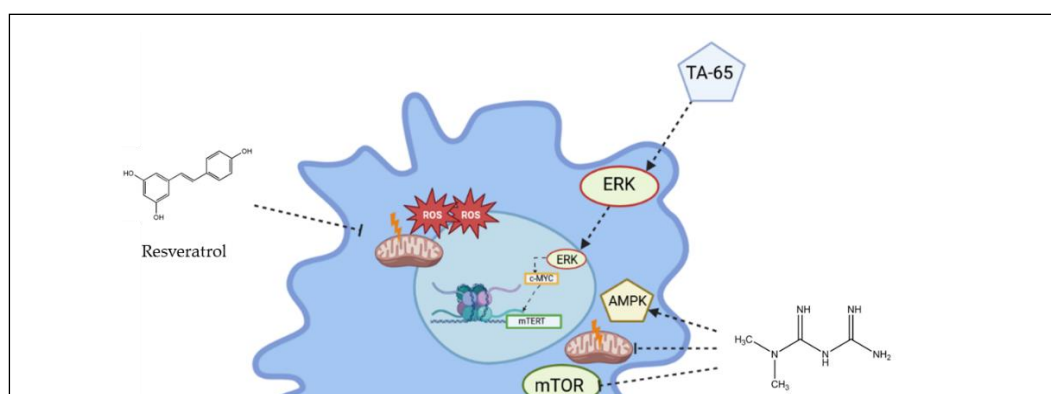


Figure 7. Anti-aging drugs. Resveratrol is known to ameliorate mitochondrial dysfunction associated with aging. Senolytics are drugs that selectively eliminate senescent cells. On the other hand, rapamycin and metformin increase lifespan by inhibiting the mTOR pathway. *Adapted from Hoi-Hung Cheung et al., (2015)*

I.3.1.3 Fasting and caloric restriction.

Fasting and caloric restriction (CR) are increasingly recommended not only for weight loss, but also for the reduction of obesity-induced aging-related diseases (Salvestrini et al., 2019). CR has a positive effect on DNA repair and telomere mechanisms. It has been reported that CR significantly reduces the incidence of tumors in telomerase transgenic (*TgTert*) mice, prolonging their lifespan (Vera et al., 2013). CR increases metabolic efficiency and prevents cell damage (Picca et al., 2017). CR also extends the lifespan of rodents and humans by reducing insulin, glucose, and the IGF-1 signaling pathway (Hwangbo et al., 2020; Pifferi & Aujard, 2019). Both expression and activity of sirtuins, which are closely related to aging, are induced by CR (Imai & Guarente, 2010). CR also is able to ameliorate inflammation and insulin resistance in a rat model of age-associated inflammation

through the regulation of GSH redox status and NF- κ B, SIRT1, and FoxOs (H. Y. Chung et al., 2011; Horrillo et al., 2011).

CR or CR mimickers, such as resveratrol or metformin, by reducing insulin resistance, contribute to preventing the onset and the progression of metabolic diseases (Gerhart-Hines et al., 2007). The reduction of nutrient intake can reduce cardiovascular disease (CVD) by controlling the mechanisms that maintain cardiac activity during aging, such as autophagy, proteasome-mediated turnover, apoptosis, and mitochondrial quality (Rattan, 2014). In healthy, non-obese individuals, CR could reduce the incidence of CVD by 30% (Most et al., 2018). Moreover, a long-term CR without malnutrition could reduce oxidative damage to tissues and organs (Redman et al., 2018), and induce significant suppression of inflammation (Meydani et al., 2016) (**Fig. 8**).

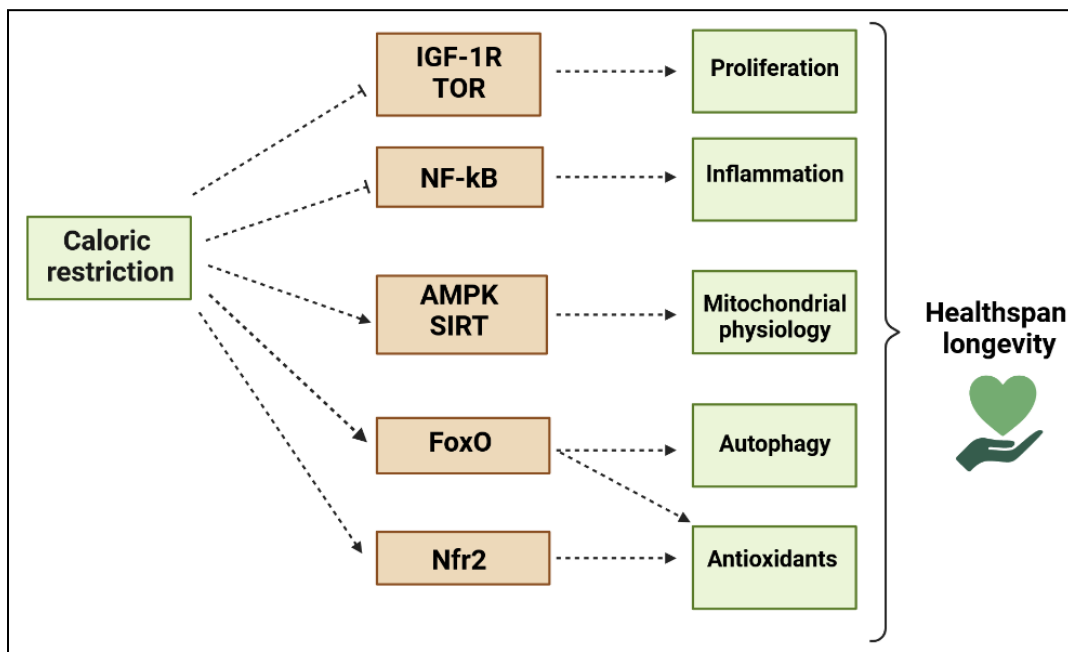


Figure 8. Caloric restriction (CR)-related processes involved in improving health and longevity. CR influences cellular pathways that produce an organism-wide response, leading to more efficient metabolism, providing greater protection against cellular damage and activation of remodelling mechanisms, whereas less efficient metabolism leads to blockade of these synthetic pathways. IGF-1, insulin-like growth factor-1; TOR, target of rapamycin; AMPK, AMP-dependent kinase; FoxOs, hairpin box proteins; eNOS, endothelial nitric oxide synthase; ROS, reactive oxygen species. *Adapted from Picca et al., (2017).*

But, again, CR can also exert negative effects. For example, CR should not be used for treating diseases in the elderly population with malnutrition (Pifferi & Aujard, 2019) or in people with a low body mass index (BMI, less than 21 kg/m²) because CR could lead to rapid weight loss increasing the risk of further health problems (Picca et al., 2017). In mice, it has been demonstrated that the combination of CR with exercise could cause bone loss (McGrath et al., 2020). In humans, CR could decrease bone mineral density, increasing the risk of osteoporotic fractures (Villareal et al., 2016). Therefore, before engaging in CR as a therapy to slow down aging, many factors should be taken into consideration.

I.4 Zebrafish models to study aging

Around 70% of human genes have at least one clear zebrafish orthologue, based on comparison with the human reference genome. Interestingly, despite having no identifiable zebrafish orthologue for a few notable human genes (Howe et al., 2013). Zebrafish proteins with functionally similar activities may exist. In addition, in the Online Mendelian Inheritance in Man (OMIM) database, 3176 genes are described that are related to different diseases, of which 82% (2601 genes) have an orthologue in zebrafish (Howe et al., 2013).

Tools have recently emerged which are able to easily manipulate the zebrafish embryo's genome and this together with the knowledge of both the

disease-leading genes in humans and the sequences of their zebrafish orthologs makes for a powerful methodology to create disease-specific models for the validation of novel drugs and the discovery of new therapeutics.

It is worth mentioning, human genes that are associated with many zebrafish genes (the 'one-human-to-many-zebrafish' class), with an average of 2.28 zebrafish genes for each human gene (Howe et al., 2013). This is because of an ancestor undergoing an additional round of whole-genome duplication. Gene redundancy, from an evolution point of view, helps an organism to survive when one copy of the homologs becomes non-functional or malfunctions or acquires a new function. However, it is undesirable for either the forward genetic approach to screen phenotypic mutants or reverse genetics to generate null alleles for target genes because the redundant genes might obscure the phenotypic drug screening or analysis.

Although the zebrafish is an aquatic animal, most zebrafish organs perform the same functions as their counterparts in humans, such as the pancreas (Matsuda, 2018), cardiovascular system (Rödel & Abdelilah-Seyfried, 2021) hematopoietic system (Robertson et al., 2016), they also conserve critical parts of the innate and adaptive immune system. The inflammatory response has also been found to be well-conserved with humans (Meijer, 2016; Y. Xie et al., 2021). The zebrafish brain and olfactory system share a significant degree of molecular and anatomical conservation with humans (Saraiva et al., 2015).

As above, processes such as aging or cancer are conserved (Anchelin et al., 2011, 2013). Interestingly, the human telomere length is more like that of zebrafish than of rodents, adding to a list of cases in which zebrafish physiology may be more relevant than its rodent counterpart as has been observed in their cardiac electrophysiology, vision dominated by cones, and diurnal behavior (Calado & Dumitriu, 2013; MacRae & Peterson, 2015).

Due to all these advantages, in recent decades, the zebrafish has positioned itself as an excellent *in vivo* model for studying a multitude of both physiological, pathological processes, including aging (Cayuela et al., 2019) (**Fig. 9**).

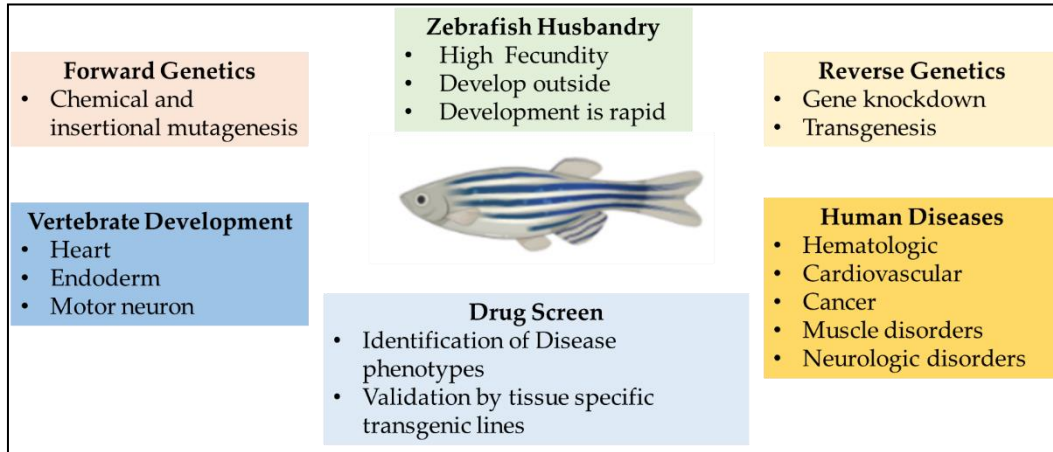


Figure 9. Advantages of the zebrafish model. Besides being an excellent model to study development, the application of genetic approaches makes the zebrafish a good model to study the function of genes and signalling pathways involved in different diseases. *Adapted from Chitramuthu et al., (2013).*

I.4.1 Telomeres and telomerase in zebrafish.

Since the coding sequence of the catalytic subunit of zebrafish telomerase (*zftert*) was sequenced and cloned, and the expression of telomerase at both mRNA, protein, and functional levels carried out a few years ago (Spence et al., 2008), the zebrafish has been considered a good model for conducting studies on aging, regeneration, and cancer. In addition, the RNA component of telomerase (*zfTR*), was also characterized through bioinformatic studies of secondary structure analysis and functional analysis in comparison with other known small vertebrates of five teleost fish, including zebrafish, observing that both structure and function are conserved, thus supporting the use of zebrafish as a model organism for the study of telomerase biology (Xie et al., 2008).

The characterization of the behavior of telomeres and telomerase in both aging and regeneration in zebrafish demonstrates that both telomeric length and telomerase activity are closely linked throughout the life cycle of zebrafish.

Therefore, these two parameters can be used as biomarkers for the study of aging in zebrafish (Anchelin et al., 2011; Carneiro, de Castro, et al., 2016; Carneiro, Henriques, et al., 2016). As both telomere length and telomerase expression are

limiting factors for the useful life of zebrafish, it is possible to study telomere shortening in normal individuals. Unlike the mouse model, zebrafish show limited telomerase activity and a telomeric length like that of humans so, with each cell division, telomere shortening occurs just as it occurs in humans, as a biological clock for cell division (Anchelin et al., 2011; Henriques & Ferreira, 2012).

The aging phenotype of zebrafish has been well described by using a premature aging model, the telomerase-deficient zebrafish line (*tert*^{-/-}). This publicly available *tert* mutant line generated by ENU mutagenesis at the Sanger Institute (hu3430) has a nonsense mutation (T>A) resulting in a premature stop codon and truncated protein with only the first 156 aa out of 1088 aa, as well as the absence of the RNA binding and reverse transcriptase domains.

The phenotype included lacking telomerase activity, telomere shortening, chromosomal instability, sustained decrease in cell proliferation, acute apoptotic response, accumulation of DNA damage responses (DDRs), senescence, and, finally, tissue atrophy (Anchelin et al., 2013; Henriques et al., 2013). For these reasons, the zebrafish is another complementary model to the murine (mouse) model for the study of diseases caused by a dysfunction in telomerase. Other studies have highlighted that telomerase is necessary for the useful life of zebrafish, since zebrafish with telomerase deficiency presents a series of symptoms of premature aging from the first generation, such as infertility, curvature in the spine, weight loss, degeneration of both the liver and the retina (Henriques et al., 2013) (**Fig. 10**).

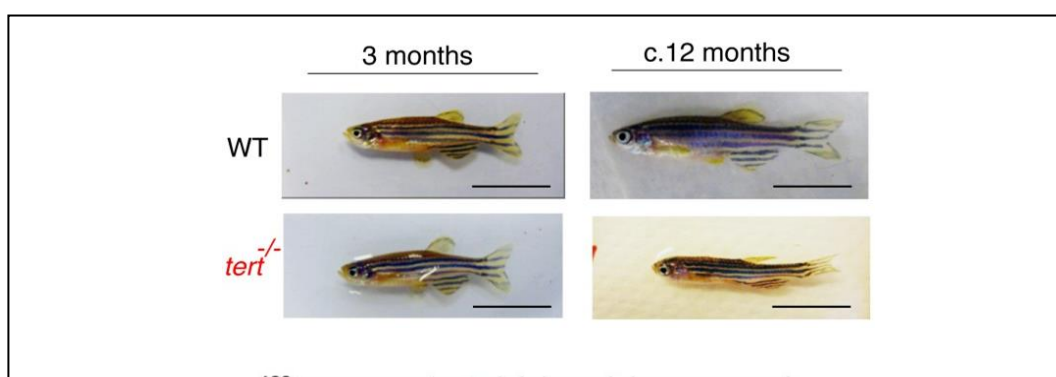


Figure 10. Telomerase-deficient premature aging zebrafish model. First-generation telomerase mutant zebrafish show progressively body wasting and die prematurely. *Adapted from Henriques et al. (2013).*

However, while the life expectancy of the first-generation Tert-deficient zebrafish model is still too long, the second-generation show a morphological phenotype so severe that larvae do not survive (Anchelin et al., 2013). For this, the generation of a hasty aging zebrafish model that is useful to do drug screening is very desirable.

I.4.2 Immunosenescence in zebrafish.

In mammals, recombination activating gene 1 and 2 (*RAG1* and *RAG2*) translate a lymphoid-specific endonuclease (*RAG1/2*), initiating a programmed DNA rearrangements in progenitor lymphocytes to assemble the vastly diverse immunoglobulin (Ig) and T-cell receptor (TCR) genes (Bassing et al., 2002). *Rag1*-deficient zebrafish present a point mutation that results in a premature stop codon in the *rag1* catalytic domain, which completely blocks Ig gene assembly removing the adaptive immune system (Wienholds et al., 2002). Contrary to *RAG1*-deficient humans, *Rag1*-deficient zebrafish reach adulthood and become fertile without obvious signs of infectious disease in standard, non-sterile aquarium facilities. In fact, *rag1*^{-/-} zebrafish respond faster to a viral infection and have increased survival (García-Valtanen et al., 2017). However, compared to their wild-type siblings, the *Rag1*-deficient zebrafish show: i) a premature aging phenotype, with a reduced lifespan; ii) a higher incidence of cell cycle arrest and apoptosis; iii) a greater amount of phosphorylated histone H2AX and oxidative stress; iv) an upregulated expression of senescence-related genes and senescence-associated β -galactosidase (SA β -gal) activity; v) diminished telomere length; and vi) abnormal self-renewal and repair capacities in the retina and liver. As expected, the treatment of *rag1*^{-/-} zebrafish with the senolytic navitoclax can reduce both the expression of senescence markers and SA β -gal staining in the skin. (**Fig. 11**).

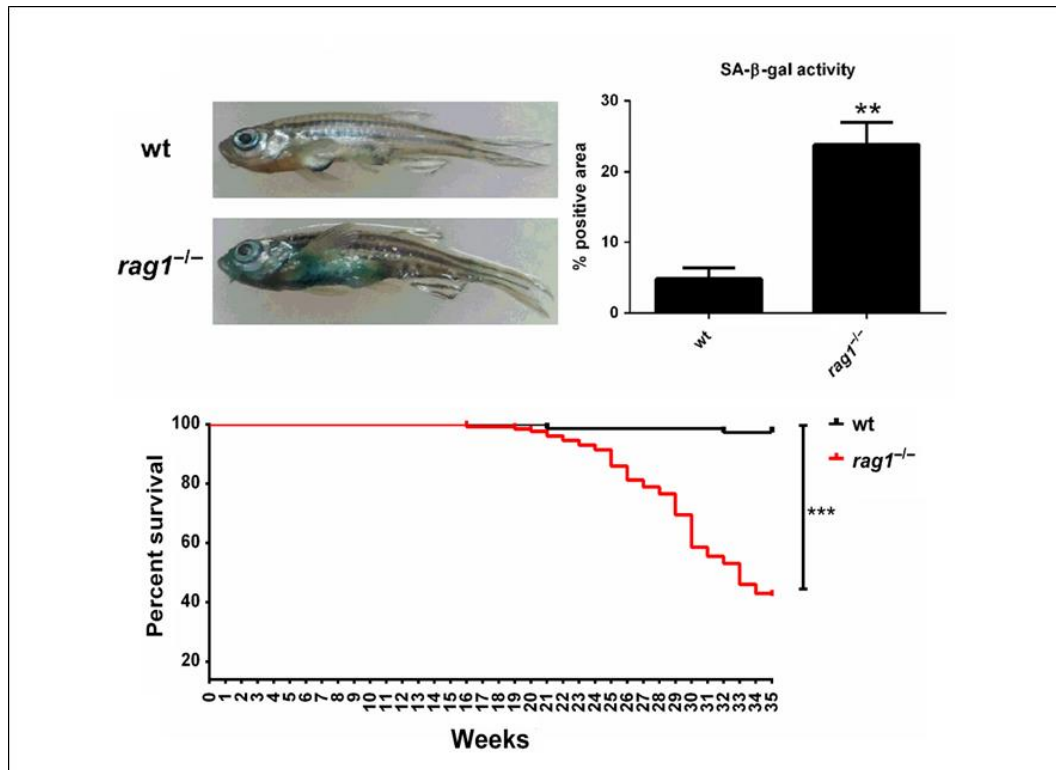


Figure 11. Rag1-deficient zebrafish immunosenescence model. 1 year-old *rag1^{-/-}* zebrafish show SA-β-gal activity in the skin and altered survival. *Adapted from Novoa et al., (2019).*

The accumulation of DNA damage over time and the involvement of chronic inflammation and oxidative stress, along with the fact that the absence of mature lymphocytes in *rag1^{-/-}* fish generate a higher accumulation of senescent cells, explain the premature aging phenotype, and presents Rag1-deficient zebrafish line is an excellent model of immunosenescence (Novoa et al., 2019).

I.4.3 Chronic inflammation and oxidative stress in zebrafish.

The zebrafish line with a hypomorphic mutation of *spint1a*, the gene encoding the serine protease inhibitor, kunitz-type, 1a (a growth factor also known as hepatocyte-activator inhibitor 1, hai1a) has been described as a chronic skin inflammation model. *Spint1a*-deficient larvae show; i) neutrophil infiltration in the skin; ii) keratinocyte hyperproliferation that results in aggregate foci; iii) epithelial

integrity disruption; and iv) chronic skin inflammation (Carney et al., 2007; Mathias et al., 2007). This inflammatory process is mediated by parthanatos cell death because of hyperactivation of poly (ADP-ribose) polymerase 1 (Parp1) in response to ROS-induced DNA damage and is fuelled by nicotinamide phosphoribosyltransferase (NAMPT)-derived NAD⁺ (Martínez-Morcillo et al., 2021). So, the chronic skin inflammation *Spint1a*-deficient model shows all the characteristics that define inflammaging (Franceschi et al., 2000) (**Fig. 12**).

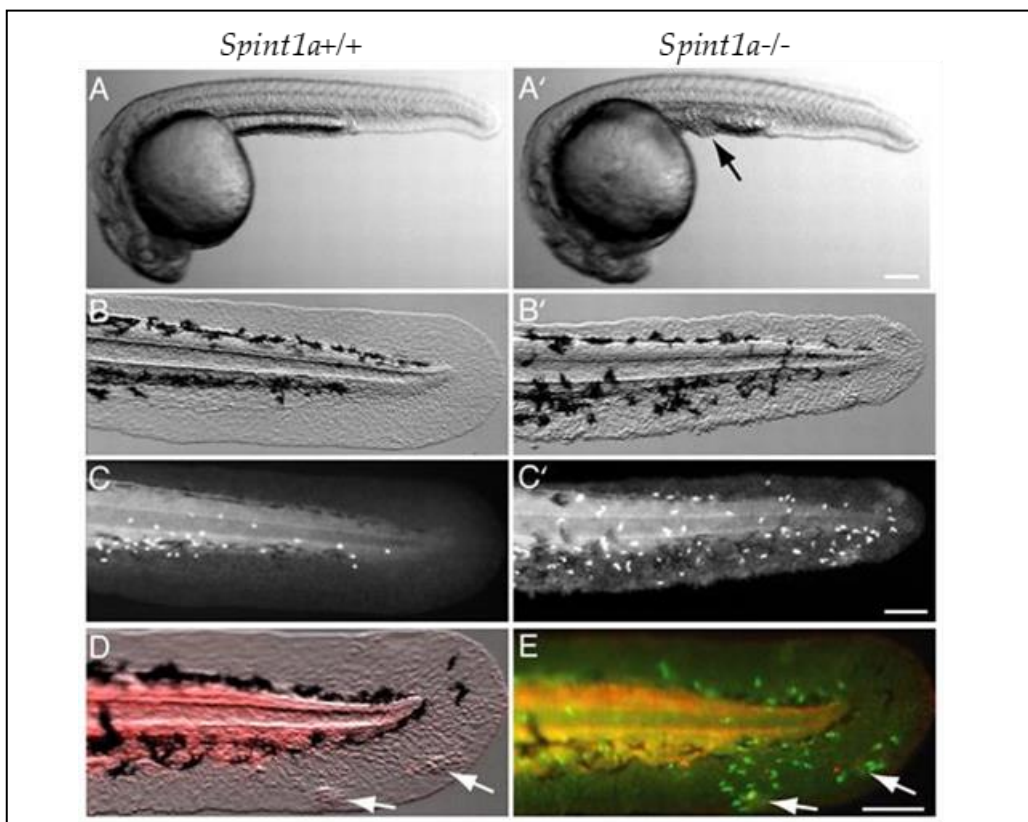


Figure 12. *Spint1a*-deficient zebrafish inflammaging model. 24-hpf *Spint1a*-deficient larvae (A') showing (48 hpf): epithelial integrity disruption (B'), neutrophil infiltration in the skin (C'), keratinocyte aggregate foci (D), and skin inflammation (E). Adapted from Mathias et al., (2007).

Another zebrafish model originally described as a non-alcoholic fatty liver disease/non-alcoholic steatohepatitis (NAFLD/NASH) model, can be also described as a nutrient excess-induced chronic inflammation or metainflammation

model. Fish fed with a high-cholesterol diet (HCD) for 11 days develop non-resolving inflammation in the liver with increased neutrophil infiltration, altered macrophage polarization, reduced T-cell density, and enhanced cancer progression (de Oliveira et al., 2019) (Fig. 13). This metainflammation model is very useful to search for new drugs with preventive-aging or anti-aging effects.

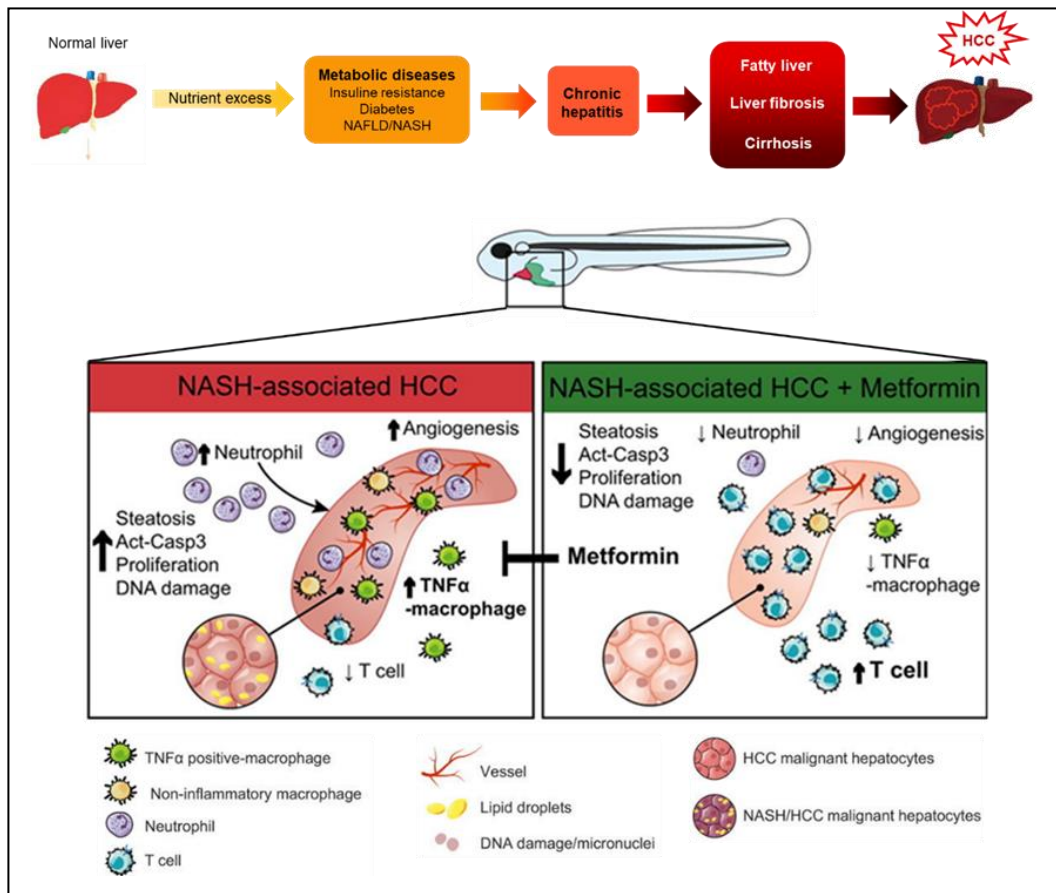


Figure 13. NAFLD/NASH zebrafish metainflammation model. At the top, nutrient excess triggers to inflammatory stress that leads to DNA damage and cell cycle dysregulation in hepatocytes. Eventually, this metainflammation leads to the development of HCC. At the bottom, zebrafish fed with HCD shows metainflammation in the liver, with changes in macrophage polarization, increased infiltration of neutrophils and TNF α -positive macrophages and reduced T cell infiltration. Metformin treatment can ameliorate this metainflammation phenotype. NAFLD: non-alcoholic fatty liver disease; NASH: non-alcoholic steatohepatitis. HCD: high cholesterol diet. Adapted from Lu et al., (2015) and de Oliveira et al., (2019).

I.5 Virtual Screening (VS)

Virtual screening techniques were born in the 1980s, but it was not until 1997 that the first virtual screening publication appeared (Horvath, 1997).

This is a computational or *in silico* technique, which allows cost-effective identification of new bioactive substances from large libraries of compounds (Surabhi & Singh, 2018) consisting of 1 dimension (D), 2D, and 3D chemical structures (Duan et al., 2010; Ivanciuc et al., 2000; Jørgensen & Pedersen, 2001; Rollinger et al., 2008). Virtual screening acts as a funnel, filtering large libraries of compounds that are available, producing a selection of the best or most promising molecules for subsequent *in vitro* assays (Cheng et al., 2012; Maia et al., 2020; Svensson et al., 2012). The fundamental premise of virtual screening is based on ligand-protein recognition, therefore only the most promising molecules are synthesized (Shen et al., 2003).

On the other hand, VS is also able to identify compounds that may be potentially toxic or present unfavorable pharmacokinetics or pharmacodynamics (Ma et al., 2009; Maia et al., 2017; Shen et al., 2003). VS can be classified in 2 types: structure-based virtual screening (SBVS) and ligand-based virtual screening (LBVS) (Fig. 14).

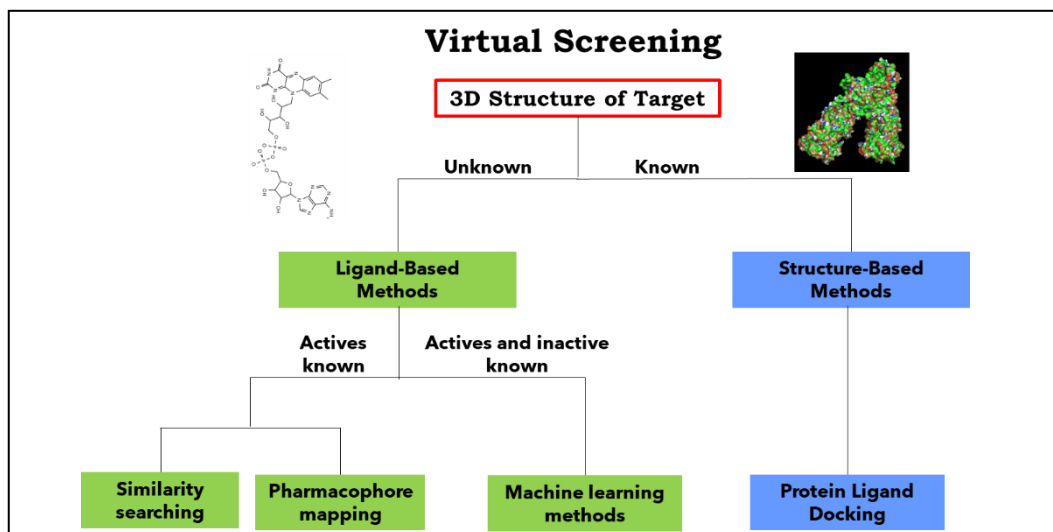


Figure 14. Schematic representation of the different types of VS methods.

I.5.1 Structure-Based Methods (SBVS)

Structure-based virtual screening (SBVS) methods predict the interaction between the ligand and the molecular target (ligand-receptor). In this type of VS, compounds are ranked from a database by a scoring function that predicts ligand-receptor affinity and is implemented in the molecular docking process (Brink & Exner, 2009; S. Y. Huang et al., 2010; Leelananda & Lindert, 2016). SBVS shows the following advantages (Leelananda & Lindert, 2016): i) Regarding computational cost of VS methods, SBVS methods are generally more expensive than LBVS methodologies (Batool et al., 2019; Gorgulla et al., 2020; Vázquez et al., 2020); ii) Since each docking simulation typically only needs a few minutes (Bender et al., 2021) when using a single CPU core; iii) When compared to full library wet-lab screening, fewer molecules are synthesized or purchased since only the top-ranked compounds are evaluated in the laboratory; iv) Existence of available software tools (<https://www.click2drug.org/>) that help to perform SBVS.

Nevertheless, SBVS also have disadvantages that are detailed as follows (Leelananda & Lindert, 2016). Other tools work better in specific cases (Lionta et al., 2014). Low accuracy in predicting ligand-receptor binding affinity and subsequent classification of compounds although it can be increased when using

more advanced SB methods such as Free Energy Perturbation (Cournia et al., 2020) of Thermodynamic Integration (Sahakyan, 2021); and finally, they can generate false positives as well as false negatives.

Search algorithms are used to predict the orientations (Carpenter et al., 2018; Carregal et al., 2017; Dutkiewicz & Mikstaka, 2018) and conformations that ligands can adopt at the binding site by the target molecule (Carpenter et al., 2018; Carregal et al., 2017; Dutkiewicz & Mikstaka, 2018; Mugumbate et al., 2017; Nunes et al., 2019; Surabhi & Singh, 2018; Wójcikowski et al., 2017).

Accordingly, a good docking protocol will obtain more realistic ligand-receptor conformations and binding positions at the binding site. When processing a large compound database during a virtual screening calculation, a good docking protocol should be able to efficiently rank the compounds according to the predicted binding affinity values (Huang et al., 2006; Palacio-Rodríguez et al., 2019), and to predict the 3D structure of resulting binding poses (Huang et al., 2006). But also important, the docking workflow should have a high computational throughput (Puertas-Martín et al., 2020) and be as fast as possible when predicting both ranking and structure.

This algorithm performs a global search for most of the possible positions that can occur between the ligand and the receptor-binding site including rotational and translational degrees of freedom to the ligand (Maia et al., 2020).

In addition, include the descriptions of algorithms used in molecular docking and a list of software used: i) *Autodock Vina* (Trott & Olson, 2009); ii) *Glide* (Friesner et al., 2004; Repasky et al., 2007); iii) *Lead Finder* (Stroganov et al., 2008); iv) *FRED* (McGann, 2012); and v) *Autodock 4* (Morris et al., 1639).

I.5.2 Ligand-Based Methods (LBVS)

Ligand-based virtual screening (LBVS) uses both structural information and the physicochemical properties of the structure of molecules, and if these molecules are active, it performs a VS under the principle of a previously defined similarity metric.

Thus, from a set of known active molecules, new candidate compounds can be identified that should bind to a molecular target by a similar mechanism and hence exert a similar biological effect on the starting molecule. This method

includes different molecular descriptors, these descriptors can be 1D and 2D that offer information about the chemical nature and topological characteristics of the compounds, on the other hand, we find the 3D molecular descriptors that are associated with molecular fields both in shape and volume and pharmacophores (Rollinger et al., 2008; Vázquez et al., 2020) (Fig. 15).

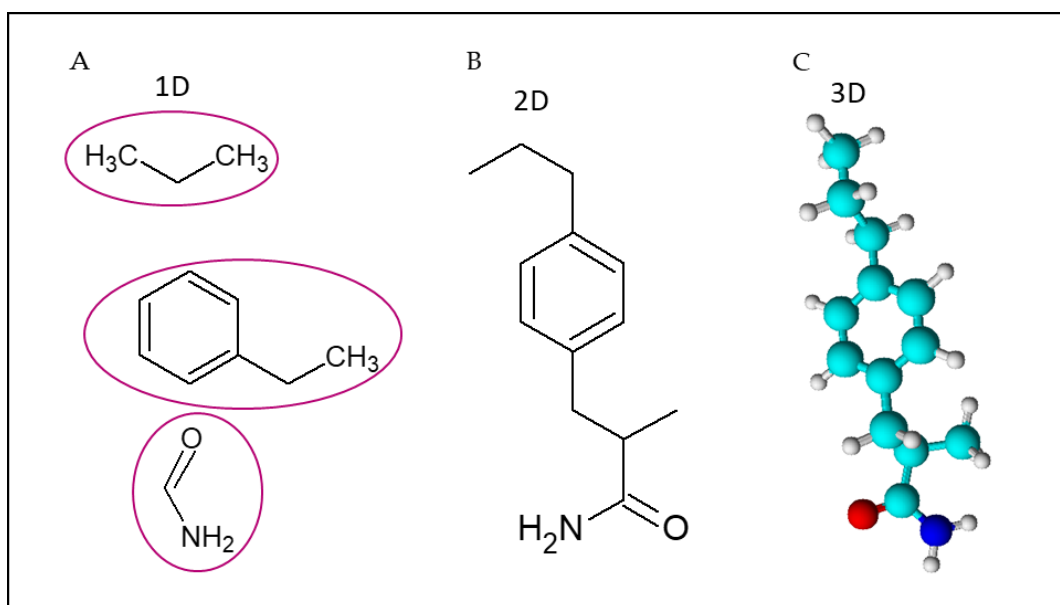


Figure 15: Graphic representation of the different molecular descriptors. A) Molecular descriptors 1D., B) Molecular descriptors 2D. C) Molecular descriptors 3D.

I.5.3 Pharmacophoric Methods

According to the International Union of Pure and Applied Chemistry (IUPAC) definition, a pharmacophore is 'a set of steric and electronic characteristics that is necessary to ensure optimal supramolecular interaction with a specific biological target and to activate or block its biological response'. This concept is based on the interactions observed in molecular recognition. Such interactions can be hydrogen bonds, positive or negative charges of the molecules, and hydrophobic regions. This type of mapping has proved to be a very useful and

successful tool in understanding the recognition process between the protein (receptor) and the ligand (Rojas et al., 2012).

To generate a pharmacophore model, in addition to knowing the interaction that occurs between the receptor protein and the ligand, in this case of structure-based virtual screening (SBVS), it is necessary for the 3D structure of the receptor to be known (Sanders et al., 2012). Currently, there is a platform in which we can find 3D structures of proteins, expressly, the Brookhaven Protein Data Bank (PDB) (Berman et al., 2000; Rollinger et al., 2008; Scapin, 2006). Along with the ligand-binding site, where we can generate a 3D structural model of the most relevant ligand-based interactions (Rollinger et al., 2008) (**Fig. 16**).

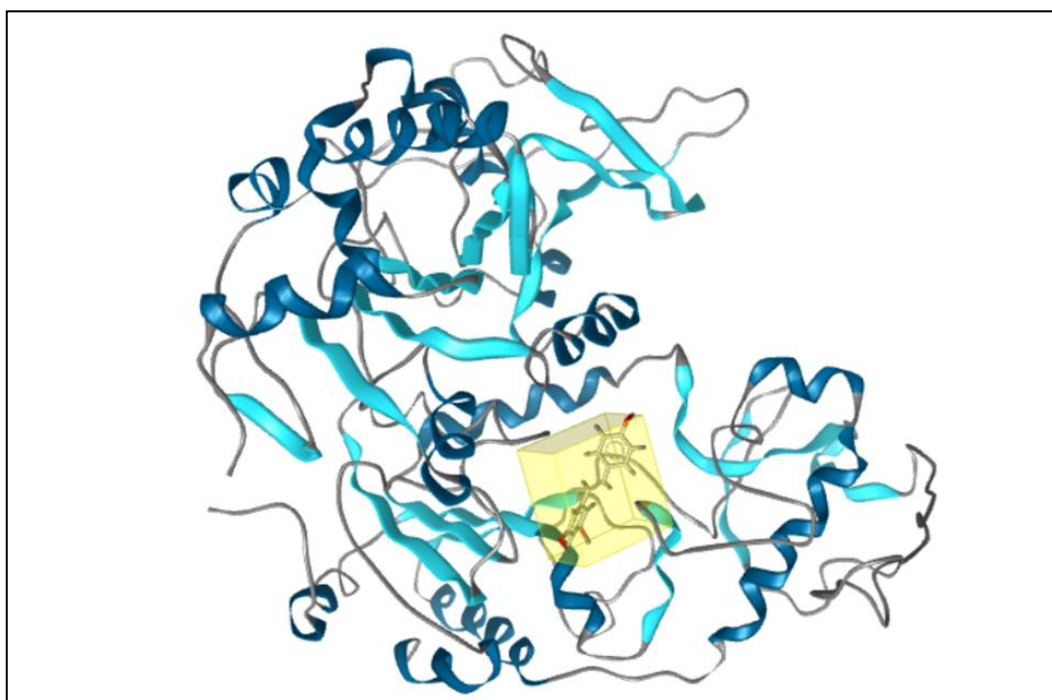


Figure 16: Ligand-protein interaction zone, the conformation of the ligand in the active center (yellow box). Figure obtained from PDB: 4HDA. Graphic representation obtained with *Ligand Scout 4.4*.

The *LigandScout* software (Wolber & Langer, 2005) allows the analysis and interpretation of the structural information of ligands and the posterior generation of pharmacophore models. This software allows the detection of the most relevant interaction site that exists between the ligand and the receptor protein, and the

binding that is generated between them can be visualized in a very detailed way (Rollinger et al., 2008) (Fig. 17).

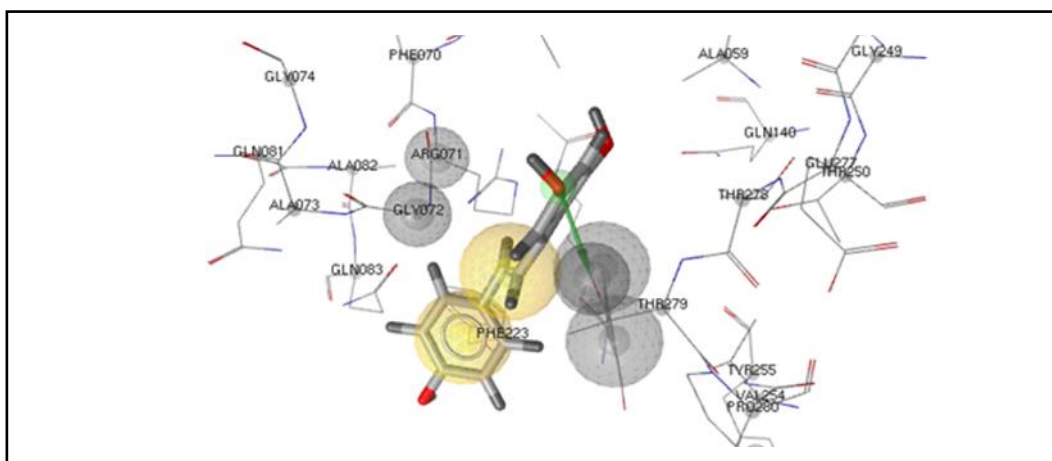


Figure 17: Pharmacophoric model of the ligand. The interaction between the ligand and the protein. Spheres of exclusion are represented gray spheres exclusion. Hydrophobic sites are represented by yellow spheres. Electron donor are represented by green arrow. Molecule obtained from *PDB: 4HDA*. Graphic representation obtained with *Ligand Scout 4.4*.

In contrast, when pharmacophore models are used for screening new ligands, the ranking prediction is based on a similarity metric (Rollinger et al., 2008) with respect to the initial pharmacophore model derived from the experimental protein-ligand crystallographic structure. This type of screening yields many possible candidates, although it has a several other advantages including discrimination of non-binder compounds. Furthermore, the computational level has a lower cost when compared to other techniques such as high throughput docking (Rollinger et al., 2008).

This VS method can be used if a group of ligands (compounds) is active and their 3D structure is known, so their pharmacophores can be defined (Gad, 2008). Such a pharmacophore can serve as a model to perform VS, especially since this

model is used when the 3D structure of the receptor is unknown and thus, SBVS cannot be performed (Rollinger et al., 2008).

With this pharmacophoric approach, better performance is usually obtained than using just ligand similarity, since this method operates using a wider set of active molecules containing completely different chemical structures but showing the same pharmacophoric features (Rollinger et al., 2008).

However, Pharmacophore-based VS methods do show some disadvantages: i) both conformation and molecule overlap might be inaccurate or insufficient (Leach et al., 2010); ii) they might exhibit ambiguities in the pharmacophore model (this is related to the protonation and tautomer state of the compounds) (Leach et al., 2010); iii) they might show inadequate binding sites in the active center of the target molecule when ligand structures are not available, leading to incorrect ligand-receptor binding affinity (Leach et al., 2010).

I.5.3.1 Combination OF SBVS and LBVS

Molecular modeling methods based on both ligands and structure that exist today have been very successful in VS by retrieving new compounds as potential candidates for the process of creating new drugs. These methods, as well as others, display some disadvantages. For example, in the structure-based (SB), pharmacophoric method, the selection of the main pharmacophoric features is not trivial, having to consider the potential ligand conformations.

These types of disadvantages must be considered when choosing the method to be used (Lavecchia & di Giovanni, 2013).

The pharmacophore model is a very important when we do not know the active form of the ligand or the structure of the target protein (receptor), because in this case, it offers an advantage, aside from being able to identify a novel compounds, which is that a series of profiles can be designed to avoid the side effects that can occur when exerting a function foreign to the target protein (Schuster, 2010). The SB pharmacophore model is provided by the structure of the target protein, after a prior investigation of all possible interaction zones in the binding cavity is performed (Leach et al., 2010).

Relevant interaction zones can be identified by energy- or geometry-based methods, resulting in a pharmacophore method. When all the necessary

information about the ligand is available, such as 3D structure and pharmacophoric characteristics, among others, the structure-based pharmacophore model is used, where all possible interaction zones between the protein and the ligand are described.

The magnified advantage the SB pharmacophore method possesses is the higher probability for the identification of compounds that can be potentially active, leading to a higher computational cost which is a disadvantage (Leach et al., 2010; Miles & Ross, 2021). The combination of both techniques has delivered both good and bad results since at present there is an inability in the fusion strategies between the two methods to be able to consistently offer superior performance concerning techniques separately (Leach et al., 2010).

Different drugs discovery by VS techniques are already commercial, including saquinavir, ritonavir, and indinavir (anti-retroviral agents), saquinavir, ritonavir and indinavir (three drugs for the treatment of human immunodeficiency virus,) and others, that are in clinical phase III, such as nolatrexed, for the treatment of liver cancer (Devi et al., 2015; Nunes et al., 2019; Sliwoski et al., 2014; Talele et al., 2010). As previously, there are also different studies in which the combination of both VS techniques (SBVS and LBVS) is applied, where different drugs were found that are much more potent than that which currently exists, such as inhibitors of 17 β -hydroxysteroid dehydrogenase type 1 (17 β -HSD1) (Debnath et al., 2019; Spadaro et al., 2012). It is worth mentioning that the use of these techniques for the development, improvement, and repositioning of drugs is in general terms a much faster and less expensive way than using a traditional experimental method. A key example is the discovery of specific inhibitors of histone deacetylase 8 (HDAC8).

I.6 Combination of virtual screening and zebrafish models.

Surprisingly, despite the success in drug discovery (DD) using virtual screening (VS) and high throughput screening (HTS) in zebrafish, the combination of both tools has not been fully exploited. Using both models in tandem provides a way of offering great potential for both new drug discovery and drug repurposing for different diseases. Importantly, innovations *in silico* target identification tools,

mentioned above, allow faster and more accurate specific target determination, making target-based screening popular again (**Fig. 18**).

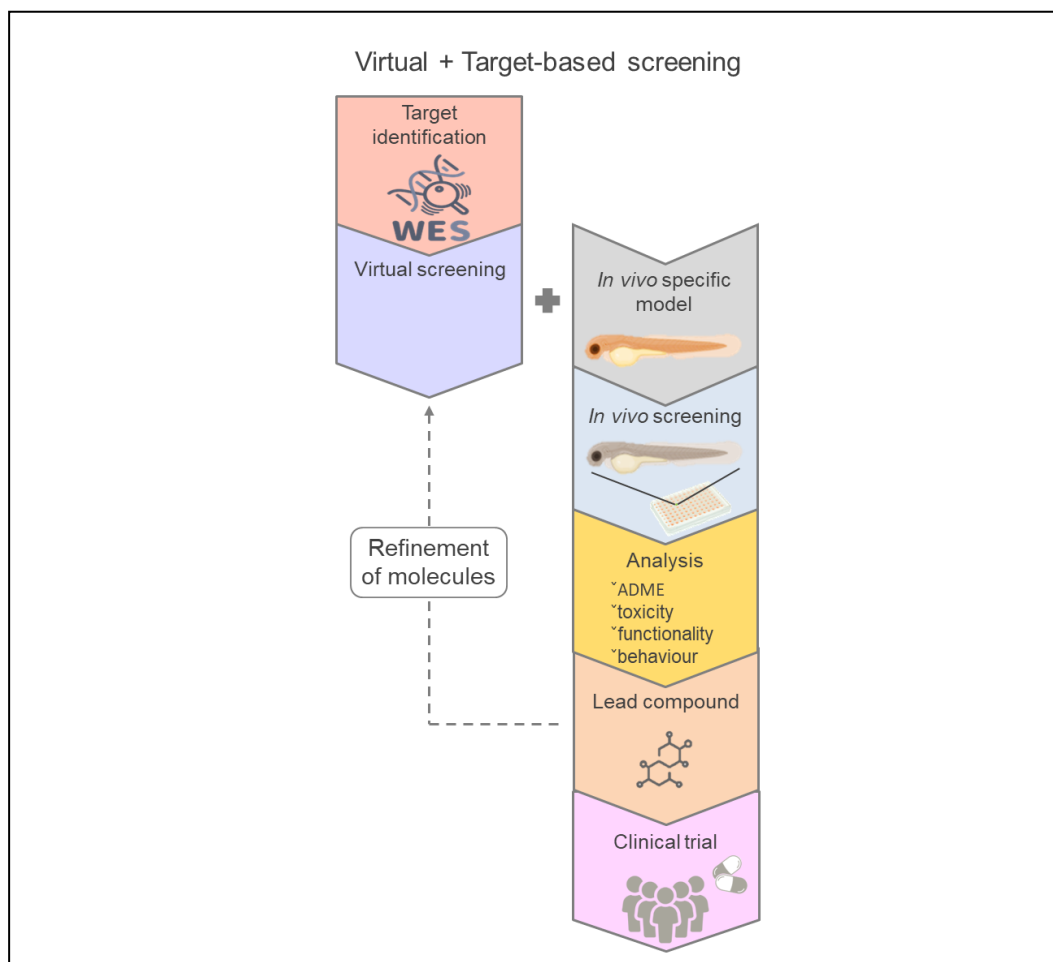


Figure 18. Combination of virtual screening and *in vivo* target-based screening in zebrafish. A second round of screening is indicated in case of refinement of molecules is necessary.

A selection of different combined VS and *in vivo* target-based screening strategies is illustrated below.

I.6.1 Xenograft.

Fascin 1 is a vital actin-bundling protein involved in cancer invasion and metastasis whose expression correlates with poor prognosis. Therefore Fascin 1 is an excellent therapeutic target in cancer treatment. *In silico* screening calculations of 9591 compounds, including 2037 approved by the FDA, were performed, and analyzed by VS to identify a potential fascin1 blocker (Albuquerque-González et al., 2020). Among the 20-30 top candidate compounds, imipramine (anti-depressants) and raltegravir (anti-retroviral) were selected by different techniques such as thermofluor, fluorescence titration and *in vitro* characterization. Finally, both compounds were tested using the xenograft transplantation in zebrafish larvae approach to evaluate their inhibitory activity in tumor growth, invasion, and metastasis. Imipramine is being already tested in an approved phase II clinical trial (Albuquerque-gonzález et al., 2021). The combination screenings allowed the repurposing to take place in less than 3 years and the number of compounds tested *in vitro/in vivo* was greatly reduced (99,5 % of the library were eliminated *in silico*).

I.6.2 Infection models.

Tuberculosis (TB) is the second leading infectious disease-causing mortality worldwide. It is caused by *Mycobacterium tuberculosis* (Mtb). Topoisomerase I (Topo I), an essential mycobacterial enzyme, is heavily involved in the viability of the Mtb pathogen. Accordingly, the protein structure of Mtb Topo I 3D was employed for VS of 5 million compound libraries in an identification process of various Mtb Topo I inhibitors (Ott et al., 2016). Hydroxycamptothecin was one of the compounds identified. Its structural derivatization yielded a set of 15 compounds that were screened *in vivo* for anti-mycobacterial activity by using a zebrafish infection model (Bouz & al Hasawi, 2018). One of them was found to be more effective when compared to first-line anti-tuberculosis drugs, such as isoniazid and rifampicin (Bouz & al Hasawi, 2018).

Currently, there is an ongoing global pandemic of coronavirus disease 2019 (COVID-19) caused by severe acute respiratory syndrome coronavirus 2 (SARS-CoV-2). This has caused a serious global public health emergency and with it, an unprecedented challenge to identify novel drugs for prevention and treatment.

Although a concerted effort has been undertaken for DD using VS (Aloufi et al., 2022; Hakami et al., 2022; Yamamoto et al., 2022) nothing has yet been published regarding the combination of VS with zebrafish.

Several laboratories have tried to analyze how useful zebrafish is as a model for COVID. These studies revealed that zebrafish showed an inflammatory reaction to SARS-CoV-2 rSpike protein (fragment N-terminal 16 to 165), which led to organs (liver, kidney, ovaries, and brain) being damaged in a similar pattern to what happens in severe cases of COVID-19 in humans (Ventura Fernandes et al., 2022). In addition, it is known that anosmia or loss of smell is a prevalent symptom of SARS-CoV-2 infection. Interestingly, the RBD fragment of SARS-CoV-2 S1 protein, caused olfactory pathology and loss of smell in adult zebrafish (Kraus et al., 2022). But all these experiments have been performed in adult zebrafish, while only larvae are most suitable for high-throughput drug screening.

Despite the low infectivity of SARS-CoV-2 observed in zebrafish larvae, it has been described a viral RNA stabilization after virus inoculation in the swim bladder, which is an aerial organ sharing similarities with the mammalian lung (Laghi et al., 2022). In this regard, a humanized model has been generated by xenotransplantation with human lung epithelial cells (A549 cell line), into zebrafish swim bladder to study DD and test the safety of vaccines and immune response against SARS-CoV-2 and COVID-19 (Bauer et al., 2021). Future generation of transgenic zebrafish expressing human ACE2, will be needed to unlock the full potential of the zebrafish larvae in the DD to fight against COVID-19.

I.6.3 Drug toxicity testing.

Zebrafish is fast becoming an *in vivo* platform to predict toxicity (with a particular focus on cardio-, neuro-, hepato-, and nephrotoxicity) and teratogenicity of new compounds in the context of the whole animal, which could help to shift compound attrition to an early stage of drug development (Bauer et al., 2021; Eimon & Rubinstein, 2009; Raldúa & Piña, 2014; Sukardi et al., 2011). As such, the developmental toxicity assay with zebrafish has become an interesting endgame for *in silico* screening.

Such is the case of a structure-based VS of the *Enamine* database with 1.7 million compounds that were applied to identify novel acetylcholinesterase

(AChE) inhibitors (Targowska-Duda KM et al., 2022). In this case, VS determined 29 compounds. Zebrafish were used as a toxicity and safety *in vivo* model. Finally, 3 compounds were chosen.

Similar strategies have been followed for detecting inhibitor toxicity of O-GlcNAc transferase (OGT), NEDD8 activating enzyme and iNOS, which would be used in potential anti-tumor, anti-inflammatory and anti-neurodegenerative applications (Check Hayden, 2014; Sukardi et al., 2011).

All this proves once again that zebrafish assays in tandem with computational screening significantly improve the efficiency of identifying specific regulators of biological targets and their toxicity, having been replicated in laboratories worldwide.

II. JUSTIFICACIÓN

II - JUSTIFICACIÓN

En los últimos 50 años la esperanza de vida ha mejorado considerablemente. Este incremento se debe a la mejora en la calidad de vida y fundamentalmente a los avances en la ciencia médica que se han producido en las últimas décadas. Los individuos están alcanzando edades que eran impensables en épocas anteriores, aumentando de manera significativa el número de personas octogenarias. Como consecuencia también ha aumentado la incidencia de enfermedades relacionadas con envejecimiento, entre las que se encuentran las enfermedades cardiovasculares, el cáncer o las enfermedades neurodegenerativas.

Sin embargo, los cambios producidos en los estilos de vida y en la dieta (rica en grasas saturadas, azúcar, con aditivos, sal y muy calóricas), así como la exposición a sustancias tóxicas o a terapias severas están haciendo que aparezcan dolencias que se asemejan a las enfermedades asociadas a edades más tempranas. Tal es el caso de la diabetes tipo 2, la obesidad, y enfermedades crónicas de hígado (hígado graso o hepatitis no infecciosas) y pérdida prematura de capacidades cognitivas. Por lo tanto, es probable que se revierta la tendencia longeva observada entre nuestros jóvenes. Por ejemplo, se predice que el número de adolescentes con diabetes tipo 2, una enfermedad prevenible, está aumentando rápidamente en sociedades con estilos de vida occidentales y altas tasas de obesidad infantil. Estos adolescentes pierden ~15 años de la expectativa de vida promedio. También cabe destacar los supervivientes de cáncer (siendo más dramático en los supervivientes de cánceres pediátricos) que, debido a los tratamientos oncológicos también ven reducida tanto sus expectativas como su calidad de vida.

Además de todo lo anterior, habría que añadir a aquellos pacientes que presentan enfermedades raras llamadas telomeropatías, que, a pesar de su baja incidencia, también sufren las consecuencias de un envejecimiento prematuro.

Por lo tanto, la búsqueda de tratamientos rejuvenecedores deberían ser objetivos urgentes de los esfuerzos de Salud Pública. De hecho, muchos son los laboratorios que están interesados en la búsqueda de compuestos que aminoren las consecuencias del envejecimiento e incluso lleguen a rejuvenecer.

La sobreexpresión de la telomerasa (*TERT*) produce el alargamiento de los telómeros presentando un efecto rejuvenecedor sobre el metabolismo y las capacidades cognitivas en modelos de ratón.

Los efectos rejuvenecedores han sido observados con los fármacos senolíticos, estos compuestos producen la eliminación específica de las células senescentes. Estas células senescentes segregan una serie de factores solubles asociados a senescencia (SASP), estos contribuyen al envejecimiento del organismo cuando se produce su acumulación al no poder ser eliminadas por el sistema inmunitario eficientemente.

Por tanto, el objetivo fundamental de esta Tesis Doctoral es la identificación de moléculas naturales (nutracéuticos) capaces de mejorar la actividad enzimática de *TERT* o de producir la lisis de células senescentes. Para ello hemos combinado la potencia de las técnicas de cribado; *in silico* e *in vivo*.

Por un lado, el escrutinio virtual *in silico* constituye una herramienta rápida y barata que nos permite procesar grandes bibliotecas de compuestos. Por otro lado, las larvas de pez cebra constituyen un modelo vertebrado que permite el cribado *in vivo* de grandes cantidades de compuestos en el contexto de un animal completo.

Es importante destacar que la fisiología y la respuesta química se conservan en su mayor parte entre el pez cebra y los mamíferos.

En este trabajo de investigación se han aunado dos campos de conocimiento (Química computacional y Biología de sistemas) para la identificación de moléculas rejuvenecedoras y ha abierto nuevas líneas de investigación donde se deberán caracterizar los mecanismos moleculares implicados en los efectos fisiológicos observados.

III. OBJETIVOS

III - OBJETIVOS

The specific objectives of the present work are:

1. Development of zebrafish models of premature aging for anti-aging drug screening.
2. Validation of the models by using two reference anti-aging compounds: resveratrol (antioxidant) and navitoclax (senolytic).
3. Discovery of new drugs with anti-aging potential by using virtual screening (VS) techniques.
4. *In vivo* validation of candidates with anti-aging potential in different aging zebrafish models for repurposing.

IV. MATERIALS AND METHODS

IV - Materials and methods:

IV.1 Maintenance of zebrafish.

Wild-type AB zebrafish (*Danio rerio*) were obtained from the Zebrafish International Resource Center and mated, staged, raised, and processed using standard procedures. Briefly, adult fish were maintained in recirculating tanks at 26°C, with a 14:10 hour light:dark cycle and were fed twice daily, once with dry flake food (PRODAC) and once with live artemia (MC 450, INVEAQUACULTURE). Zebrafish embryos were maintained in egg water at 28.5°C and were fed at 5 days with NOVOTOM and with live artemia at 11 days of life (DOI:dx.doi.org/10.17504/protocols.io.mrjc54n) (Widrick et al., 2018).

The *tert* mutant line (allele hu3430) was obtained from the Sanger Institute and has been previously described (Anchelin et al., 2013; Henriques et al., 2013).

The *spint1a*-deficient line was kindly provided by (Carney et al., 2007). The transgenic zebrafish lines Tg(*lyz:dsRED2*)^{nz50,5} (Hall et al., 2007) and Tg(*mpeg1:EGFP*)^{gl22} (Ellett et al., 2011) have been described previously. The mutant zebrafish line *spint1a*^{hi2217} (Carney et al., 2007) was isolated from an insertional mutagenesis screen.

The performed experiments comply with the Guidelines of the European Union Council (Directive 2010/63/EU) and the Spanish RD 53/2013. The animal study protocol was approved by the Institutional Ethics Committee of the University Hospital “Virgen de la Arrixaca” (protocol code A13211202) and by Albert Einstein College of Medicine Institutional Animal Care and Use Committees (IACUC) (protocol code 00001166).

IV.2 Gene expression analysis.

Total RNA was extracted from larvae 3 or 16 dpf larvae with TRIzol reagent (Thermo Fisher Scientific, Waltham, MA, USA) using a Direct-zol RNA Miniprep kit (Zymo Research) following the manufacturer's instructions. RNA was treated with DNase I, RNase free (Qiagen) on the column. SuperScript™ VILO™ cDNA Synthesis Kit (Invitrogen, Waltham, MA, USA) was used to synthesize first-strand cDNA following the manufacturer's instructions. Real-time PCR was performed with a StepOnePlus instrument (Applied Biosystems) using SYBR® Premix Ex Taq™ (Perfect Real Time) (Takara). Reaction mixtures were incubated for 30 seconds (sec) at 95°C, followed by 40 cycles of 5 sec at 95°C, 20 sec at 60°C, and finally a melting curve protocol. Ribosomal protein S11 (*rps11*) was used for normalization of zebrafish mRNA expression (**Table I**), respectively, using the comparative Ct method ($2^{-\Delta\Delta Ct}$). In all cases, each PCR was performed with triplicate samples and repeated, at least, with two independent samples.

Table I: Primers used for gene expression.

<i>zf TERT-F</i>	5'- CGGTATGACGGCCTATCACT - 3'
<i>zf TERT-R</i>	5'- TAAACGGCCTCCACAGAGTT - 3'
<i>zf p53-F</i>	5'- GATGGTGAAGGACGAAGGAA - 3'
<i>zf p53-R</i>	5'- AAATGACCCCTGTGACAAGC - 3'
<i>zf p21-F</i>	5'- AACGCTGCTACGAGACGAAT - 3'
<i>zf p21-R</i>	5'- CGCAAACAGACCAACATCAC - 3'
<i>zfrps11-F</i>	5'- ACAGAAATGCCCCTTCACTG - 3'
<i>zf rps11-R</i>	5'- GCCTCTTCTCAAACGGTTG - 3'
<i>zf il1β-F</i>	5'- GCCTGTGTGTTTGGGAATCT-3'
<i>zf il1β-R</i>	5'- TGATAAACCAACCGGGACA-3'
<i>zf tnfa-F</i>	5'- GCGCTTTTCTGAATCCTACG-3'
<i>zf tnfa-R</i>	5'-TGCCCAGTCTGTCTCCTTCT-3'
<i>zf cxcl8b.1-F</i>	5'-GCTGGATCACACTGCAGAAA-3'

<i>zf cxcl8b.1-R</i>	5'-TGCTGCAAACCTTTTCCTTGA-3'
<i>zf bcl2-F</i>	5'- TGTTACGGGATGCTGGAGAT-3'
<i>zf bcl2-R</i>	5'- GTCCCACCAAACCTCGAAGAA-3'

IV.3 Telomerase activity assay.

A real-time quantitative TRAP (Q-TRAP) analysis was performed (Anchelin et al., 2011; Herbert et al., 2006). Briefly, a total of 20 zebrafish larvae were mechanically homogenized and proteins were extracted using ice-cold CHAPS Lysis buffer. Real-time Q-TRAP was performed with 0.1 and 1 µg protein extracts. For making the standard curve, a 1:10 dilution series of a telomerase-positive sample (HeLa cells) was used. Control samples were obtained by treating the zebrafish extracts with 1 µg RNase at 37 °C for 20 min. Data were collected and converted into Relative Telomerase Activity units performing the calculation: RTA of sample = $10^{(Ct \text{ sample} - \Delta \text{int}) / \text{slope}}$. The standard curve obtained was $y = -3.2295x + 23.802$.

IV.4 Telomeric length measurement.

gDNA from both kinds of samples was obtained using Wizard Genomic DNA Purification Kit (Promega, Madison, WI, USA) following the manufacturer's instructions. Telomere length was measured by qPCR following the protocol described by Lau (Lau et al., 2013), using the primers described in the Table II. and 40 ng of gDNA as template. Real-time PCR was performed with an ABI PRISM 7700 instrument (Applied Biosystems) using TB Green PCR Core Reagents (Applied Biosystems). Reaction mixtures were incubated for 15 min at 95°C, followed by 40 cycles of 15 s at 95°C, 2 min at 54°C, and finally, 15 s at 95°C, 1 min at 60°C, and 15 s at 95°C. For each DNA genomic, gene expression was corrected by the rRNA11S content in each sample (Table II). Using the comparative Ct method ($2^{-\Delta\Delta Ct}$). In all cases, each PCR was performed with triplicate samples.

Table II: Primers used for telomeric length.

<i>telom F</i>	5'-GGTTTTTGAGGGTGAGGGTGAGGGTGAGGGTGAGGGT-3'
<i>telom R</i>	5'-TCCCGAACTATCCCTATCCCTATCCCTATCCCTATCCCTA-3'
<i>rps11 F</i>	5'-ACAGAAATGCCCTTCACTG-3'
<i>rps 11 R</i>	5'-GCCTCTTCTCAAGGTG-3'

IV.5 Senescence-associated β -galactosidase (SA β -gal) activity assay.

The measurement of the senescence-associated with β -galactosidase (SA β -gal) activity is recognized as a standard procedure for detecting cellular senescence (Dimri et al., 1995). At 24 hpf, larvae were treated with 1-phenyl 2-thiourea (PTU) (3.8 μ M) added to avoid the formation of melanocytes. After 4 days, the larvae were fixed in 4% paraformaldehyde (PFA) at 4 °C overnight with stirring, then washed 3 times with PBS (pH 7.4) and a fourth wash with PBS (pH 6.0) at 4 °C. Staining was carried out overnight at 37 °C with the corresponding staining solution (40 mM phosphate/citrate buffer (pH 6.0), 150 mM NaCl, 5 mM potassium ferrocyanide, 5 mM potassium ferricyanide, MgCl₂ 2 mM, and 1 mg/ ml X-gal in DMSO), with stirring. After staining, the larvae were transferred to a Petri dish with PBS (pH 7.0) and imaged using a Leica M150C magnifying glass equipped with a digital camera (DMC 5400, Leica). The quantification of SA- β -gal activity staining was performed with *ImageJ* software by calculating the percentage of a blue area at the indicated a common region of interest (ROI).

IV.6 Measurement the oxidative stress levels (H₂O₂ analysis).

H₂O₂ release was quantified using the live cell fluorogenic substrate acetyl-pentafluorobenzene sulfonyl fluorescein (Cayman Chemical) (Candel et al., 2014; de Oliveira et al., 2015). About 72 hpf embryos were collected in a 96-well plate with 50 μ M of the substrate in 1% DMSO for 1 hr. *ImageJ* software was used to determine the mean intensity fluorescence of a region of interest (ROI) placed in the dorsal fin for quantification of H₂O₂ production.

IV.7 Acridine Orange (AO) Staining Assay.

gDNA from both kinds of samples was obtained using Wizard Genomic DNA Purification Kit (Promega, Madison, WI, USA) following the manufacturer's instructions. It was performed by staining Acridine Orange, preparation the Acridine Orange (Sigma A6014) is prepared at 1 mg/mL (100X) in milliQ water and stored at -20°C (light protected). Zebrafish larvae at 3 dpf were incubated in E3 medium with Acridine Orange 1X for 30 min at room temperature (RT). The staining was stopped by washing 3 times for 10 min. After staining, zebrafish larvae with tricaine (200 mg/ml) or an equivalent anaesthetic (1X) and visualize dead cells. Imaging was performed with a fluorescence magnifying glass, Leica M205 FA equipped with a digital camera Leica DFC 365 FX with a green, fluorescent filter.

IV.8 Imaging of zebrafish larvae.

Live imaging of 3 or 16 dpf larvae was obtained employing buffered tricaine (200 mg/mL) dissolved in egg water. Images of 3 dpf larvae were captured with a fluorescence magnifying glass (Leica M205 FCA) equipped with a digital camera (Leica DFC 365 FX) and set up with green and red fluorescent filters. The images were analyzed to quantify the number of neutrophils, their distribution in the larvae, the number of macrophages, and the keratinocyte aggregates in a common region of interest (ROI) indicated in each figure. For 16 dpf larvae, images were taken by using a Nikon CSU-W1 spinning disk confocal and analysed with *Imaris* software (version 9.7.2).

IV.9 Survival curves.

A total of 30 zebrafish larvae with different genotypes treated with senolytics or flavonoids were monitored every 24 h over 18 days for clinical signs of disease and mortality under the magnifying glass Leica M150C equipped with a digital camera (DMC 5400, Leica). 20 larvae per condition were plated in 6-well plates, making triplicates of each condition.

IV.10 Molecule File.

Pymol software, 2.3.4. version, was used as a ligand resource, (RCSB PDB, PDB:4hda; 3sxx; 4lvt, resource). For ligand conversion, MOE software, extension .mol2, and Autodock Tools software, extension .pdbqt, were used.

IV.11 Ligand database.

Drugbank database, extensions .pdbqt and .mol2, where 15000 entries (DB), including 2,700 approved small molecule drugs, 1,500 approved biologics (proteins, peptides, vaccines, and allergens), 132 nutraceuticals, and over 6,700 experimental (discovery-phase) drugs can be found, was used as the main resource of main resource of ligands.

IV.12 Virtual Screening.

AutoDock, *AutoDock Vina*, *LeadFinder* software was used for docking calculations.

IV.13 Ligand-Based Virtual Screening.

Pharmacophore models development and candidate screening were performed using *Ligand Scout 4.4*. software.

IV.14 Toxicity assay.

The test doses of all the chosen compounds were determined in wt larvae and observed during the first 72 hours for both morphology and physiology of the larvae. It was decided to test first the 10 μ M dose because it is the standar concentration used in the high-throughput screening.

IV.15 Chemical treatment.

The senolytics were re-suspended in 1mM DMSO, the treatment was added zebrafish models wt, ST2 and *spint 1a* $-/-$; $+/+$, larvae were maintained for 3 days with the different treatments: ABT-263 (10 μ M + 1% DMSO), dasatinib (0.1 μ M + .1 % DMSO) or vehicle alone (1% DMSO), the antioxidants using a (10 μ M + 1% DMSO), the genistein (5 μ M + 1% DMSO). The chemotherapy doses (indicated in

each figure) were established according to developmental criteria. The water was renewed daily throughout the experiment period, in all the trials the treatment was added at 1 dpf.

IV.16 Diet Preparation and Feeding of Zebrafish Larvae.

Prior to any experimental procedure, the larvae were fasted for 24 h. At 3 dpf, the larvae were pre-selected for *mpeg1:EGFP* (green macrophages), and *lyz:dsRED2* (red neutrophils), using a fluorescence magnifier (Leica M205 FCA) equipped with a digital camera (Leica DFC 365 FX), and green and red fluorescence filters. Normal and high cholesterol diets (ND and HCD, respectively) were prepared as described previously (Michael et al., 2021), using Golden Pearl Diet 5–50 nm — Active Spheres. At 5 dpf, zebrafish larvae were separated in different tanks and maintained in the system. They were kept in medium size tanks with a density of 80 larvae per tank and fed for 8 days with ND or HCD (4 mg per day). At 13 dpf, the larvae were separated into small breeding boxes (20–30 larvae) and treated with vehicle (0.1% DMSO) or navitoclax (10 μ M in 0.1% DMSO) for 3 days or apigenin (10 μ M in 0.1% DMSO), naringenin (10 μ M in 0.1% DMSO) and sakuranetin (10 μ M in 0.1% DMSO) for 3 days with daily water renewal and fed with ND or HCD (2.5 mg per day).

IV.17 Statistical analysis.

Statistical analysis was performed by using *GraphPad Prism 8*. The differences between the two samples were analyzed by parametric or non-parametric test. Data with more than two samples were analyzed by analysis of variance (ANOVA) or mixed-effect analysis (see Figure legends for further details).

V. RESULTS

V – Results

V.1 *In vivo* models of premature aging in zebrafish.

V.1.1 Shortened telomere-induced premature aging, the ST2 model.

We generated a new zebrafish model to study aging and rejuvenation at the larvae stage from the Tert-deficient model (*tert*^{-/-}) and corresponding to the 2nd generation of Tert-deficient zebrafish (Fig. 19A-B). By 48 hours post fertilization (hpf), most of the larvae showed a wild-type phenotype (94.9%), while the rest presented a mild (0.85%) or severe phenotype (4.24%) (Fig. 19C).

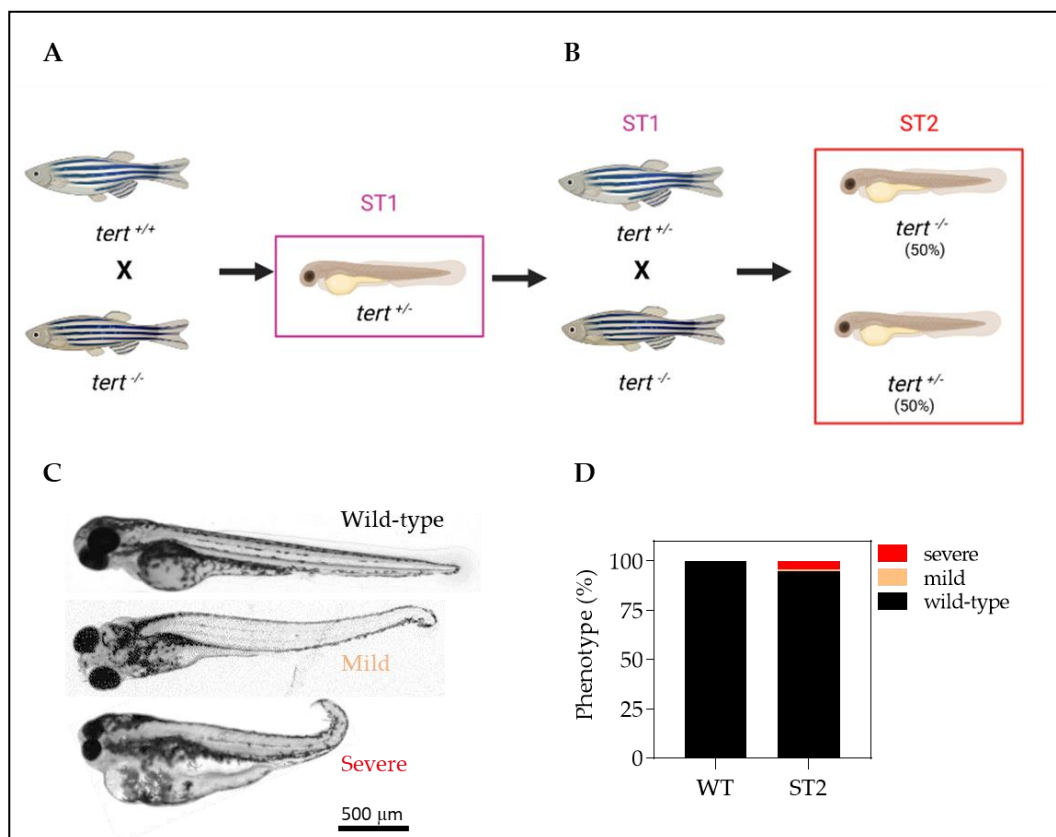


Figure 19. Workflow for the generation of the ST2 model and phenotype. A) Generation of telomerase-haplodeficient fish (*tert* +/-, ST1) by crossing wild-type fish (*wt*, *tert* +/+) with telomerase-deficient fish (*tert* -/-). **B)** The ST2 model was generated by crossing ST1 with *tert* -/- fish. The spawn was made up of 50% *tert* +/- and 50% *tert* -/- fish. **C)** Representative images and **D)** Classification of 48 hpf larvae according to phenotype. In D, differences are not statistically significant according to Two-way ANOVA followed by Sidak's multiple comparison test. Scale bar: 500 μ M.

From the telomeric point of view (**Fig. 20**), at 3 days post fertilization (dpf) this new model presented a significant reduction of *tert* mRNA level (**Fig. 20A**). Consequently, telomerase activity was also significantly reduced (**Fig. 20B**), and this translated into a significant telomere shortening (**Fig. 20C**), for which we have called the new model as ST2 (Short Telomere, 2nd generation).

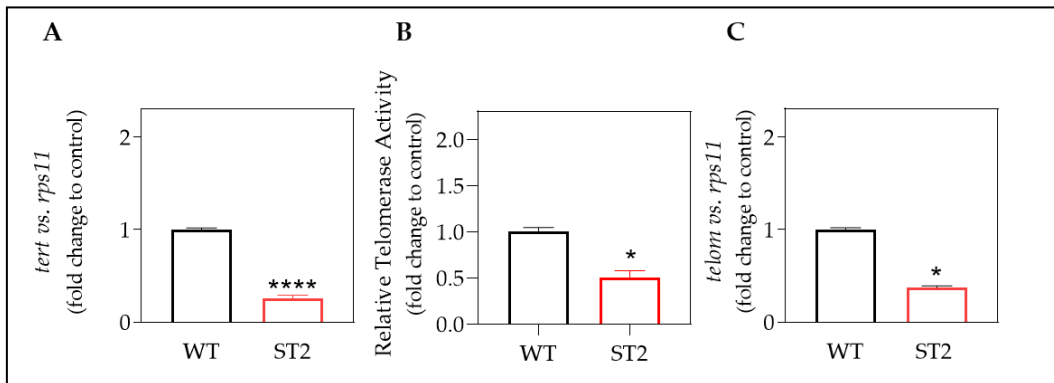


Figure 20. Telomeric characterization of the ST2 model. **A)** The mRNA level of *tert* was determined by real-time RT-qPCR and normalized against *rps11* in 3 dpf zebrafish larvae. The graph shows the mean \pm SEM of 20 pooled larvae (n=20) and triplicate samples from 2 independent experiments (N=2). **B)** Telomerase activity was measured quantitatively in 3 dpf zebrafish larvae by Q-TRAP (relativized to telomerase-positive cells) using 0.1 μ g of protein extract. Results are expressed as the mean \pm SEM of 25 pooled larvae (n=25) and triplicate samples from 2 independent experiments (N=2). **C)** The telomere length was measured in 3 dpf zebrafish larvae by qPCR using 16 ng of gDNA and determined as the telomere content relative to the single copy gene *rps11*. The graph shows the mean \pm SEM of 25 pooled larvae (n=25) and triplicate samples from 2 independent experiments (N=2). ns, non-significant; * $p < 0.05$; *** $p < 0.0001$, according to Mann-Whitney test.

Next, as telomere attrition leads cellular senescence, and cellular senescence can trigger premature aging, we determined the level of cellular senescence in the ST2 model by measuring the senescence-associated β -galactosidase (SA β -gal) biomarker in 3 dpf larvae. The whole larvae β -gal staining revealed a high level of cellular senescence compared to control (**Fig. 21**).

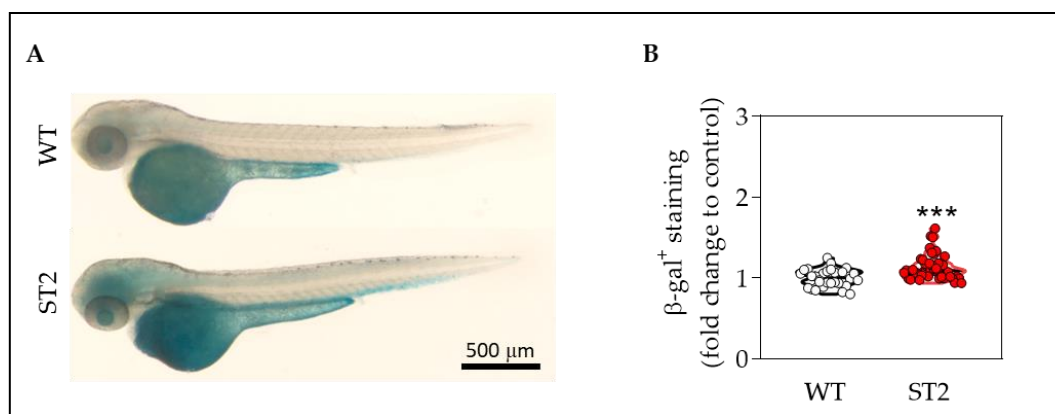


Figure 21. The ST2 larvae show increased cellular senescence. A) Representative images of b-gal staining of 3 dpf WT and ST2 larvae where b-gal⁺ cells are stained in blue. **B)** Quantification of the cellular senescence levels. The violin plots with the median shown as a horizontal line show the distribution of b-gal⁺ cells. The graph shows the accumulation of 3 independent experiments (N= 3). *** $p < 0.01$, according to unpaired t-test with Welch's correction. b-gal: b-galactosidase. Scale bar: 500 μm .

The increase in senescence also affects the mitochondria, which was reflected as an increase in the production of reactive oxygen species (ROS) in the ST2 model (Fig. 22).

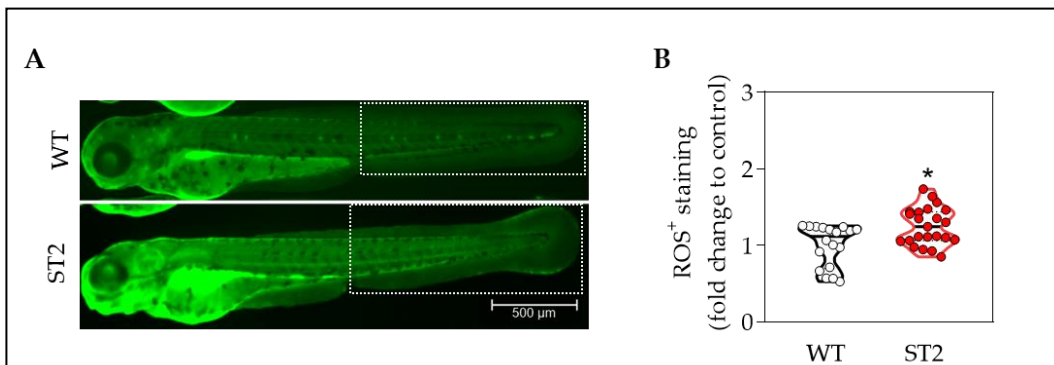


Figure 22. The ST2 larvae show increased oxidative stress levels. A) Representative images of ROS staining of 3 dpf WT and ST2 larvae, where ROS⁺ cells are stained in green. The discontinuous white square represents the ROI for quantification. **B)** Quantification of the cellular oxidative stress levels. The violin plots with the median shown as a horizontal line show the distribution of ROS⁺ cells. The graph shows the accumulation of 2 independent experiments (N= 2). *** $p < 0.001$, according to unpaired t-test with Welch's correction. ROS: reactive oxygen species. ROI: region of interest. Scale bar: 500 μm .

On the other hand, as both critically short telomeres and the increase in ROS induce apoptosis, we evaluated the cell death level in the ST2 model by performing an acridine orange (AO) assay, and we found an increased DNA fragmentation level in the ST2 larvae compared to control (Fig. 23B). We also checked the gene

expression profile of the pro-apoptotic genes *p53* and *p21*, and the anti-apoptotic gene *bcl-2*. In our ST2 model, the expression of both *p53* and *p21* was induced, while the expression of *bcl-2* was inhibited compared to control, supporting the previous results (Fig. 23C).

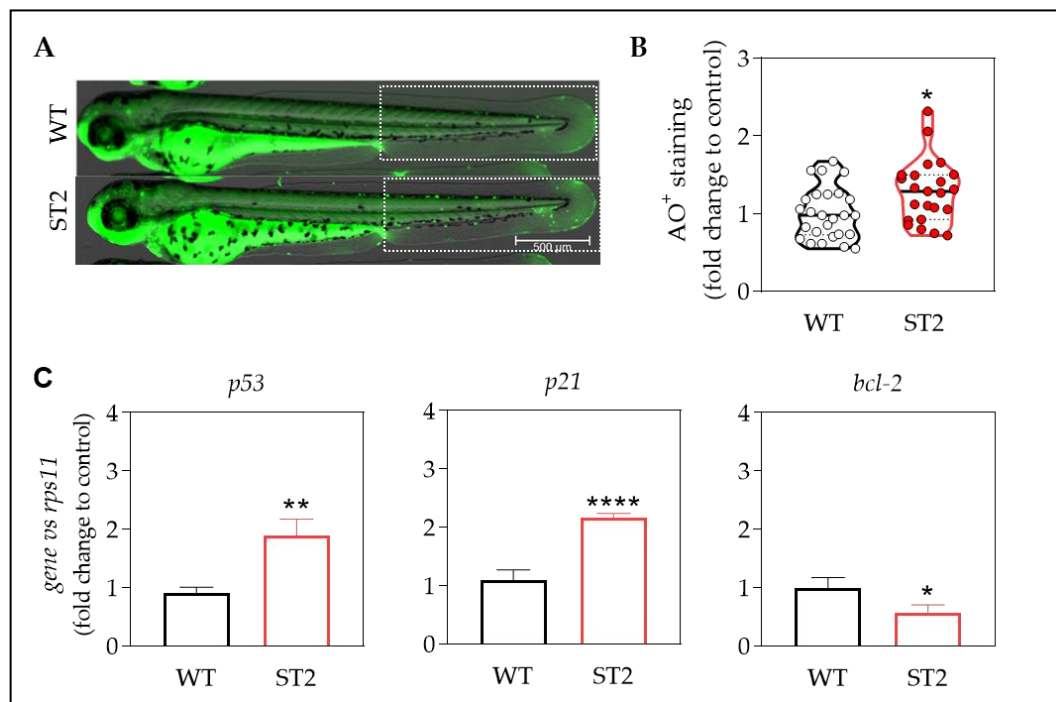


Figure 23. The ST2 larvae show increased cell death levels. **A)** Representative images of AO staining of 3 dpf WT and ST2 larvae, where AO⁺ cells are stained in green. The discontinuous white square represents the ROI for quantification. **B)** Quantification of the DNA fragmentation levels. The violin plots with the median shown as a horizontal line show the distribution of AO⁺ cells and are overlaid with the raw data, where each dot represents an individual. **C)** The mRNA levels of apoptosis-related genes were determined by real-time RT-qPCR and normalized against *rps11* in 3 dpf zebrafish larvae. The bars show the mean \pm SEM of 20 pooled larvae (n=20) and triplicate samples from 2 independent experiments (N=2). * $p < 0.05$; ** $p < 0.01$; **** $p < 0.0001$, according to unpaired t-test with Welch's correction (B-C). AO: acridine orange. ROI: region of interest. Scale bar: 500 μm .

Finally, although spawning viability was good and the larvae did not present any striking phenotype (**Fig. 19C**), the overall survival of the ST2 larvae was drastically compromised compared with the wild-type (wt) control. The ST2 larvae died prematurely during the second week of life, being unable to exceed the larval stage (**Fig. 24**).

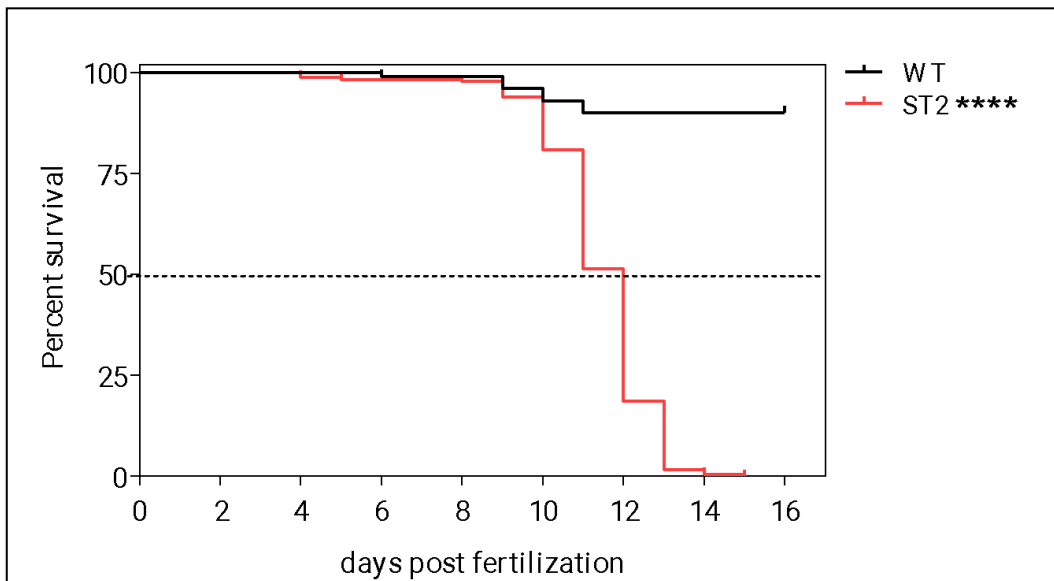


Figure 24. The ST2 larvae show premature death. Kaplan-Meier representation of the survival of WT ($n=101$) and ST2 larvae ($n=183$). The discontinuous line represents the half-life. The graph shows the accumulation of 5 independent experiments ($N=5$). **** $p<0.0001$, according to Log Rank test.

Altogether, these results validate the ST2 model as an excellent model of premature aging in larvae. This new model will be very useful for the rapid evaluation of the anti-aging effect of molecules through drug screening by using as read out, for instance, the survival or the telomere length.

V.2 Premature aging induces by DNA damage caused by chemotherapy, the QiDD model.

We have generated chemotherapy-induced DNA damage-induced premature aging, the QiDD model, by treating wild-type zebrafish larvae with the chemotherapeutic agents used for the treatment of acute lymphoid leukemia (ALL) (Fig. 25).

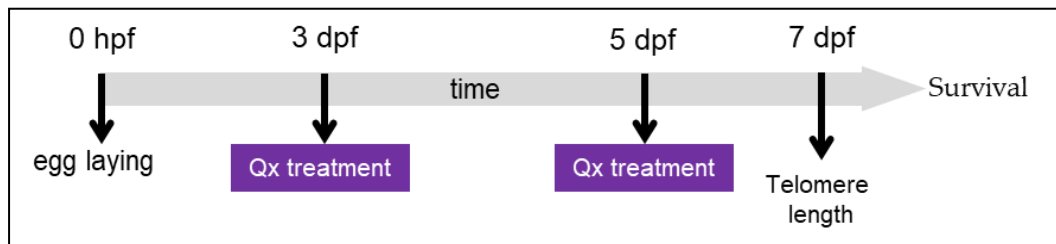


Figure 25: General workflow for the generation of the QiDD model. Zebrafish larvae were treated with chemotherapeutic drugs at 3 dpf and 5 dpf for telomere length and survival study. Qx: chemotherapy.

As suspected, two cycles of treatment with cytarabine, daunoblastina, dexamethasone, methotrexate, and vincristine in and 7-dpf larvae were sufficient to trigger a significant telomere shortening (Fig. 26).

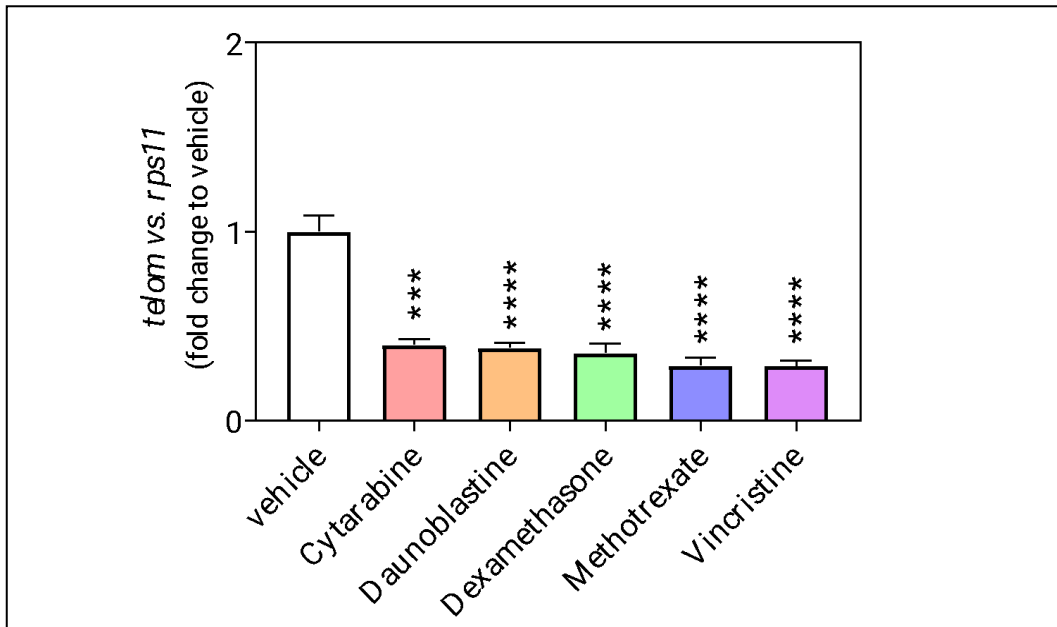


Figure 26. The QiDD larvae show a drastic attrition of telomere length. Telomere length was measured in 7 dpf zebrafish larvae by qPCR using 16 ng of gDNA and determined as the telomere content relative to the single copy gene *rps11*. The graph shows the mean \pm SEM of 25 pooled larvae (n=25) and triplicate samples from 2 independent experiments (N=2). **** $p < 0.0001$, according to Kruskal-wallis/Dunnett's.

This telomere shortening caused a notable reduction in half-life to around 8-9 days in all cases but methotrexate to 15 dpf, and a limited survival (**Fig. 27**).

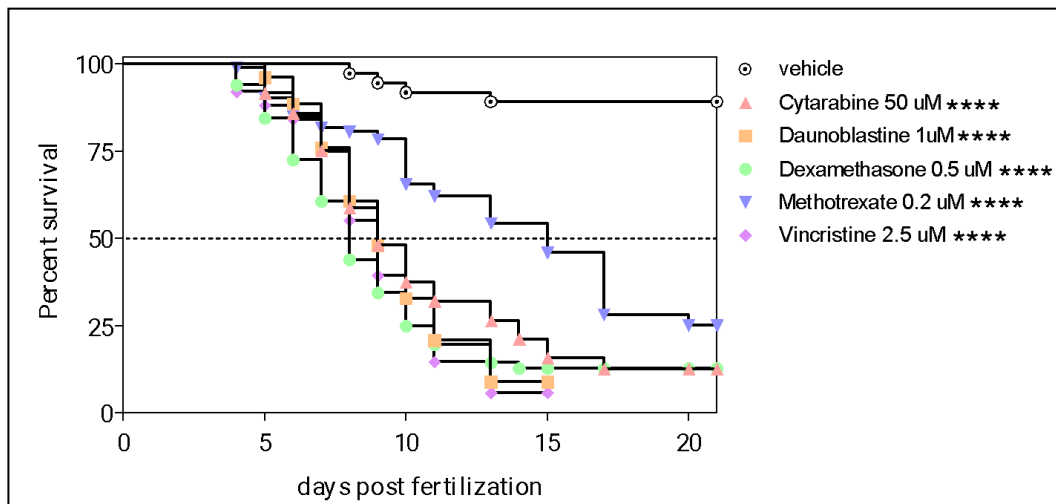


Figure 27. The QiDD larvae show a limited survival. Kaplan-Meier representation of the survival of vehicle ($n=37$), cytarabine ($n=85$), daunoblastina ($n=79$), dexamethasone ($n=84$), methotrexate ($n=93$), and vincristine ($n=76$) treated larvae. The discontinuous line represents the half-life. The graph shows the accumulation of 5 independent experiments. **** $p<0.0001$, according to Log Rank test.

This new model will be very useful for the rapid evaluation of the anti-aging effect of molecules through drug screening by using as read out, for instance, survival or telomere length.

V.3 High-cholesterol diet-induced metainflammation zebrafish model, the HCD model.

We also generated a zebrafish model with metainflammation induced by nutrient excess by feeding wild-type larvae with a high-cholesterol diet (HCD) for 11 days (Fig. 28).



Figure 28: General workflow for the generation of the zebrafish model of metainflammation produced by a 10% cholesterol diet. 5 dpf zebrafish larvae were fed with a high (10%) cholesterol diet for 11 days, for imaging and sampling at 16 dpf.

Fish fed with a HCD developed non-resolving inflammation throughout the larvae (Fig. 29A), with increased neutrophil numbers (assayed in a transgenic line with labelled neutrophils, *lyz:DsRED2*) and macrophage numbers (assayed in a transgenic line with labelled macrophages, *mpeg1; EGFP*) (Fig. 29B, C).

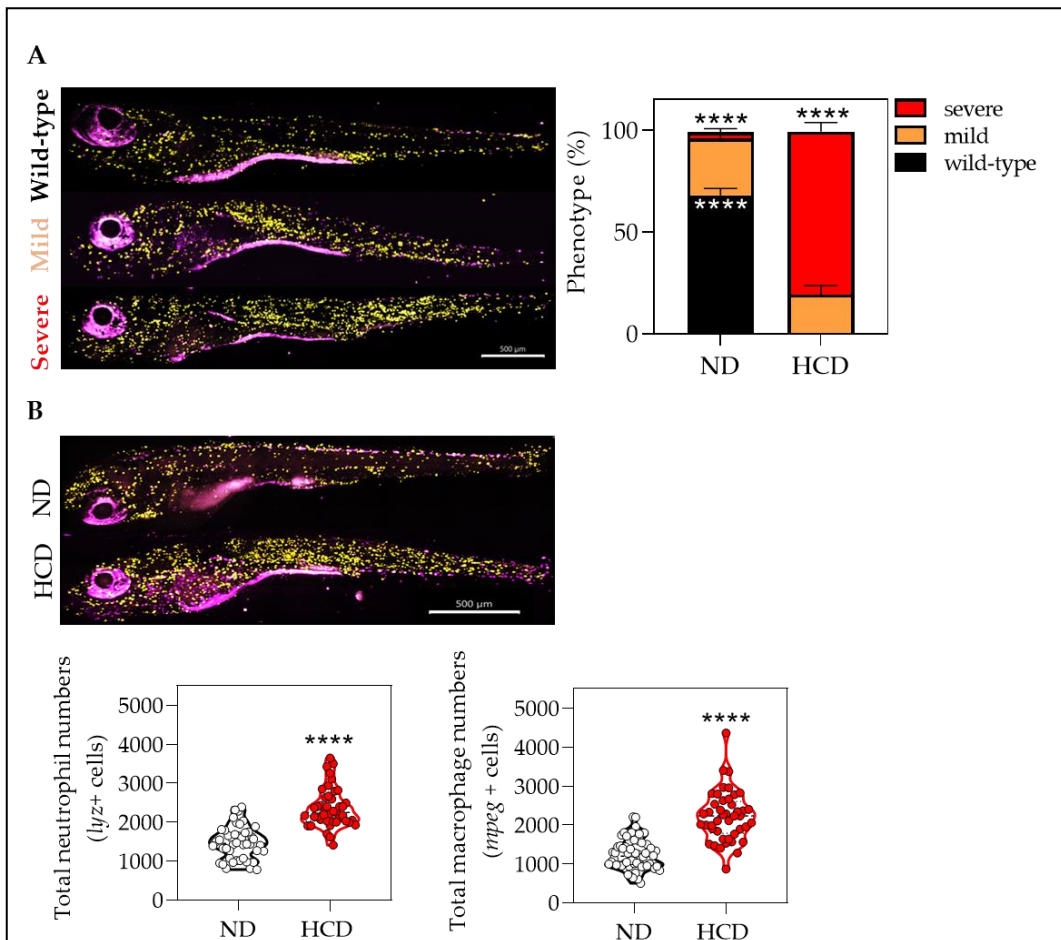


Figure 29. Characterization of the HCD-induced metainflammation zebrafish model. **A)** Representative images and classification of the phenotype of neutrophils (yellow) and macrophages (purple) distribution of 16 dpf (*lyz*: DsRED2; *mpeg1*:EGFP) larvae. **B)** Representative images and quantification of total neutrophils (yellow, *lyz*⁺ cells) and macrophages (purple, *mpeg*⁺ cells). The violin plots with the median shown as a horizontal line show the distribution of the neutrophils and the macrophage cells and are overlaid with the raw data, where each dot represents an individual. The graphs show the accumulation of 3 independent experiments (N= 3). **** $p < 0.0001$, according to Two-way ANOVA followed by Sidak's multiple comparison test (A) and unpaired t test with Welch's correction (B). HCD: high-cholesterol diet. Scale bar: 500 μ m.

Then, we studied the effect of nutrient excess on telomere length, observing that larvae fed with HCD showed mild but not statistically significant telomere shortening compared to larvae fed with a normal diet (ND) (**Fig. 30**).

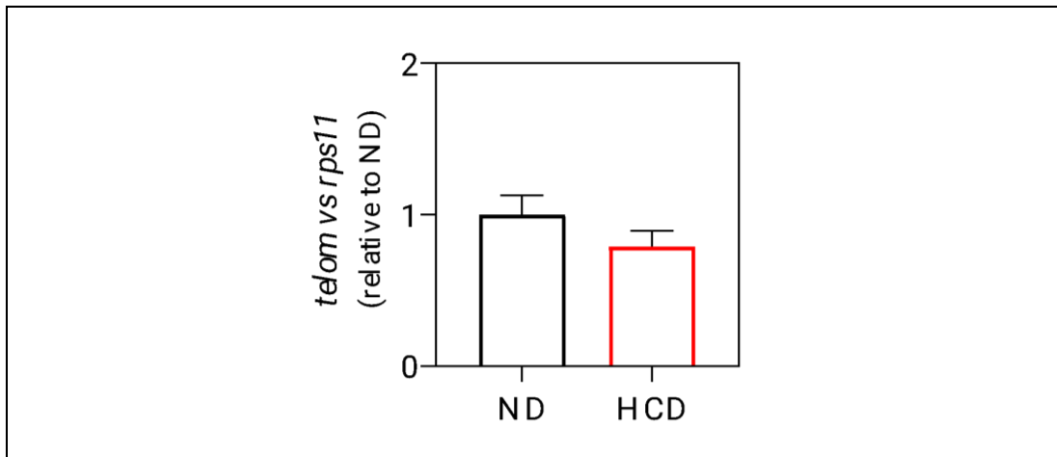


Figure 30. HCD-induced metainflammation larvae do not show telomere shortening. Telomere length was measured in 16 dpf zebrafish larvae by qPCR using 16 ng of gDNA and determined as the telomere content relative to the single copy gene *rps11*. The graph shows the mean \pm SEM of 25 pooled larvae (n=25) and triplicate samples from 3 independent experiments (N=3). Results were non-significant according to unpaired t-test.

This model will be very useful for the rapid evaluation of the anti-inflammatory effect of molecules through drug screening by using as read out, the inflammatory phenotype or the total neutrophil numbers.

V.4 Inflammaging zebrafish model, the *Spint1a*-deficient model.

The *spint1a*-deficient model was previously characterized, showing neutrophil infiltration in the skin, keratinocyte aggregate foci, and epithelial integrity disruption (Carney et al., 2007; Mathias et al., 2007). Although it is well-established that chronic inflammation leads to premature aging, we checked the aging stage in the *spint1a*-deficient model at 3 dpf. First, telomere length was not affected (**Fig. 31A**) and, consequently, the senescence-associated β -galactosidase (SA β -gal) staining revealed development-associated senescence in the head and muscle of both wild type and *spint1a*-deficient larvae, whereas no staining was observed in the skin (**Fig. 31B**).

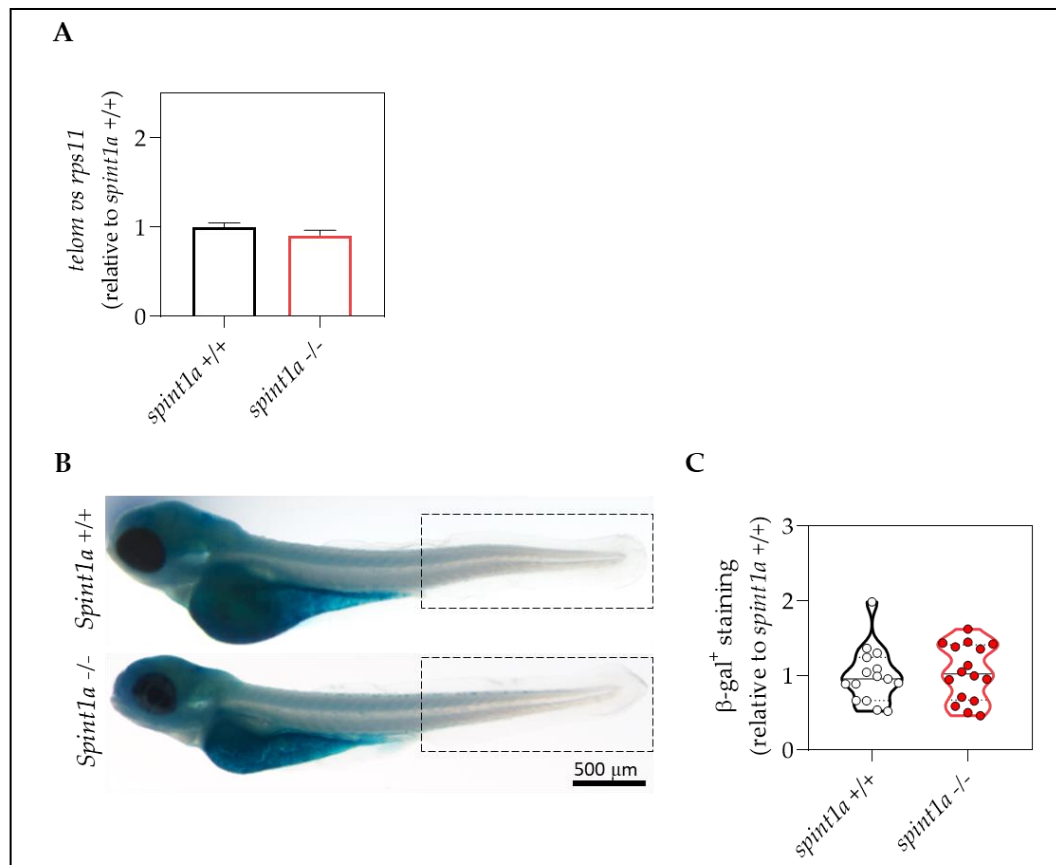


Figure 31. Spint1a-deficient zebrafish larvae do not show premature aging.

A) Telomere length was measured in 3 dpf zebrafish larvae by qPCR using 40 ng of gDNA and determined as the telomere content relative to the single copy gene *rps11*. The graph shows the mean \pm SEM of 25 pooled larvae (n=25) and triplicate samples from 2 independent experiments (N=2). **B)** Representative images of b-gal staining of 3 dpf *spint1a*^{+/+} and *spint1a*^{-/-} larvae, where β -gal⁺ cells are stained in blue. **C)** Quantification of the cellular senescence levels in the Spint1a-deficient larvae by b-gal staining assay. The violin plots with the median shown as a horizontal line show the distribution of b-gal⁺ staining and are overlaid with the raw data, where each dot represents an individual. The graph shows the accumulation of 2 independent experiments (N= 2). Results were non-significant according to unpaired t-test with Welch's correction (A, C). Discontinuous black squares represent the ROI for quantification. β -gal: β -galactosidase. Scale bar: 500 μ m.

Next, we determined the cell death level with an acridine orange (AO) assay, and *spint1a*-deficient larvae showed high levels of cell death in the skin (**Fig. 32**).

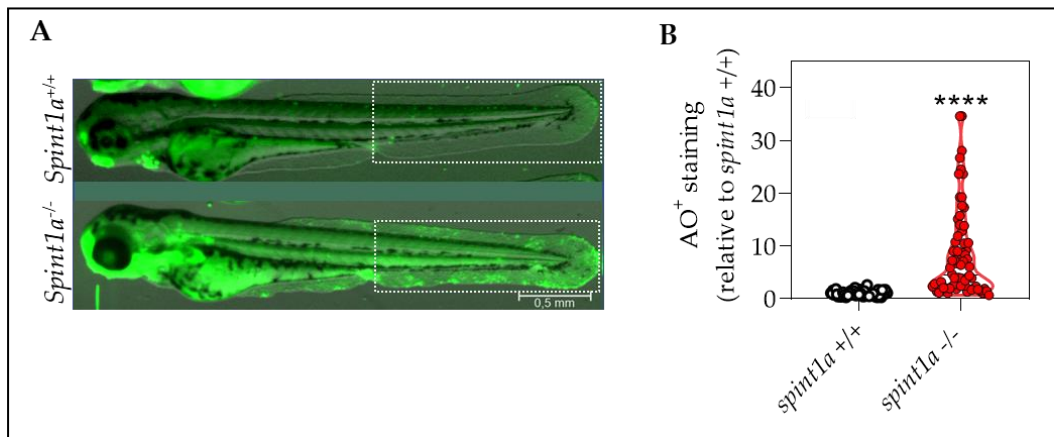


Figure 32. The Spint1a-deficient larvae show increased cell death levels. A) Representative images of AO staining in 3 dpf larvae, where AO⁺ cells are stained in green. Discontinuous white squares represent the ROI for quantification. **B)** Quantification of the DNA fragmentation levels in 3 dpf *spint1a*^{+/+} and *spint1a*^{-/-} larvae. The violin plots with the median shown as a horizontal line show the distribution of AO⁺ cells and are overlaid with the raw data, where each dot represents an individual. The graph shows the accumulation of 3 independent experiments (N= 3). **** $p < 0.0001$, according to unpaired t-test with Welch's correction. AO: acridine orange. ROI: region of interest. Scale bar: 500 μm .

This new model will be very useful for the rapid evaluation of the anti-inflammatory effect of molecules through drug screening by using as read out, neutrophil dispersion or the state of skin.

V.5 Evaluation of the anti-aging potential of resveratrol and navitoclax in the ST2 model. A proof of concept.

Once validated the ST2 model as a good premature aging model, we decided to evaluate the effect of two reference molecules, resveratrol and navitoclax, representing polyphenols and senolytics, respectively (Fig. 33).

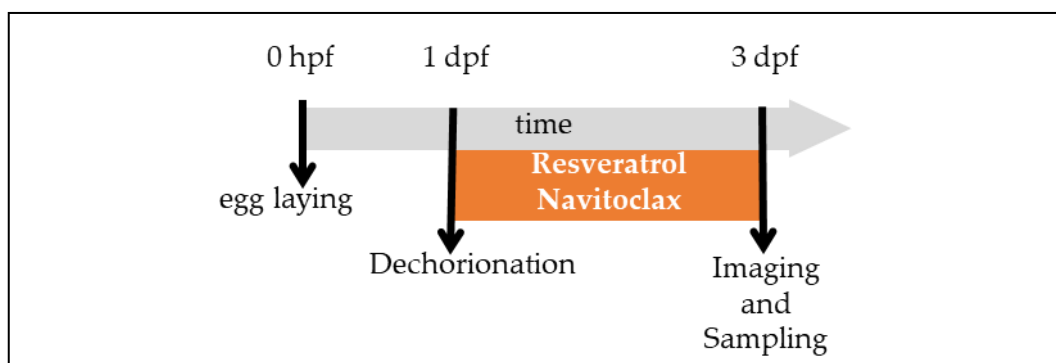


Figure 33: General workflow for the treatment the ST2 zebrafish larvae. Zebrafish larvae were treated with resveratrol and navitoclax at 1 dpf and 2 dpf.

Related to telomeres, the treatment with both resveratrol and navitoclax resulted in an increase of the mRNA level of *tert* (Fig. 34A). However, only resveratrol was able to induce telomerase activity (Fig. 34B) and, consequently, to increase the telomere length (Fig. 34C).

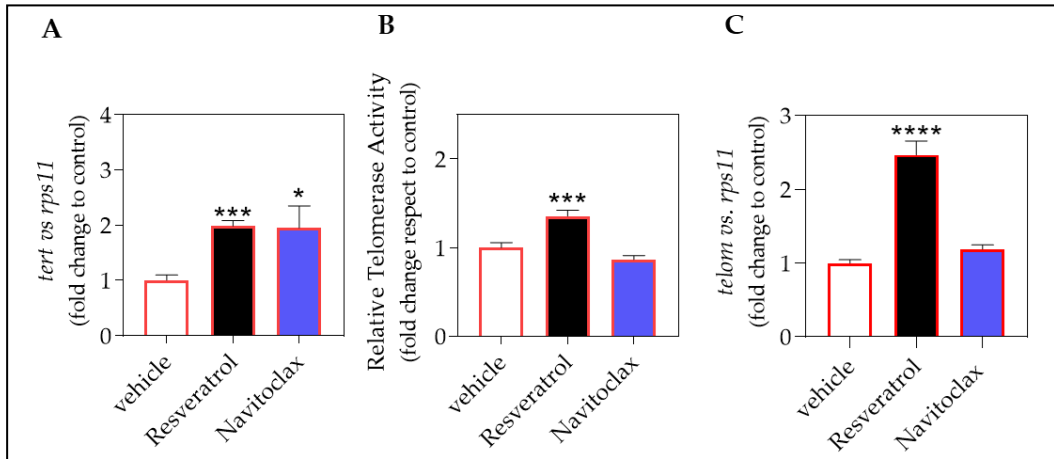


Figure 34. Resveratrol improves telomerase expression, activity, and telomere length in the ST2 model of premature aging. **A)** The mRNA level of *tert* was determined by real-time RT-qPCR and normalized against *rps11* in 3 pdf ST2 larvae treated with resveratrol or navitoclax. **B)** Relative telomerase activity was measured quantitatively in 3 dpf zebrafish larvae treated with resveratrol or navitoclax by Q-TRAP using 0.1 μ g of protein extract. **C)** Telomere length was measured in 3 dpf larvae treated with resveratrol or navitoclax by qPCR using 16 ng of gDNA and determined as the telomere content relative to the single copy gene *rps11*. In **A, B, C)** the graph shows the mean \pm SEM of 25 pooled larvae (n=25) and triplicate samples from 2 independent experiments (N=2). * $p < 0.05$; **** $p < 0.0001$, according to Kruskal-Wallis followed by uncorrected Dunn's multiple comparison test (A, B, C).

Regarding cellular senescence, only navitoclax was able to reduce the senescence-associated β -gal positive area compared to untreated ST2 control (Fig. 35).

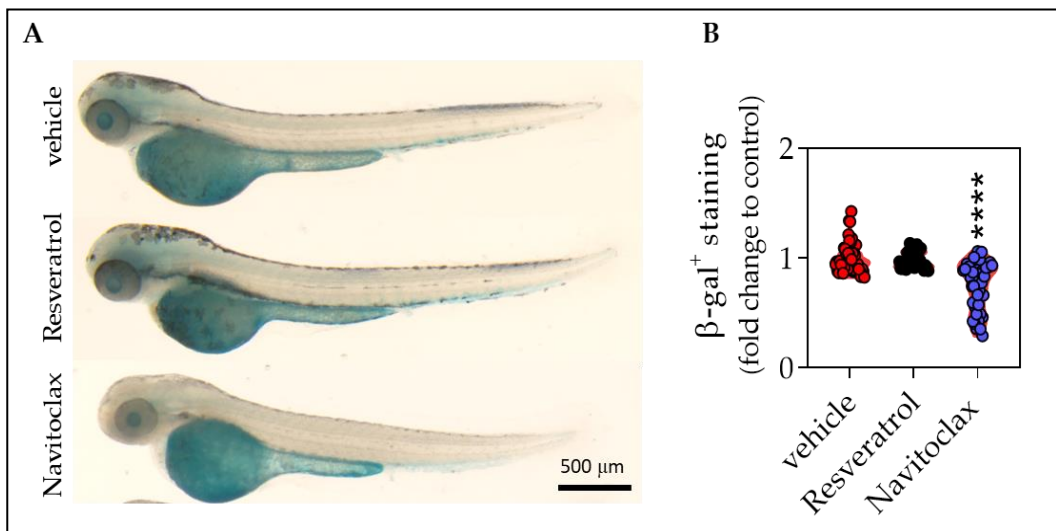


Figure 35. Navitoclax treatment decreases cellular senescence levels in the ST2 model of premature aging. **A)** Representative images of β -gal staining of 3 dpf ST2 larvae after treatment, where β -gal⁺ cells are stained in blue. **B)** Quantification of the cellular senescence levels. The violin plots with the median shown as a horizontal line show the distribution of β -gal⁺ cells. The graph shows the accumulation of 3 independent experiments (N= 3). **** $p < 0.0001$, according to Brown-Forsythe and Welch ANOVA test. B-gal: β -galactosidase. Scale bar: 500 μ m.

The effect of these molecules on telomere length was reflected in cell death levels. While the treatment with resveratrol was able to reduce the DNA fragmentation level significantly, navitoclax did not affect it (**Fig. 36**).

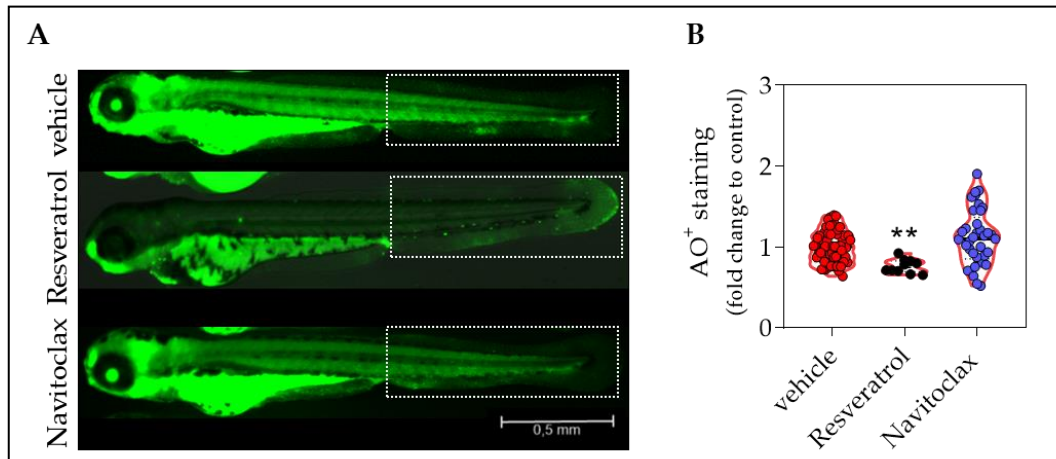


Figure 36. Resveratrol treatment decreases cell death levels in the ST2 model of premature aging. **A)** Representative images of AO staining in 3 dpf ST2 larvae after treatment, where AO⁺ cells are stained in green. The discontinuous white square represents the ROI for quantification. **B)** Quantification of the DNA fragmentation levels in 3 dpf larvae. The violin plots with the median shown as a horizontal line show the distribution of AO⁺ cells and are overlaid with the raw data, where each dot represents an individual. The graph shows the accumulation of 2 independent experiments (N= 2). ** $p < 0.001$, according to Kruskal-Wallis followed by uncorrected Dunn's multiple comparison test. AO: acridine orange. ROI: region of interest. Scale bar: 500 μm .

Finally, we evaluated the effect of resveratrol and navitoclax on the life expectancy of ST2 larvae. The treatment with resveratrol, but not with navitoclax, was able to increase the half-life of ST2 larvae by 12.5%, and survival by 6.25%, (**Fig. 37**).

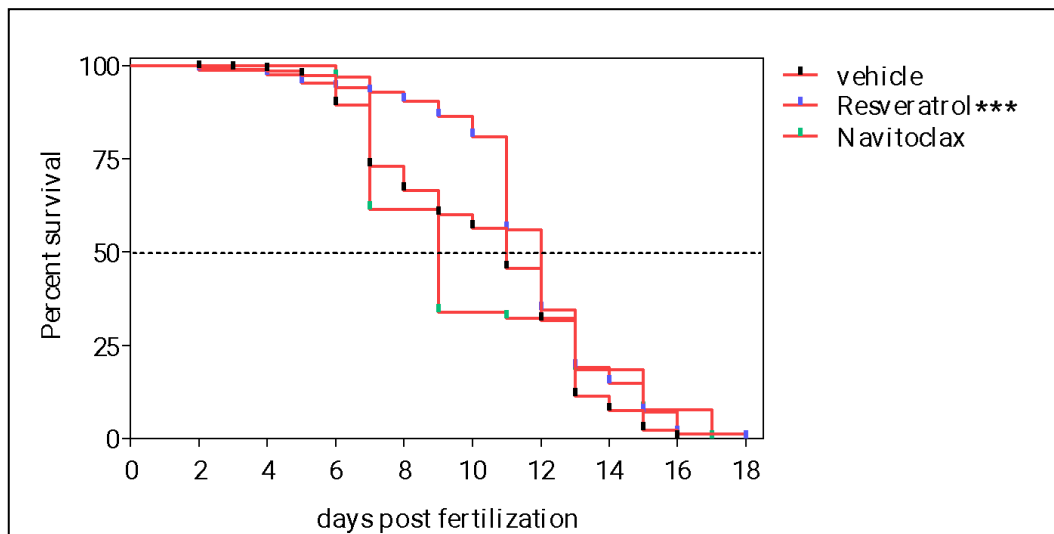


Figure 37. Resveratrol treatment increase the ST2 larvae survival. Kaplan-Meier representation of the survival of vehicle ($n=446$), resveratrol ($n=168$) and navitoclax ($n=65$) ST2 treated larvae. The discontinuous line represents the half-life. The graph shows the accumulation of 5 independent experiments. *** $p < 0.001$, according to Log Rank test.

At this point, due to the good results obtained with resveratrol, we decided to do an *in silico* screening to find new drugs with anti-aging potential for repurposing. And we did the same with navitoclax, although its anti-aging profile was not as evident as resveratrol.

V.6 In silico discovery of new drugs with anti-aging potential.

V.6.1 Natural antioxidants derived from resveratrol.

V.6.1.1 Structure-based virtual screening (SBVS) method: protein-ligand docking.

As one of the main targets of resveratrol is the protein sirtuin-1 SIRT1 (Konrad T. Howitz *et al.*, 2003), different virtual screening calculations were carried out based on their structure by using the protein data bank (*PDB:4hda*). First, we located the interaction sites between resveratrol and SIRT1 and thus knowing all the residues involved in the interaction. With the use of the docking engines *LeadFinder (LF)*, *Autodock 4 (AD)* and *Autodock Vina (AK)*, we checked the reliability in the prediction of the interactions between resveratrol and SIRT1. Next, by using the docking engines *LF*, *AD* and *AK*, and the target SIRT1, we performed the calculations against the Drugbank (DB) compound library, containing more than 10000 compound entries. We obtained a list of compounds for each of the docking engines used. Finally, we cross-checked the three lists of candidates, and we obtained a single list with the 550 compounds that were common.

V.6.1.2 Ligand-based virtual screening (LBVS) method: pharmacophore mapping.

In this case, continuing with resveratrol as a reference (**Fig. 38A**), we carried out an *in silico* approach based on its pharmacophoric properties. First, we obtained a pharmacophore map of resveratrol by using the software *Ligand Scout 4.4*. According to IUPAC, the pharmacophore is the set of structural features in a molecule necessary to ensure the optimal supramolecular interactions responsible for the biological activity of that molecule. The analysis showed 3 pharmacophoric characteristics for resveratrol corresponding to; i) six hydrogens bonds, both electron donors (3) and acceptors (3); ii) two hydrophobic sites and iii) two aromatics rings that correspond with the blue circles (**Fig. 38B, C**).

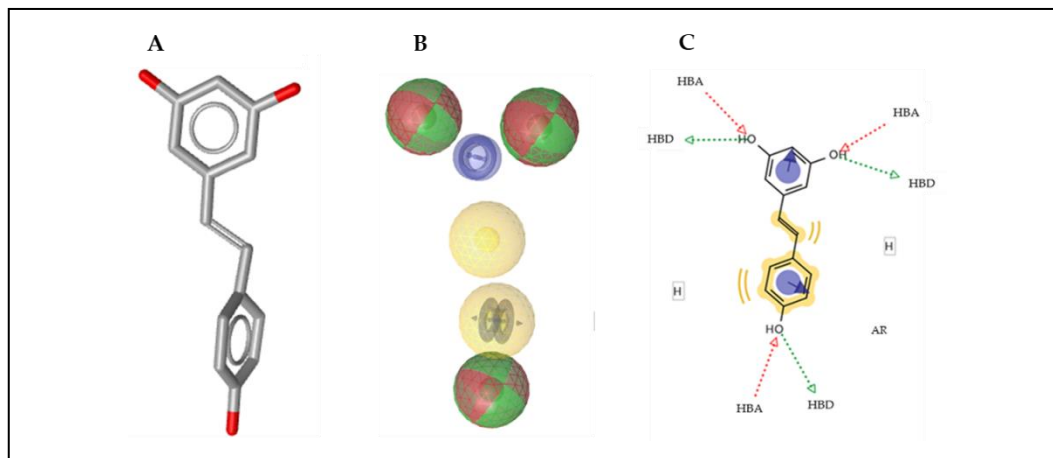


Figure 38. Schematic representation of pharmacophoric features. A) The three-dimensional (3D) structure of resveratrol. B) The pharmacophoric characteristics of resveratrol obtained with the *LigandScout* software. Hydrogen bonds are represented green and red spheres, respectively. Hydrophobic sites are represented by yellow spheres. Aromatic rings are represented by blue circles. C) Pharmacophoric features of resveratrol molecule. *PDB: 4hda*.

Next, we performed the calculations against the more than 10000 compound entries of the DB library, obtaining a list with more than 5000 compounds like resveratrol, both in structure and pharmacophoric characteristics. Then, we classified these compounds by the degree of similarity between structures and pharmacophoric characteristics, being resveratrol with score 1, and the candidates sorted by descending score. We selected a total of 10 compounds (apigenin, naringenin, isoliquiritigenin, quercetin, kaempferol, hesperetin, sakuranetin, tricetin, genestein and liquiritigenin), whose score was in a range of 1-0.70 (**Fig. 39**).

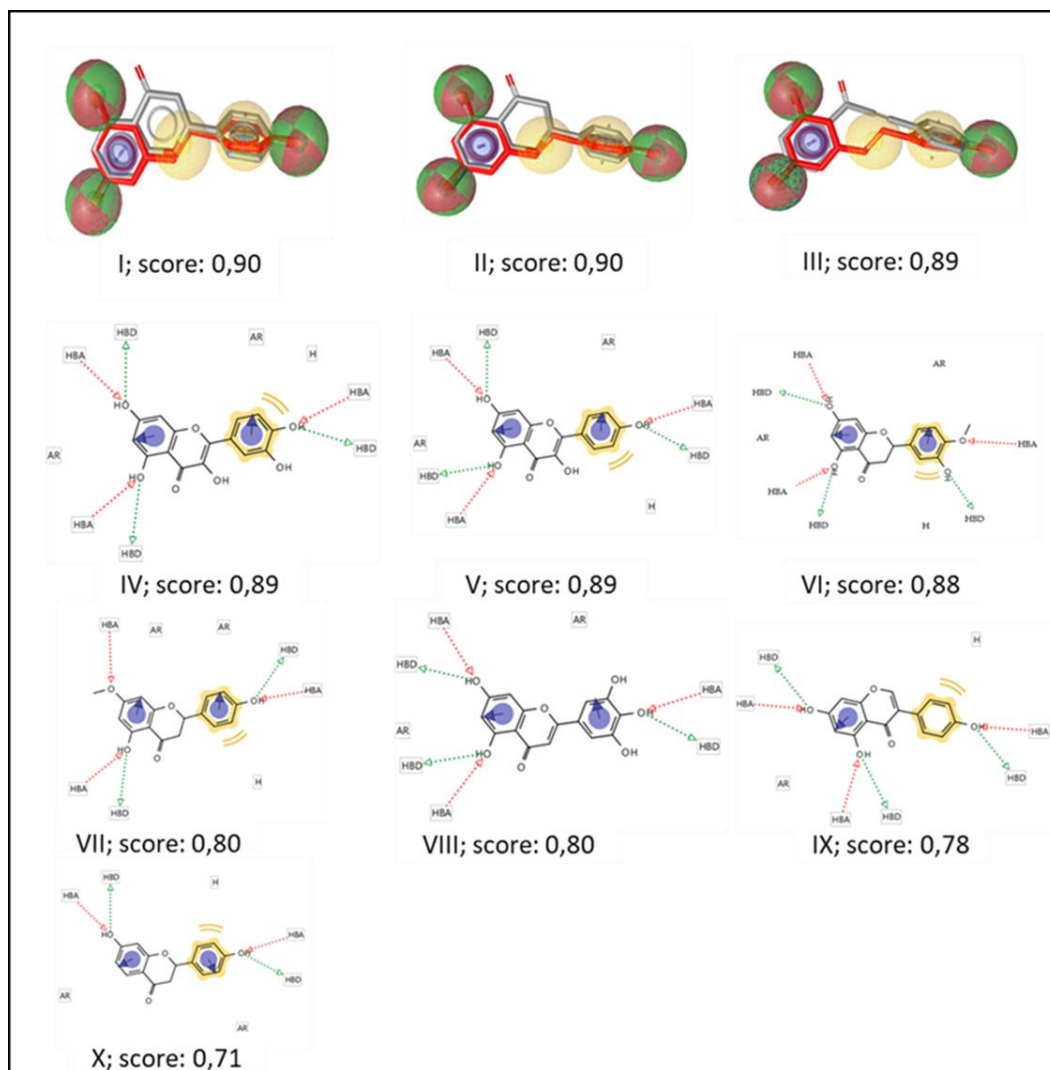


Figure 39. Pharmacophoric method. The structure of resveratrol is shown in red and in gray, the antioxidants selected by the VS method and the pharmacophoric characteristics. The pharmacophoric characteristics: i) hydrogen bonds are represented green and red spheres, respectively. ii) hydrophobic sites are represented by yellow spheres. iii) aromatic rings are represented by blue circles. 3 compounds are shown overlaid with resveratrol, to show their similarity. **I:** Apigenin, **II:** Naringenin, **III:** Isoliquiritigenin, **IV:** Quercetin, **V:** Kaempferol, **VI:** Hesperetin, **VII:** Sakuranetin, **VIII:** Tricetin, **IX:** Genestein, **X:** Liquiritigenin.

A further cross-checked between these 10 compounds and the final list obtained by the protein-ligand docking technique, confirmed their presence. Finally, we repeated the protein-ligand docking approach with the docking engines *LF*, *AD* and *AK*, taking the catalytic subunit of telomerase (TERT) as protein and using protein data bank (*PDB:3du6*), and each of the 10 compounds plus resveratrol as ligand to identify the interaction sites between TERT and the candidates and to highlight the aminoacids responsible for interaction in base of their conservation (**Table III**).

Table III. Interaction between resveratrol-derived candidates and the telomerase catalytic subunit (TERT). The interaction results have been performed with the AD docking. They were also performed with AK and LF docking, obtaining similar results (data not shown for clarity).

Docking	AD	AD	AD	AD	AD	AD	AD	AD	AD
Candidates	Apigenin	Genestein	Hesperetin	Liquiritigenin	Naringenin	Quercetin	Resveratrol	Sakuranetin	Tricetin
414 Arg	X	X	X	X	X	X	X	X	X
419 Leu	X	X	X	X	X	X	X	X	
480 Ala						X			X
592 Arg	X	X	X	X	X	X		X	X
76 Lys		X	X	X	X	X			X
84 Glu	X			X	X		X	X	
483 Met				X			X		
547 Arg									X
593 Lys		X							X
Cluster	3	2	2	1	3	2	3	2	2
Energy	-7,76	-7,73	-8,92	-8,29	-7,69	-9,12	-6,81	-7,59	-7,85

The docking calculations showed the same protein-ligand interaction zone between TERT and apigenin, naringenin and sakuranetin. Tricetin presents almost the same interaction zone as the compounds mentioned above. It is noteworthy that all protein-ligand binding predictions occurred in cluster 1, 2 and 3, which means they are very likely interactions that can occur in the *in vivo* model. Surprisingly, the reference molecule resveratrol does not present a great homology in the binding residues compared to the other compounds, which indicates that the interaction is not very likely to occur. The results obtained with the *AD* docking, also with the *LF* and *AK* docking that have obtained similar results (data not

shown) (**Table III**). We can observe the interaction zone of the telomerase complex with the different polyphenols (**Fig. 40**).

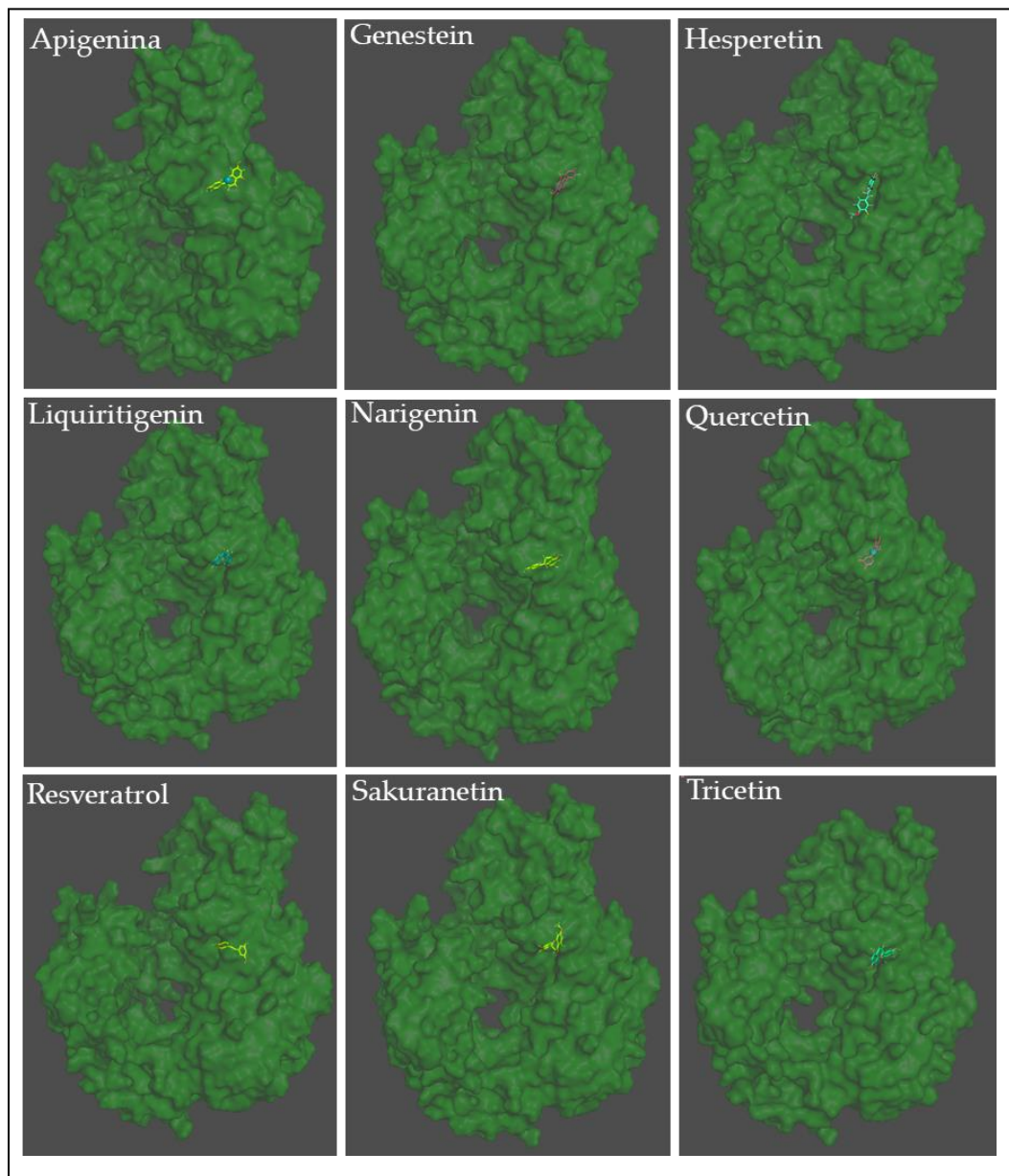


Figure 40. 3D representation of the predicted interaction between resveratrol-derived candidates and the catalytic subunit of telomerase (TERT). TERT is represented in green. Candidates, represented in different colors, are located at the calculated interaction zone by AD docking.

In summary, using the VS approach we have been able to select 10 natural antioxidant compounds with anti-aging potential out of a total of 10000, based on the similarity of both their structure and pharmacophoric properties compared to resveratrol. These compounds would have the ability to bind to TERT, favoring its biological function and, therefore, are candidates for screening in zebrafish aging models.

V.7 Drugs derived from senolytics.

V.7.1 Ligand-based virtual screening (LBVS) method: navitoclax pharmacophore mapping.

We also took as reference the senolytic navitoclax (**Fig. 41**) to perform the *in silico* approach. First, by using the software *Ligand Scout 4.4*, we obtained the pharmacophoric map (**Fig. 41B**). Navitoclax showed 5 pharmacophoric characteristics corresponding to: i) eight hydrogen bonds, both electron donors (3) and acceptors (5). Among them, one hydroxyl group behaves both as an electron donor and acceptor; ii) four hydrophobic sites; iii) four aromatic rings; iv) one nitrogen group that is positively ionized; and finally, v) one chloride group acting as a halogen bond donor, (**Fig. 41C**). Next, we performed the calculations against the more than 10000 compound entries of the DB library, but no satisfactory results were obtained.

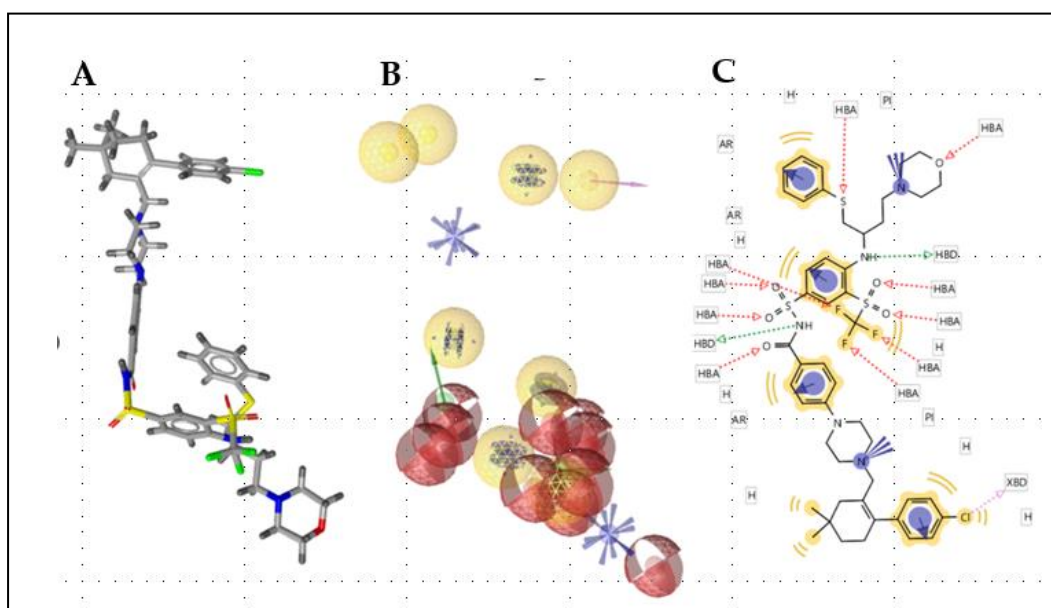


Figure 41. Schematic representation of pharmacophoric features. A) The three-dimensional (3D) structure of navitoclax. B) The pharmacophoric characteristics of navitoclax were obtained with the *Ligand Scout* software. Electron-donor and -acceptor hydrogen bonds are represented by green and red spheres, respectively. Hydrophobic sites are represented by yellow spheres. Aromatic rings are represented by blue circles. C) Pharmacophoric features diagram for navitoclax molecule. *PDB: 4LVT*.

V.7.2 Ligand-based virtual screening (LBVS) method: Dasatinib pharmacophore mapping.

In view of the lack of results with navitoclax, we decided to perform the *in silico* approach with another senolytic, dasatinib (**Fig. 42**). We obtained its pharmacophoric map by using the software *Ligand Scout 4.4* (**Fig. 42B**). Dasatinib showed 5 pharmacophoric characteristics corresponding to: i) five hydrogen bonds, both electron donors (3) and acceptors (2). Among them, one hydroxyl group behaves both as an electron donor and acceptor; ii) five hydrophobic sites; iii) aromatic rings that correspond to the blue rings; iv) one nitrogen group that is

positively ionised and represented by a blue star; and finally, v) one chloride group acting as a halogen bond donor and represented by a violet arrow (Fig. 42C).

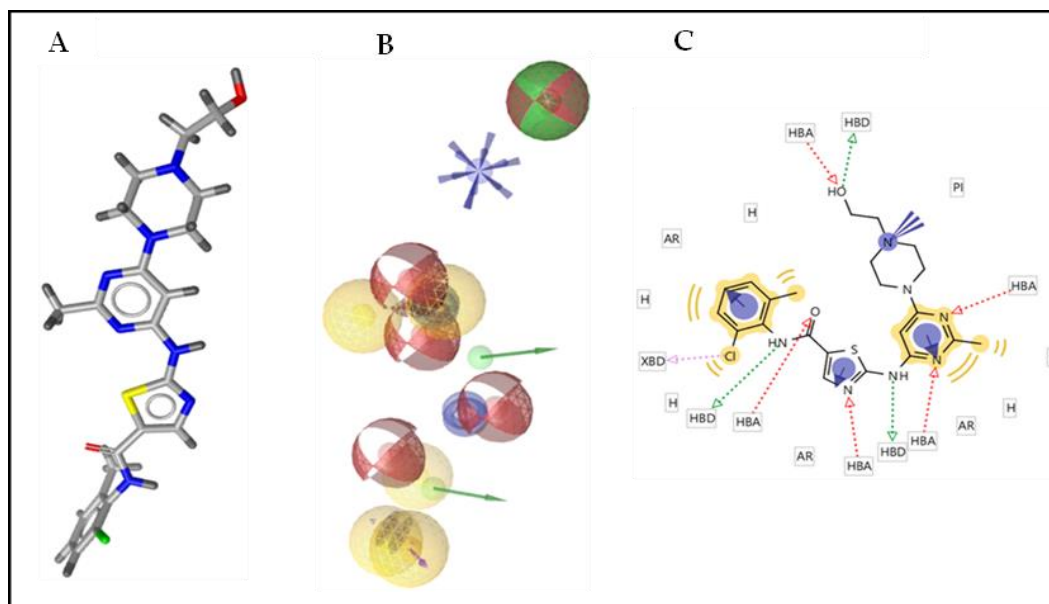


Figure 42: Schematic representation of pharmacophore features: **A)** The three-dimensional (3D) structure of dasatinib. **B)** The pharmacophore characteristics of Dasatinib were obtained with the *Ligand Scout* software. Electron-donor and -acceptor hydrogen bonds are represented by green and red spheres, respectively. Hydrophobic sites are represented by yellow spheres. Aromatic rings are represented by with blue circles. **C)** Pharmacophoric features of the dasatinib molecule. *PDB: 3SXR*.

Next, we performed the calculations against the more than 10000 compound entries of the drugbank (DB) library, we obtained a list with more than 600 compounds that were similar both in structure and pharmacophore characteristics, but in this case, we did not obtain the highest score for our molecule, but we found a molecule that presented a score of 0.62 which was the highest, not having many pharmacophore characteristics in common and neither the structure (Fig. 43).

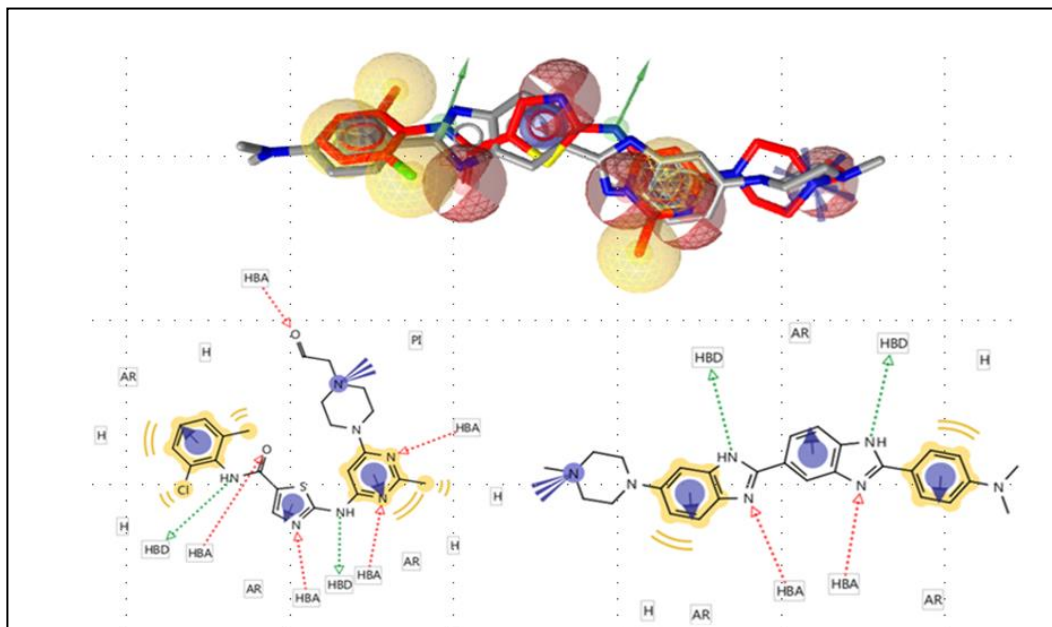


Figure 43. Pharmacophoric method. The structure of dasatinib is shown in red and in gray, the candidate obtained by the VS method. The pharmacophoric characteristic; i) electron-donor and -acceptor hydrogen bonds are represented by green and red spheres, respectively. ii) hydrophobic sites are represented by yellow spheres. iii) aromatic rings are represented by with blue circles. (I: 2'-(4-dimethylaminofenil)-5-(4-metil-1-piperazinil)-2,5'-bi-benzimidazole), the compounds are shown overlaid with dasatinib, to show their similarity.

V.8 In vivo validation of candidates with anti-aging potential in different aging zebrafish models for repurposing.

V.8.1 Analyzed the toxicity assay.

First, we evaluated toxicity at 24 hpf, 48 hpf. 72 hpf we evaluated the development during the first 72 hours of WT zebrafish larvae to determine the working doses (Fig. 44).

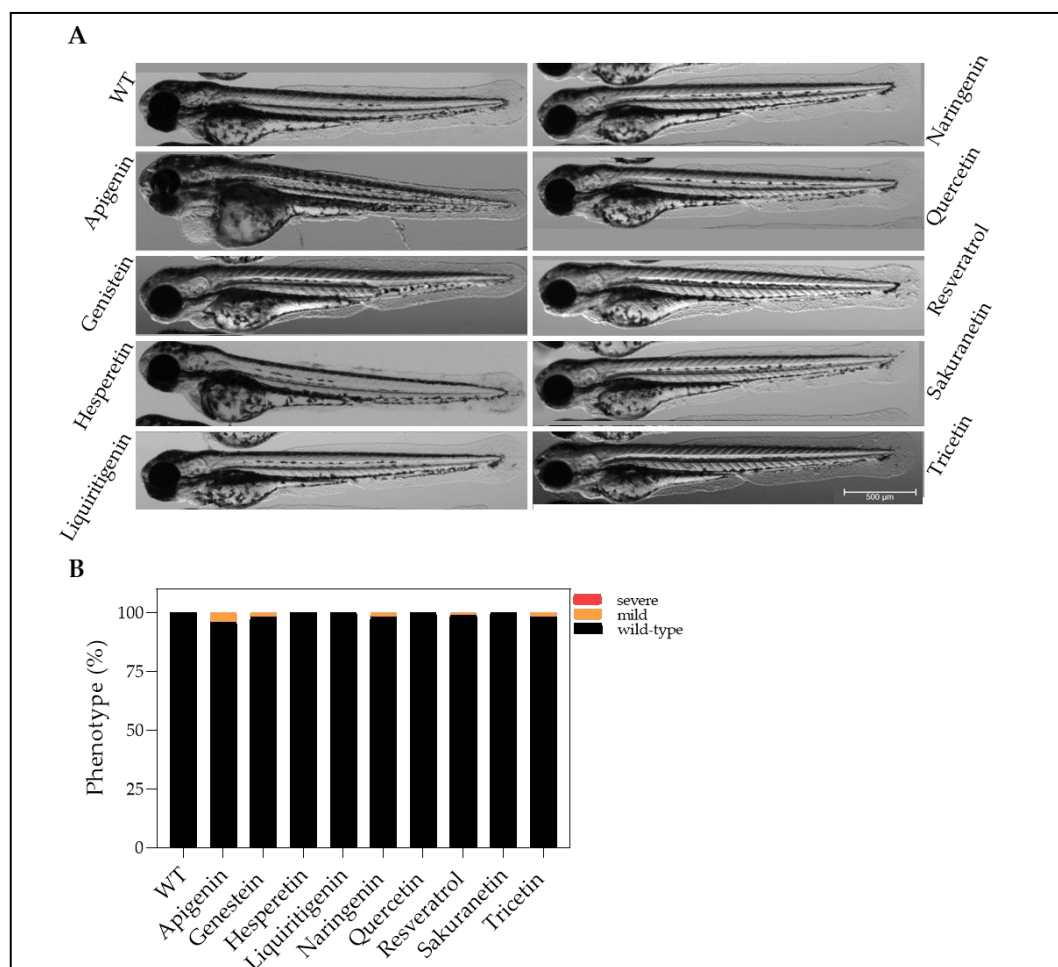


Figure 44. Candidates are non-toxic for wild-type zebrafish larvae. A) Representative images of the toxicity assay of candidates in wild-type zebrafish larvae. B) Classification of 72 hpf larvae according to phenotype. In B, differences are not statistically significant according to Two-way ANOVA followed by Sidak's multiple comparison test.

V.8.2 Shortened telomere-induced premature aging, the ST2 model.

By using the ST2 model zebrafish larvae, we evaluated the anti-aging properties of the non-toxic resveratrol-derived compounds. (Fig. 45).

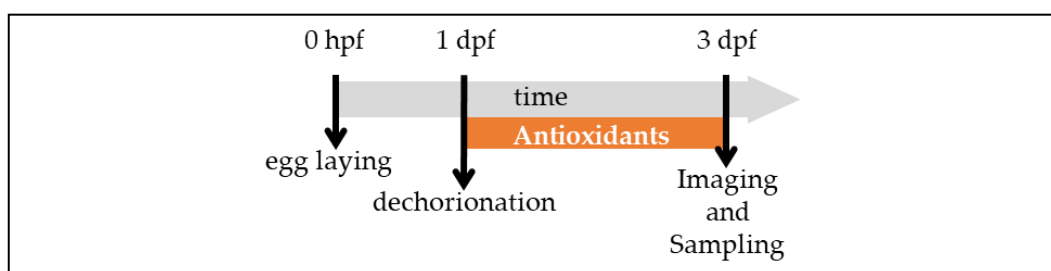


Figure 45. General workflow for antioxidant treatment in the ST2 model of premature aging. 1 dpf larvae were treated with resveratrol-derived antioxidants for 2 days before imaging and sampling.

Isoliquiritigenin and kaempferol were discarded based on toxicity assay, so we evaluated the anti-aging effects of the rest of candidates in the ST2 premature aging model. Treatment of 1-day post fertilization (dpf) ST2 larvae with naringenin, sakuranetin and tricetin for 3 days showed an induction of telomerase activity, while hesperetin caused a decrease compared to vehicle (Fig. 46A). However, the effect on telomerase activity was effective only in the case of resveratrol, as sakuranetin and tricetin did not affect telomere length. ST2 larvae treated with naringenin showed even greater telomere attrition than vehicle and, contrary, hesperetin produced a lengthening of telomeres compared to control (Fig. 46B).

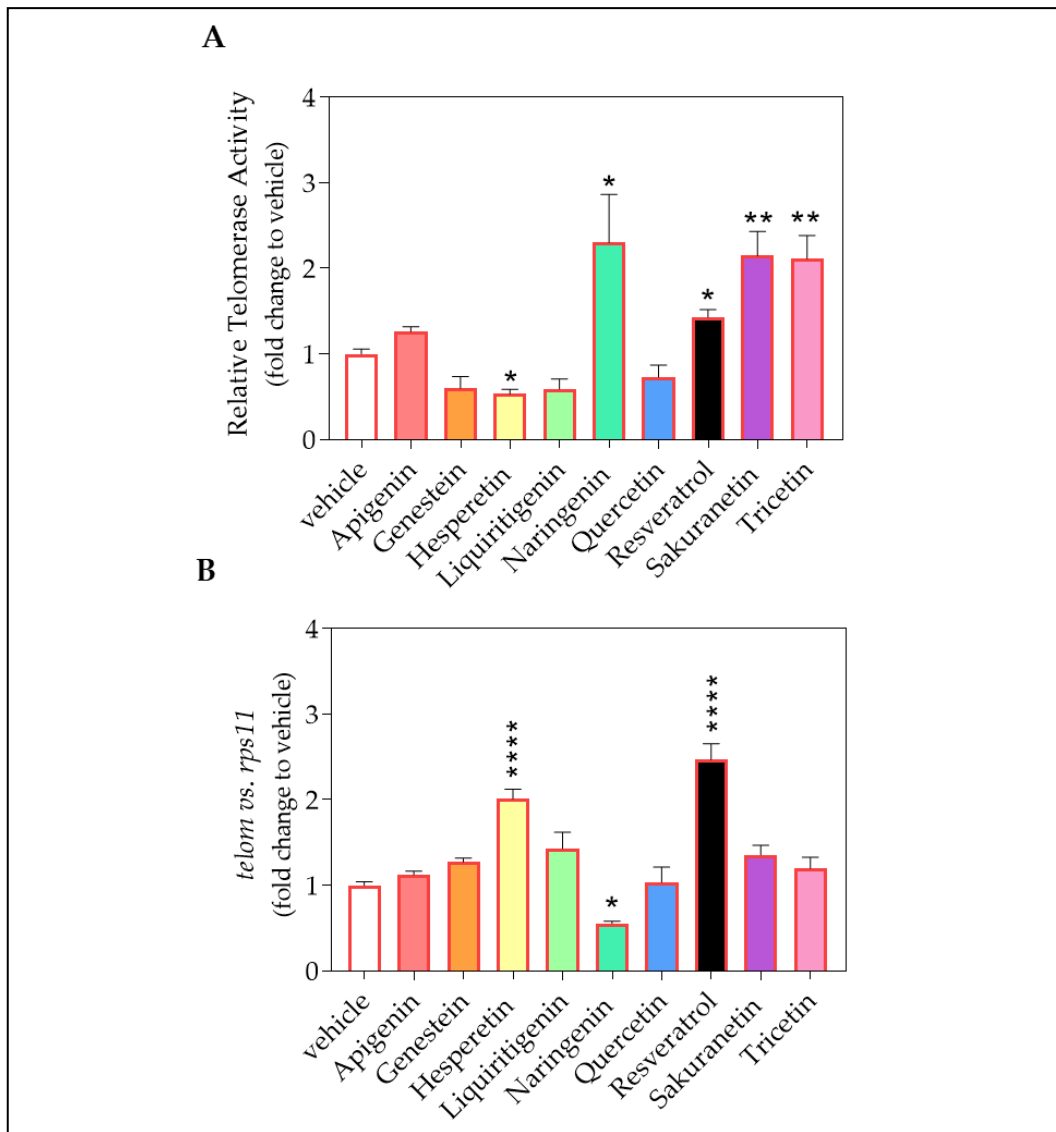


Figure 46. Telomeric characterization of the ST2 model after antioxidant treatment. A) Telomerase activity was measured quantitatively in 3 dpf ST2 zebrafish larvae treated with antioxidants by Q-TRAP using 0.1 μg of protein extract. **B)** Telomere length was measured in 3 dpf ST2 zebrafish larvae treated with antioxidants by qPCR using 16 ng of gDNA and determined as the telomere content relative to the single copy gene *rps11*. In **(A, B)** the graph shows the mean \pm SEM of 25 pooled larvae ($n=25$) and triplicate samples from 2 independent experiments ($N=2$). ns, non-significant; * $p<0.05$; ** $p<0.001$; **** $p<0.0001$, according to Kruskal-Wallis followed by uncorrected Dunn's multiple comparison test.

The effect of apigenin, naringenin, resveratrol and sakuranetin on life expectancy of ST2 larvae was consistent with telomere length results, as naringenin treatment reduced survival by 25%, resveratrol increased survival by 12.5% compared to untreated larvae. Unexpectedly, although apigenin did not improve telomere length, it was able to increase half-life by 12.5% (**Fig. 47**).

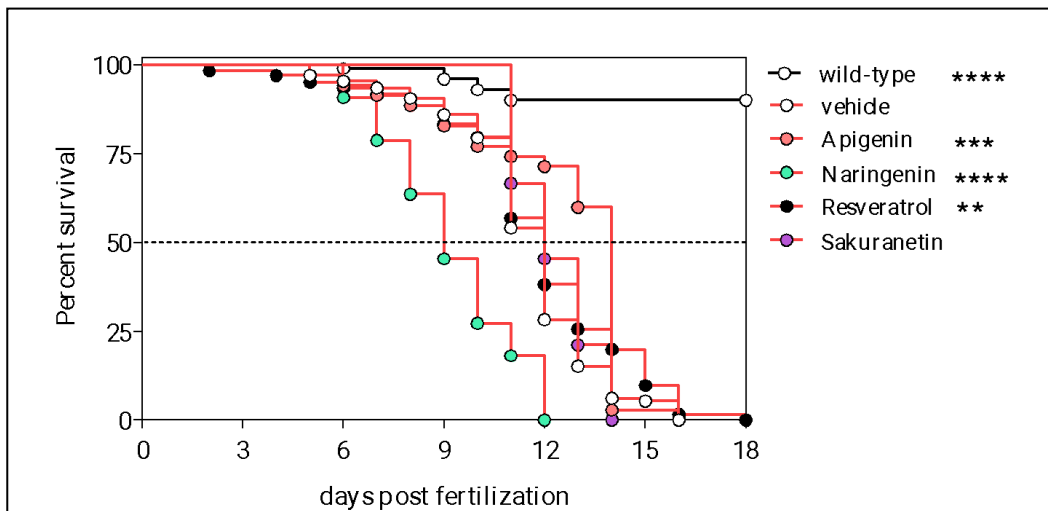


Figure 47. Effect of resveratrol-derived antioxidants on ST2 larvae survival. Kaplan-Meier representation of vehicle ($n=244$), apigenina ($n=35$), naringenin ($n=33$), resveratrol ($n=246$) and sakuranetin ($n=33$) treated ST2 larvae and wild-type ($n=101$). The graph shows the accumulation of 2-4 independent experiments ($N=2-4$). ** $p<0.05$; *** $p<0.001$; **** $p<0.0001$, according to Log Rank test respect to vehicle.

V.8.3 Premature aging induced by DNA damage caused by chemotherapy, the QiDD model.

To evaluate the anti-aging effects of some natural antioxidants candidates for their repositioning as adjuvants in cancer treatment, we used a chemotherapy-induced DNA damage, the QiDD model. We continued using apigenin, naringenin, resveratrol and sakuranetin as adjuvants in chemotherapy treatment to study their effect on larval survival compared to chemotherapeutics alone (Fig. 48).

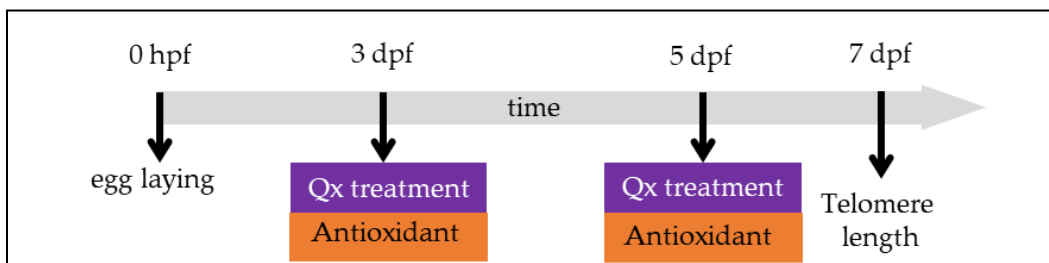


Figure 48: General workflow for the evaluation of antioxidants in the QiDD model. 3 dpf and 5 dpf zebrafish larvae were co-treated with antioxidants and Qx before telomere length measurement. QiDD: chemotherapy-induced DNA damage. Qx: chemotherapy.

We observed a clear and beneficial effect on survival when apigenin and naringenin were co-treated with cytarabine (Fig. 49).

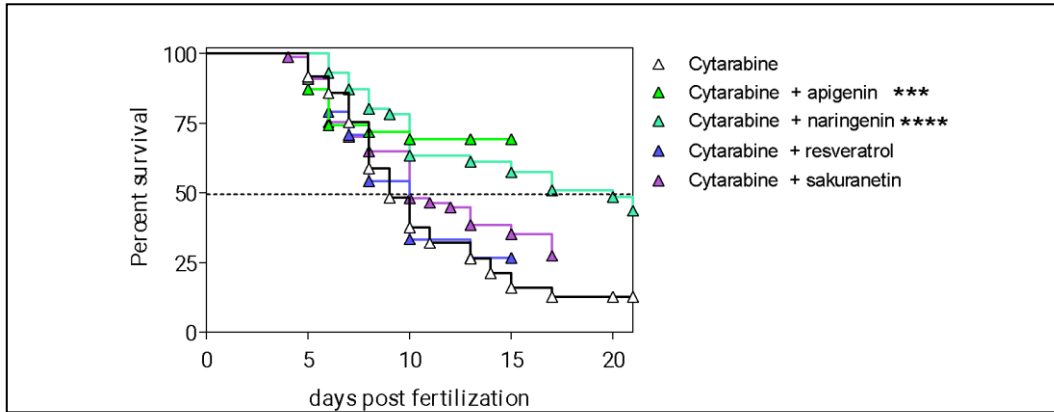


Figure 49. Effect of resveratrol-derived antioxidants on QiDD larvae survival.

Kaplan-Meier representation of cytarabine 50 μM alone ($n=85$) or in combination with apigenin 10 μM ($n=39$), naringenin 10 μM ($n=101$), resveratrol 10 μM ($n=24$) and sakuranetin 10 μM ($n=77$). The graph shows the accumulation of 3 independent experiments ($N=3$). *** $p<0.001$; **** $p<0.0001$, according to Log Rank test.

In the case of daunoblastine, co-treatment with naringenin, resveratrol and sakuranetin also improved survival compared to daunoblastine alone (Fig. 50).

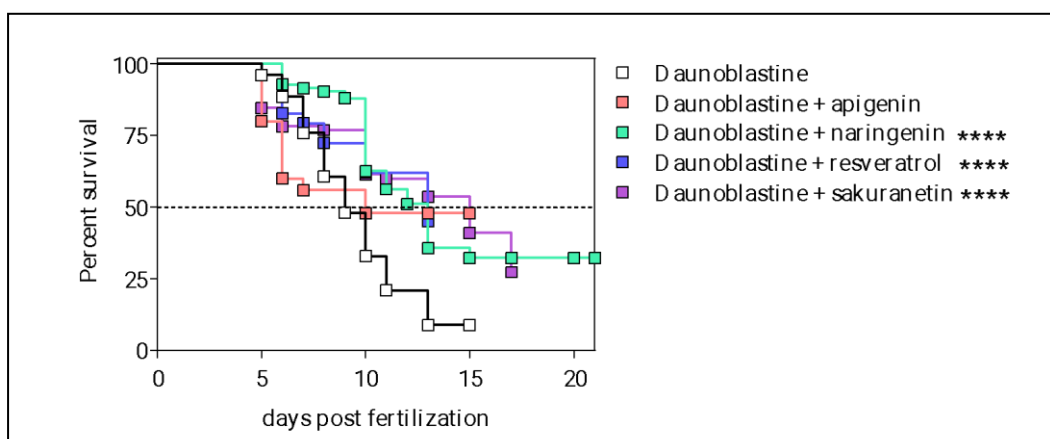


Figure 50. Effect of resveratrol-derived antioxidants on QiDD larvae survival. Kaplan-Meier representation of daunoblastine 1 μM alone ($n=79$) or in combination with apigenin 10 μM ($n=25$), naringenin 10 μM ($n=83$), resveratrol 10 μM ($n=29$) and sakuranetin 10 μM ($n=78$). The graph shows the accumulation of 3 independent experiments ($N=3$). **** $p<0.0001$, according to Log Rank test.

However, while naringenin was beneficial for larvae survival when co-treated with dexamethasone, the effect of resveratrol and sakuranetin was the opposite (**Fig. 51**).

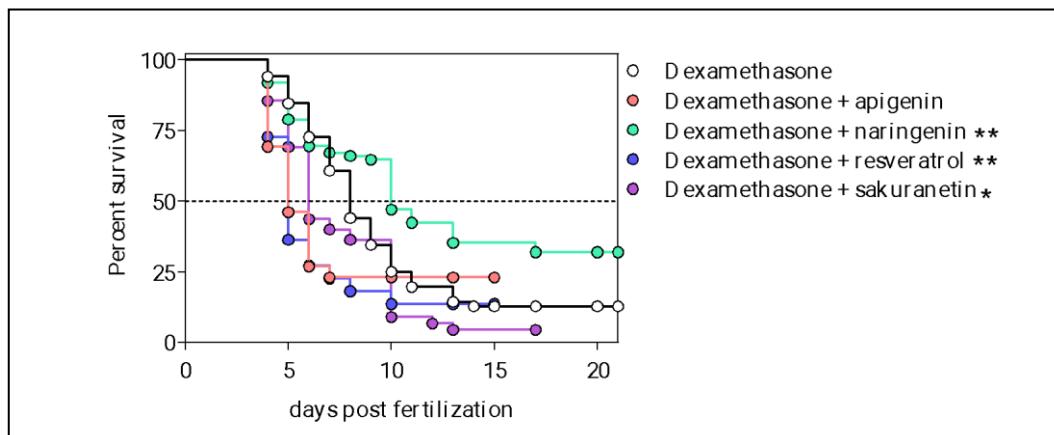


Figure 51. Effect of resveratrol-derived antioxidants on QiDD larvae survival. Kaplan-Meier representation of dexamethasone 0.5 μM alone ($n=84$) or in combination with apigenin 10 μM ($n=26$), naringenin 10 μM ($n=85$), resveratrol 10 μM ($n=22$) and sakuranetin 10 μM ($n=55$). The graph shows the accumulation of 3 independent experiments ($N=3$). * $p<0.05$; ** $p<0.001$, according to Log Rank test.

None of the antioxidant candidates improved the methatrexato-treated larvae survival (Fig. 52).

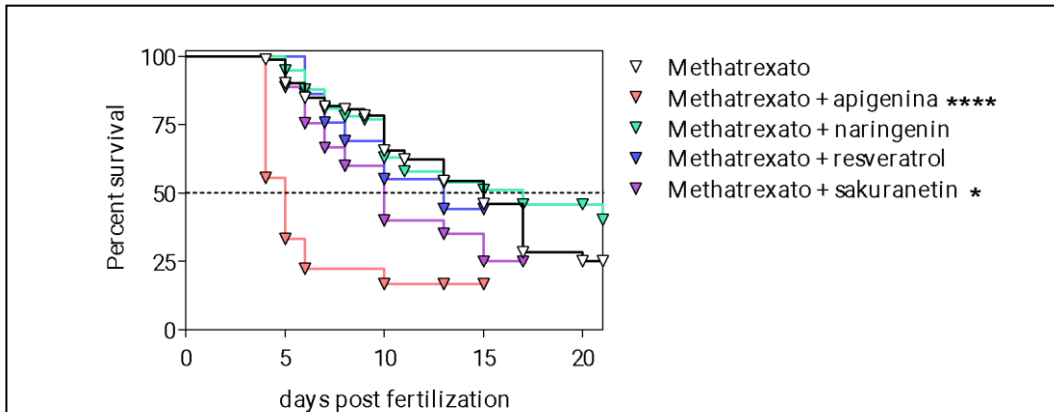


Figure 52. Effect of resveratrol-derived antioxidants on QiDD larvae survival. Kaplan-Meier representation of methatrexato 0.2 μM alone ($n=84$) or in combination with apigenin 10 μM ($n=18$), naringenin 10 μM ($n=100$), resveratrol 10 μM ($n=29$) and sakuranetin 10 μM ($n=45$). The graph shows the accumulation of 3 independent experiments ($N=3$). * $p<0.05$; **** $p<0.0001$, according to Log Rank test.

And finally, we observed a positive effect on the vincristine-treated larvae survival when co-treated with both apigenin and naringenin (Fig. 53).

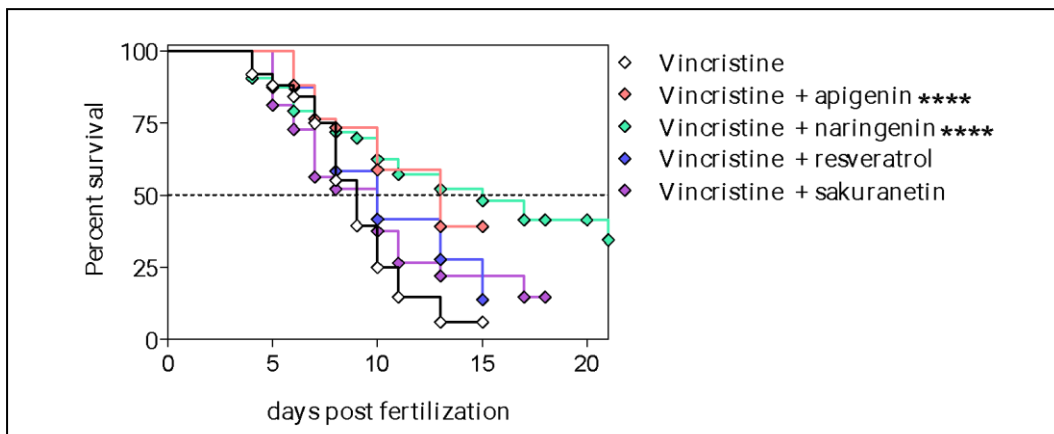


Figure 53. Effect of resveratrol-derived antioxidants on QiDD larvae survival.

Kaplan-Meier representation of vincristine 2.5 μM alone ($n=76$) or in combination with apigenin 10 μM ($n=34$), naringenin 10 μM ($n=96$), resveratrol 10 μM ($n=24$) and sakuranetin 10 μM ($n=48$). The graph shows the accumulation of 3 independent experiments ($N= 3$). **** $p<0.0001$, according to Log Rank test.

All these results are summarized for clarity in **Table IV**.

Table IV. Summary of the effect of the adjuvant treatment of apigenin, naringenin, resveratrol and sakuranetin with different chemotherapeutic agents on larval survival.

	Cytarabine 50 μM	Daunoblastine 1 μM	Dexamethasone 0.5 μM	Methotrexate 0.2 μM	Vincristine 2.5 μM
Apigenina 10 μM	<i>positive</i>	<i>no effect</i>	<i>no effect</i>	<i>negative</i>	<i>positive</i>
Naringenin 10 μM	<i>positive</i>	<i>positive</i>	<i>positive</i>	<i>no effect</i>	<i>positive</i>
Resveratrol 10 μM	<i>no effect</i>	<i>positive</i>	<i>negative</i>	<i>no effect</i>	<i>no effect</i>
Sakuranetin 10 μM	<i>no effect</i>	<i>positive</i>	<i>negative</i>	<i>negative</i>	<i>no effect</i>

V.9 High-cholesterol diet-induced metainflammation zebrafish model, the HCD model.

We also evaluated some antioxidants in a zebrafish model with metainflammation induced by a high-cholesterol diet (HCD) (**Fig. 54**).

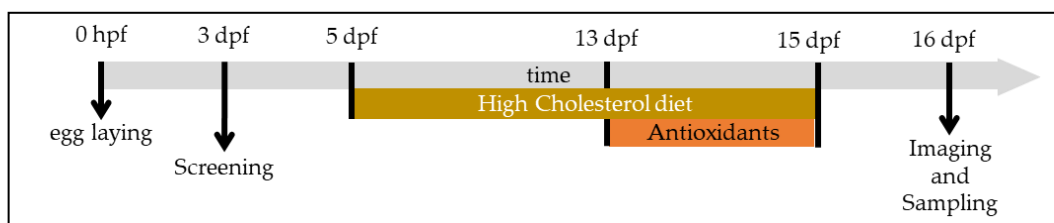


Figure 54. General workflow for the evaluation of antioxidants in the HCD-induced metainflammation model. 13 dpf HCD-fed larvae were treated with antioxidants for two days before imaging and sampling. HCD: high cholesterol diet.

The treatment with apigenin, naringenin and sakuranetin triggered an amelioration of the inflammation phenotype (Fig. 55A) characteristic of the HCD model that, in the case of naringenin, also resulted in a significant reduction in the total number of neutrophils (Fig. 55B) and macrophages (Fig. 55C).

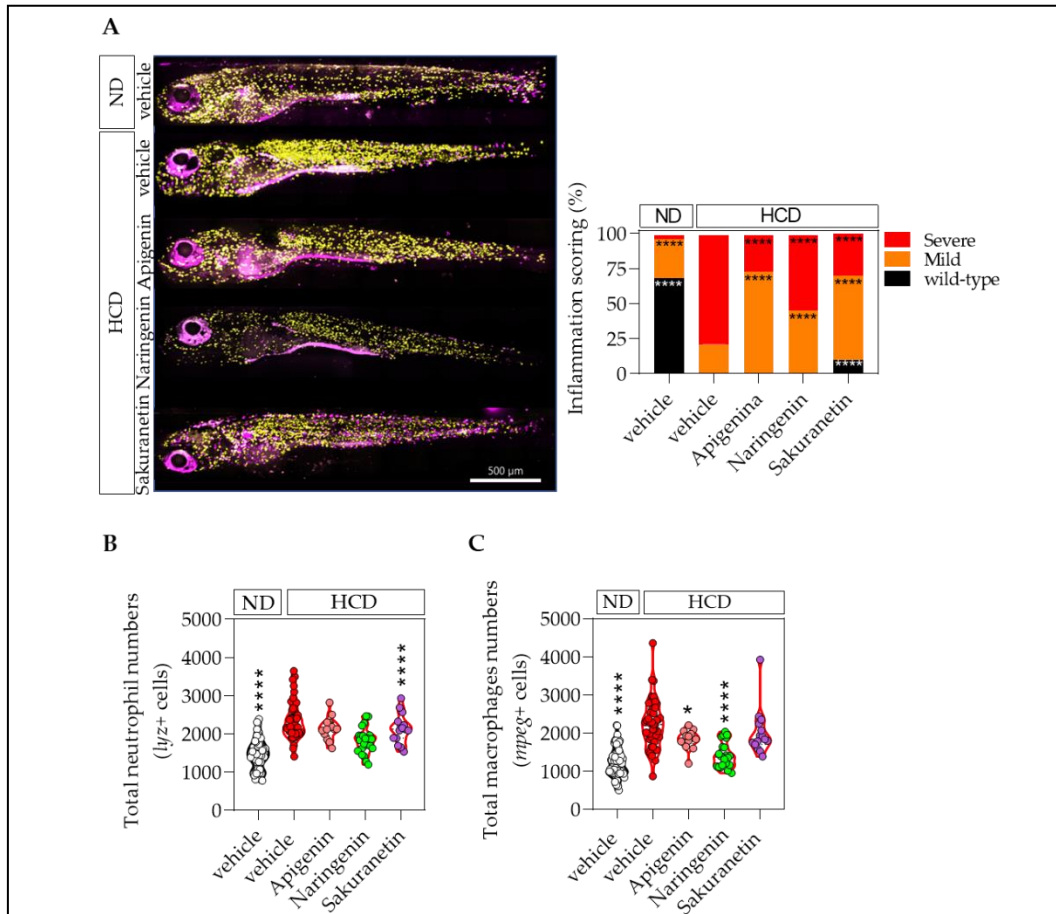


Figure 55. Evaluation of selected antioxidant compounds in the HCD-induced metainflammation model. **A)** Representative images and **classification** of the distribution of neutrophils (yellow) and macrophages (purple) of 16 dpf (*lyz:DsRED2; mpeg1:EGFP*) larvae after navitoclax treatment for 3 days. **B)** Quantification of total neutrophil numbers (*lyz+* cells). **C)** Quantification of total macrophage numbers (*mpeg+* cells). In **B, C)** the violin plots with the median shown as a horizontal line show the distribution of neutrophil and macrophage cells and are overlaid with the raw data, where each dot represents an individual. The graphs show the accumulation of 3 independent experiments (N= 3). * $p < 0.05$; **** $p < 0.0001$, according to Two-way ANOVA followed by Sidak's multiple comparison test (A) and Brown-Forsythe ANOVA followed by Dunnett's T3 multiple comparison test compared to untreated HCD larvae (B, C).

These results highlight the anti-inflammatory properties of naringenin, so it could be a candidate for preventive use against metainflammation.

Despite the little success of the *in silico* screening using navitoclax and dasatinib as a reference, we decided to evaluate the anti-aging effect of navitoclax in the context of metainflammation (**Fig. 56**).

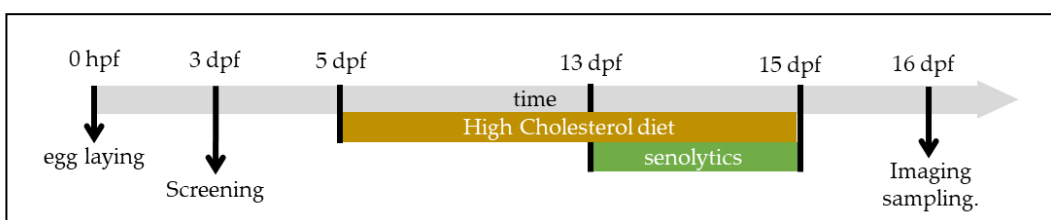


Figure 56. General workflow for the evaluation of navitoclax in the HCD-induced metainflammation model. 13 dpf HCD-fed larvae were treated with navitoclax for 3 days before imaging and sampling. HCD: high cholesterol diet.

The treatment of the HCD-fed group with navitoclax for 3 days dampens emergency myelopoiesis by reversing neutrophilia and monocytosis in the HCD-fed larvae (**Fig. 57A**). In the case of navitoclax, also resulted in a significant reduction in the total number of neutrophils (**Fig. 57B**) and macrophages (**Fig. 57C**).

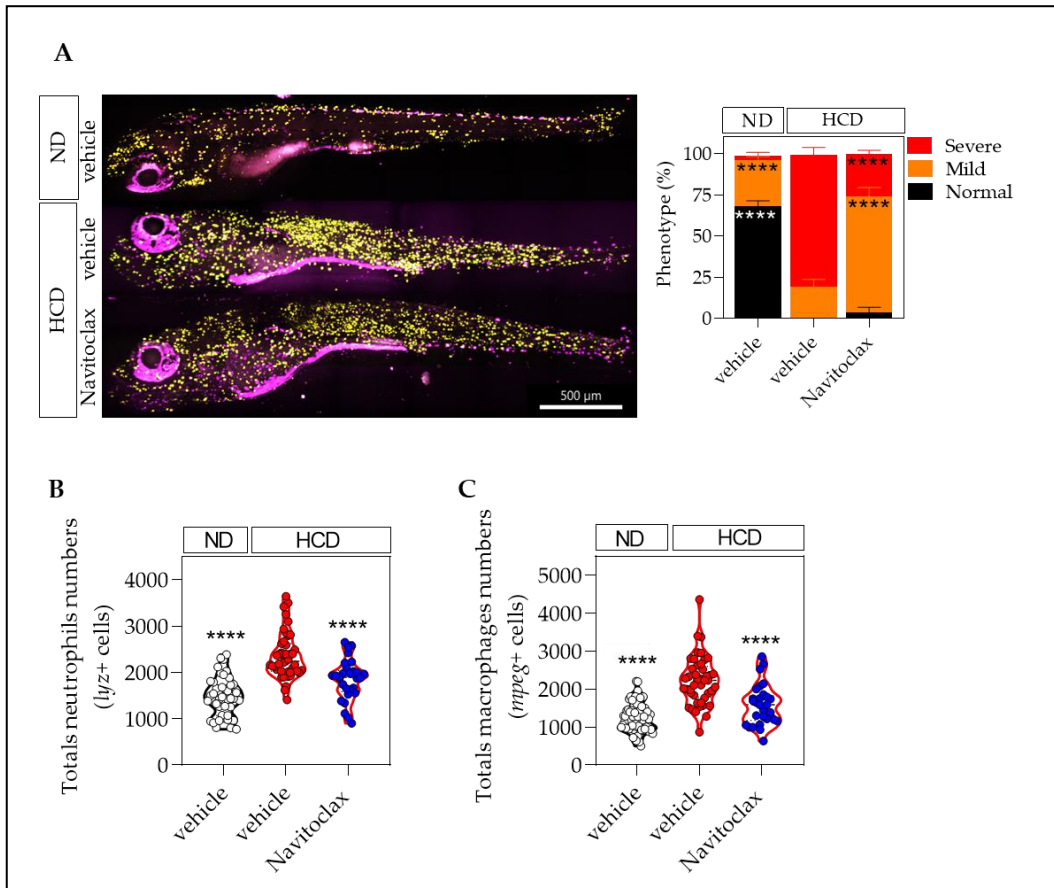
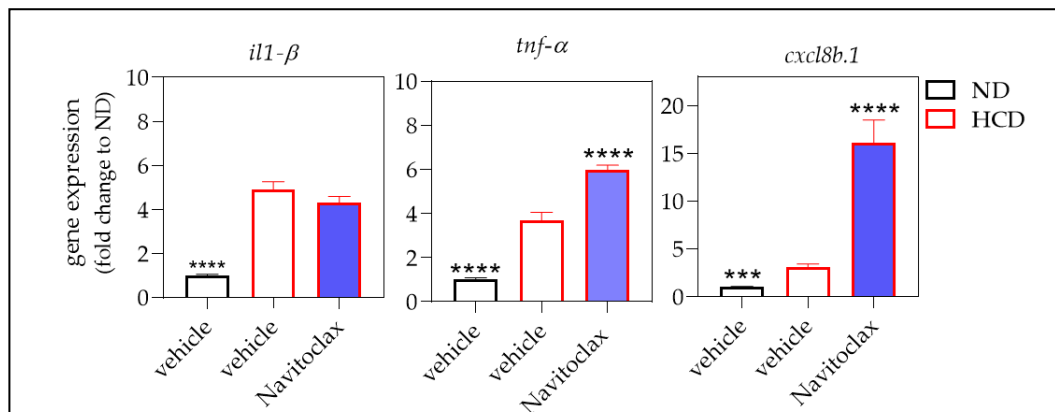


Figure 57. Evaluation of selected antioxidant compounds in the HCD-induced metainflammation model. A) Representative images and classification of the distribution of neutrophils (yellow) and macrophages (purple) of 16 dpf (*lyz:DsRED2; mpeg1:EGFP*) larvae after navitoclax treatment for 3 days. B) Quantification of total neutrophil numbers (*lyz+* cells). C) Quantification of total macrophage numbers (*mpeg+* cells). In B, C) the violin plots with the median shown as a horizontal line show the distribution of neutrophils and macrophage cells respectively and are overlaid with the raw data, where each dot represents an individual. The graphs show the accumulation of 3 independent experiments (N= 3). **** $p < 0.0001$, according to Two-way ANOVA followed by Dunnett's multiple comparison test (A) and Brown-Forsythe ANOVA followed by Dunnett's T3 multiple comparison test (B, C).

Unexpectedly, navitoclax failed to ameliorate the transcript levels of *il1 β* , *tnf- α* , and *cxcl8b.1* genes (Fig. 58).



These results confirm the senescence-independent therapeutic benefits of navitoclax in the context of chronic inflammation.

Figure 58. Navitoclax increased genes related to inflammation phenotype of HCD-fed larvae. The mRNA level of *il1b*, *tnf- α* , *cxcl8b.1* was determined by RT-qPCR and normalized against *rps11*. The bars show the mean \pm SEM of 20 pooled larvae (n=20) and triplicate samples from 2 independent experiments (N=3). ** $p<0.01$; *** $p<0,001$ **** $p<0.0001$ according to Kruskal-Wallis followed by Dunn's multiple comparison test.

V.10 Inflammaging zebrafish model, the Spint1a-deficient model.

To evaluate the anti-inflammatory properties of antioxidants in the *spint1a*-deficient model of inflammaging, 1-dpf *spint1a*-deficient larvae were treated with candidates for 48 hours (Fig. 59).

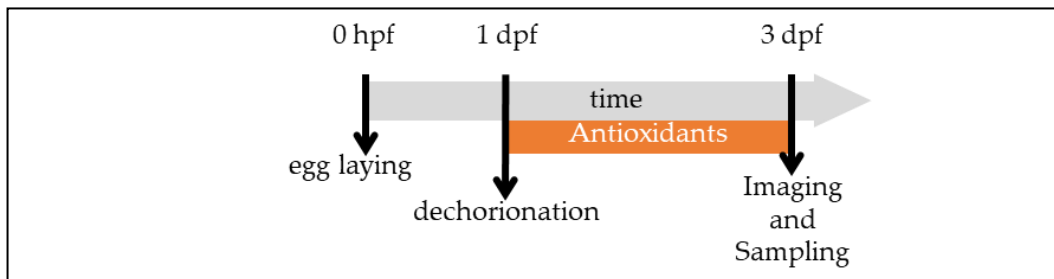


Figure 59. General workflow for the evaluation of antioxidants in the Spint1a-deficient inflammaging model. 1 dpf Spint1a-deficient larvae were treated with antioxidants for 3 days before imaging and sampling.

We observed that treatment with apigenin, genestein, naringenin, sakuranetin and tricetin was able to decrease neutrophil dispersion, assayed in a transgenic line with labelled neutrophils (*lyz:DsRED2*) (Fig. 60B), even though only apigenin, hesperetin reduced the total number of neutrophils (Fig. 60C).

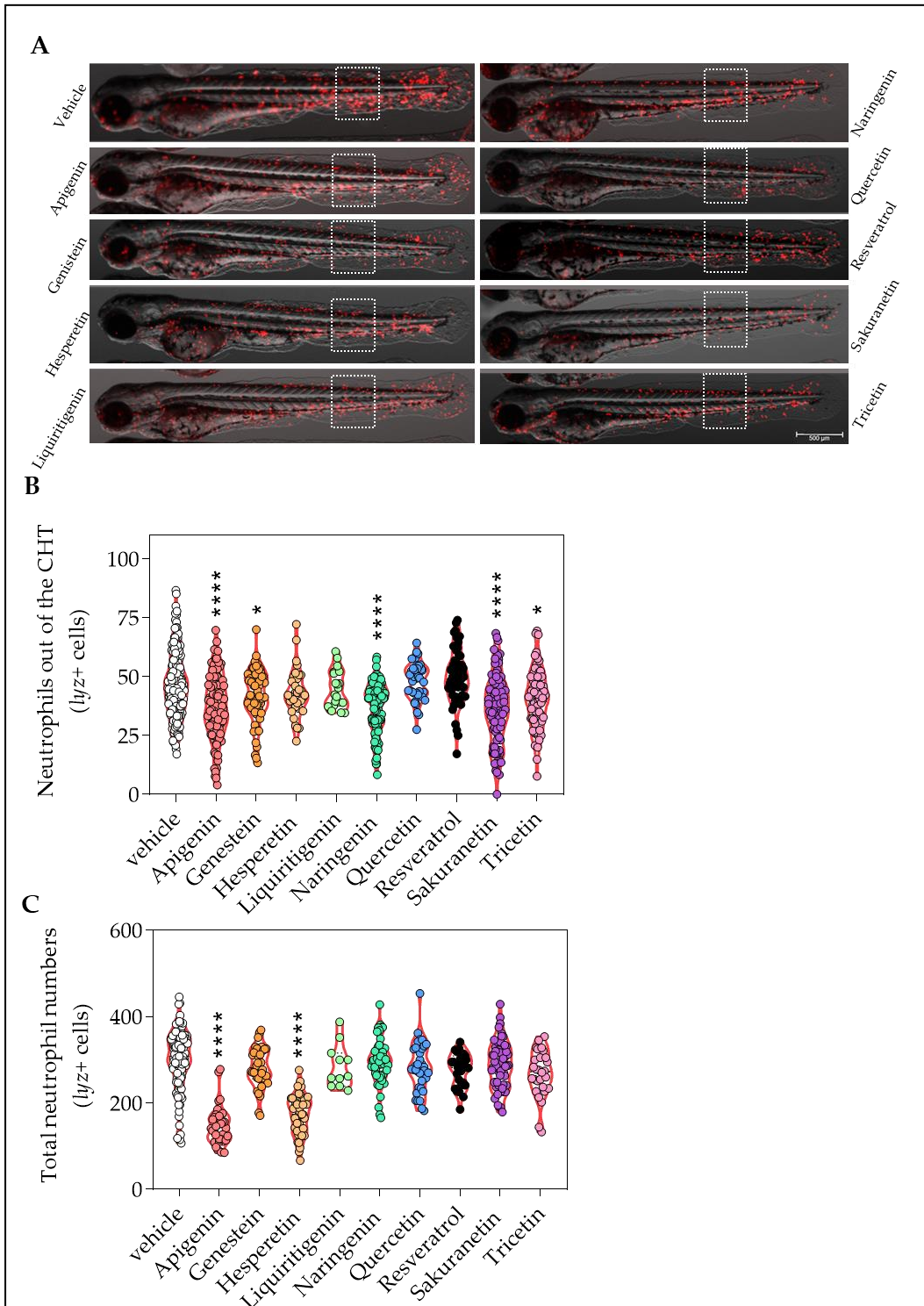


Figure 60. Apigenin, genestein, naringenin, sakuranetin and tricetin ameliorate the skin inflammation phenotype of *Spint1a*-deficient larvae. A) Representative images of neutrophil phenotype of 3 dpf larvae (neutrophils labeled in red, *lyz:DsRED2*). Discontinuous white squares represent the ROI for quantification. **B)** Quantification of the number of neutrophils out of the CHT. **(C)** Quantification of the total neutrophils numbers. In **B, C)** the violin plots with the median shown as a horizontal line show the distribution of *DsRED2*+ cells, and are overlaid with the raw data, where each dot represents an individual. The graphs show the accumulation of 3 independent experiments (N=3). * $p < 0.05$; **** $p < 0.0001$ according to Kruskal-Wallis followed by Dunn's multiple comparison test. ROI: region of interest. CHT: caudal hematopoietic tissue. Scale bar: 500 μm .

Regarding the number of keratinocyte aggregate foci, the effect of antioxidants was quite similar to that of neutrophil dispersion in the skin, observing a decrease with genestein, naringenin and sakuranetin, and a slight increase with resveratrol (**Fig. 61B**).

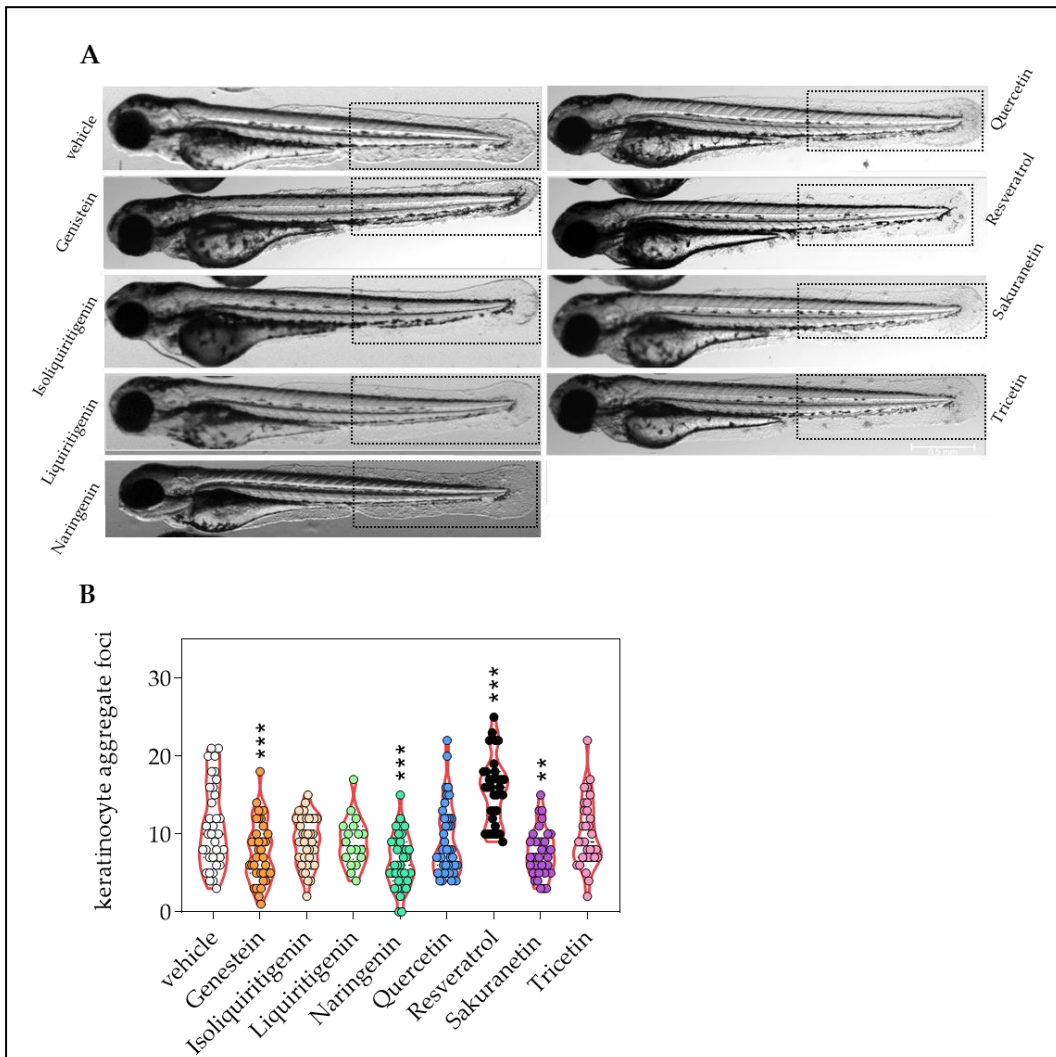


Figure 61. Genestein, naringenin and sakuranetin, contrary to resveratrol, ameliorate the skin inflammation phenotype of Spint1a-deficient larvae. A) Representative images of skin phenotype of 3 dpf larvae. Discontinuous black squares represent the ROI for quantification. **B)** Quantification of the keratinocyte aggregate foci at the skin of 3 dpf larvae. The violin plots with the median shown as a horizontal line show the distribution of keratinocyte aggregate foci, and are overlaid with the raw data, where each dot represents an individual. The graph shows the accumulation of 3 independent experiments (N= 3). ** $p < 0.01$; *** $p < 0.001$; according to Kruskal-Wallis followed by Dunn's multiple comparison test. ROI: region of interest. Scale bar: 500 μm .

With respect to oxidative stress, we found that only the treatment with apigenin and genestein resulted in a strong reduction (**Fig. 62B**).

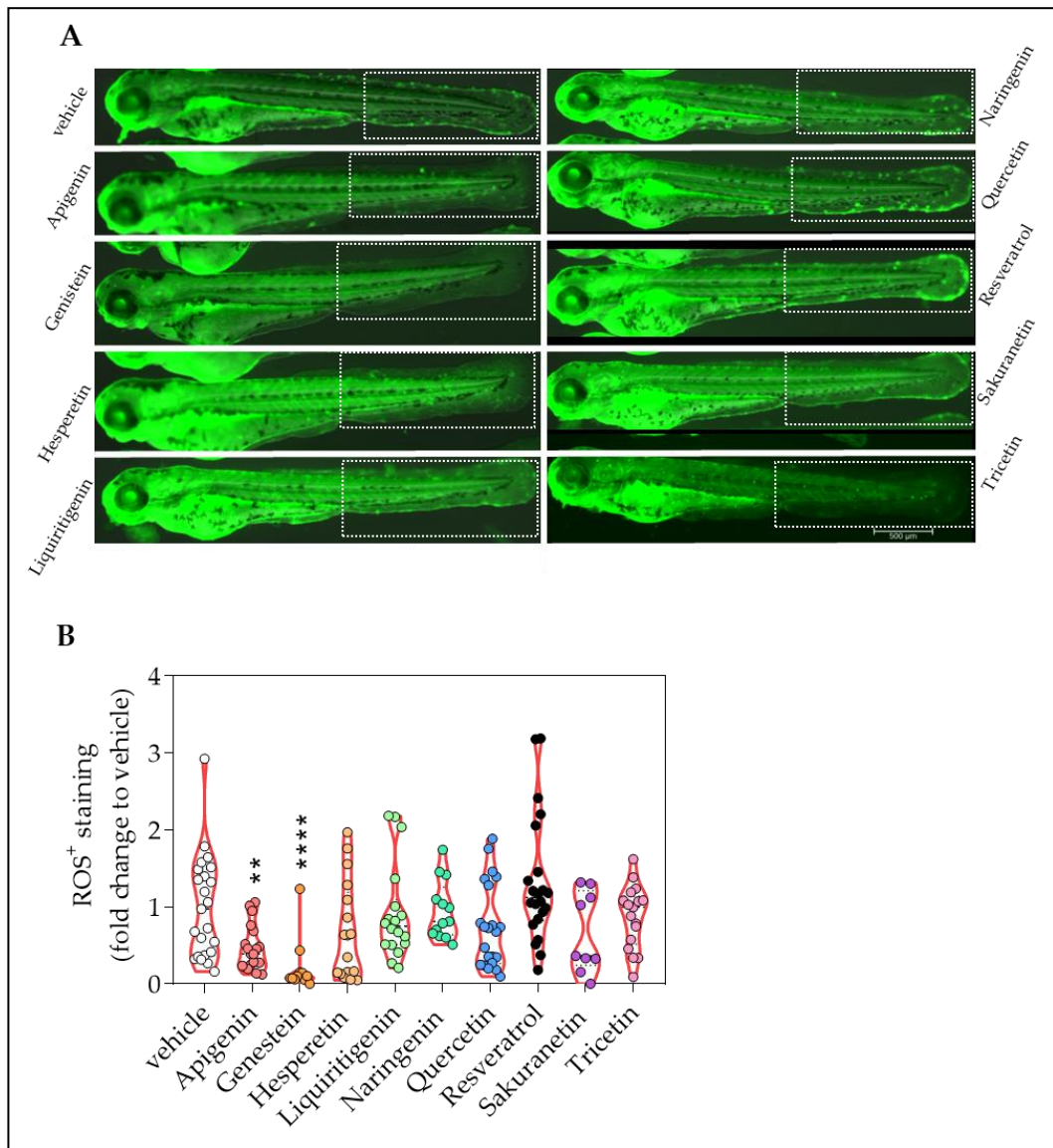


Figure 62. Apigenin and genestein ameliorate oxidative stress levels of Spint1a-deficient larvae. **A)** Representative images of ROS staining of 3 dpf Spint1a-deficient larvae, where ROS⁺ cells are stained in green. Discontinuous black squares represent the ROI for quantification. **B)** Quantification of the oxidative stress levels of 3 dpf Spint1a-deficient larvae. The violin plots with the median shown as a horizontal line show the distribution of ROS⁺ cells, and are overlaid with the raw data, where each dot represents an individual. The graph shows the accumulation of 3 independent experiments (N=3). The graph shows the accumulation of 3 independent experiments (N=3). ** $p < 0.001$; **** $p < 0.0001$, according to Kruskal-Wallis followed by uncorrected Dunn's multiple comparison test. ROS: reactive oxygen species. ROI: region of interest. Scale bar: 500 μm .

These results were further supported by the robust reduction of cell death levels, not only by apigenin and genestein, but also by hesperetin, quercetin and sakuranetin (**Fig. 63B**).

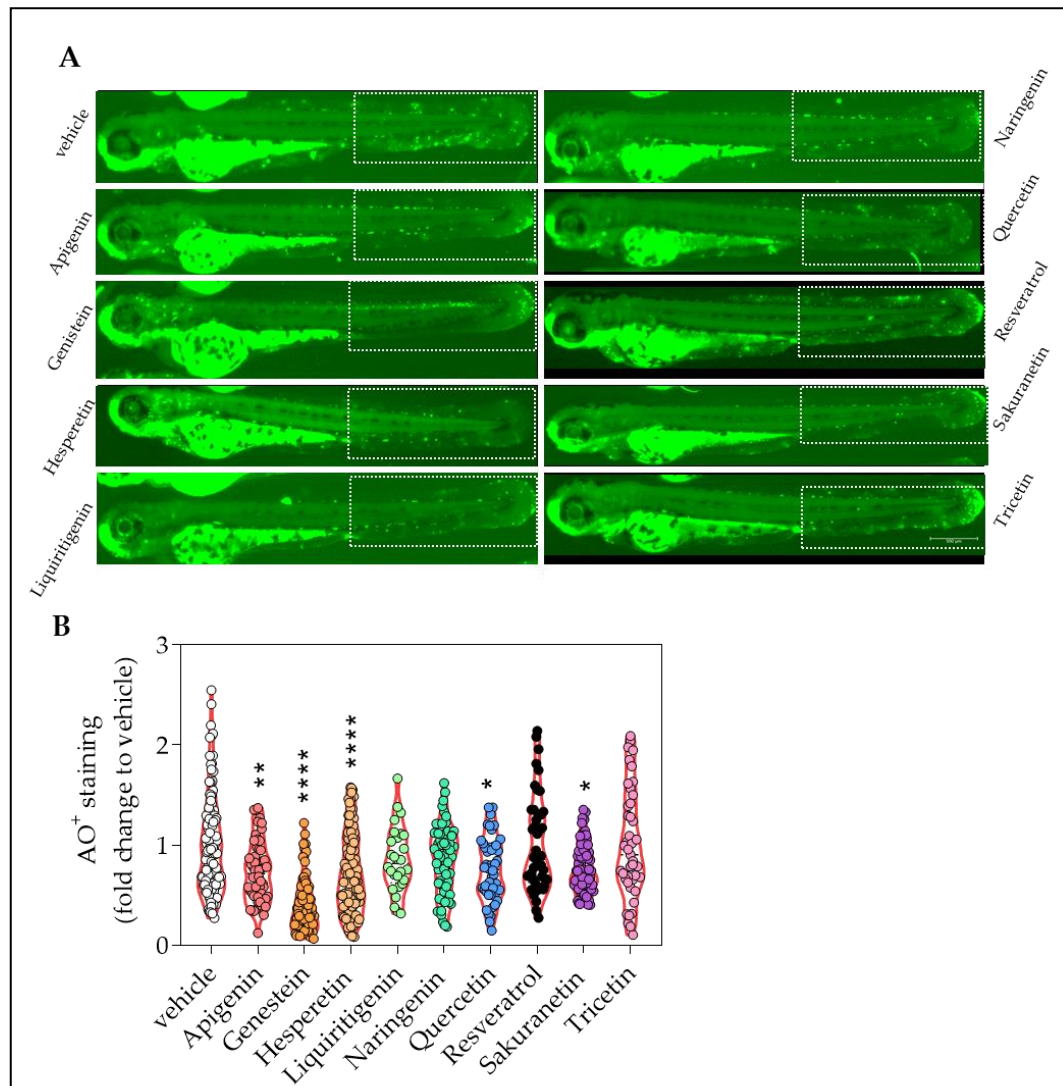


Figure 63. Apigenin, genestein, hesperetin, quercetin and sakuranetin ameliorate the cell death levels of *Spint1a*-deficient larvae. **A)** Representative images of AO staining of 3 dpf *Spint1a*-deficient larvae, where AO⁺ cells are stained in green. Discontinuous white squares represent the ROI for quantification. **B)** Quantification of the DNA fragmentation levels of 3 dpf *Spint1a*-deficient larvae. The violin plots with the median shown as a horizontal line show the distribution of AO⁺ cells, and are overlaid with the raw data, where each dot represents an individual. The graph shows the accumulation of 3 independent experiments (N= 3). * $p < 0.05$ ** $p < 0.001$; **** $p < 0.0001$, according to Kruskal-Wallis followed by uncorrected Dunn's multiple comparison test. AO: acridine orange. ROI: region of interest. Scale bar: 500 μm .

Taken together, all these results highlight the anti-inflammatory effect of apigenin and genestein especially, in the context of chronic inflammation, so their preventive use against aging associated with chronic inflammation could be assessed.

Even though we had already shown that the larvae did not present premature aging, we decided to also evaluate the effect of some senolytics, not only dasatinib and navitoclax, but also venetoclax, as it has its target on a different target (Souers et al., 2013) (**Fig. 64**).

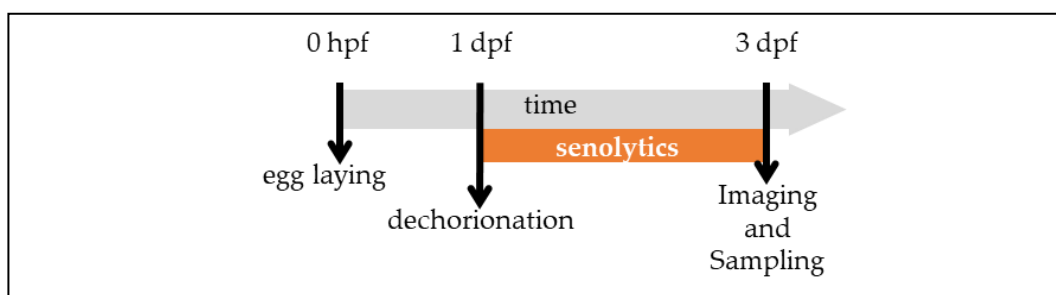


Figure 64. General workflow for the evaluation of senolytics in the *Spint1a*-deficient inflammaging model. 1 dpf *Spint1a*-deficient larvae were treated with senolytics for 3 days before imaging and sampling.

Surprisingly, treatment of larvae with dasatinib, navitoclax, and venetoclax for 48 h was able to decrease neutrophil dispersion, assayed in a transgenic line with labelled neutrophils (*lyz:DsRED2*) (Fig. 65).

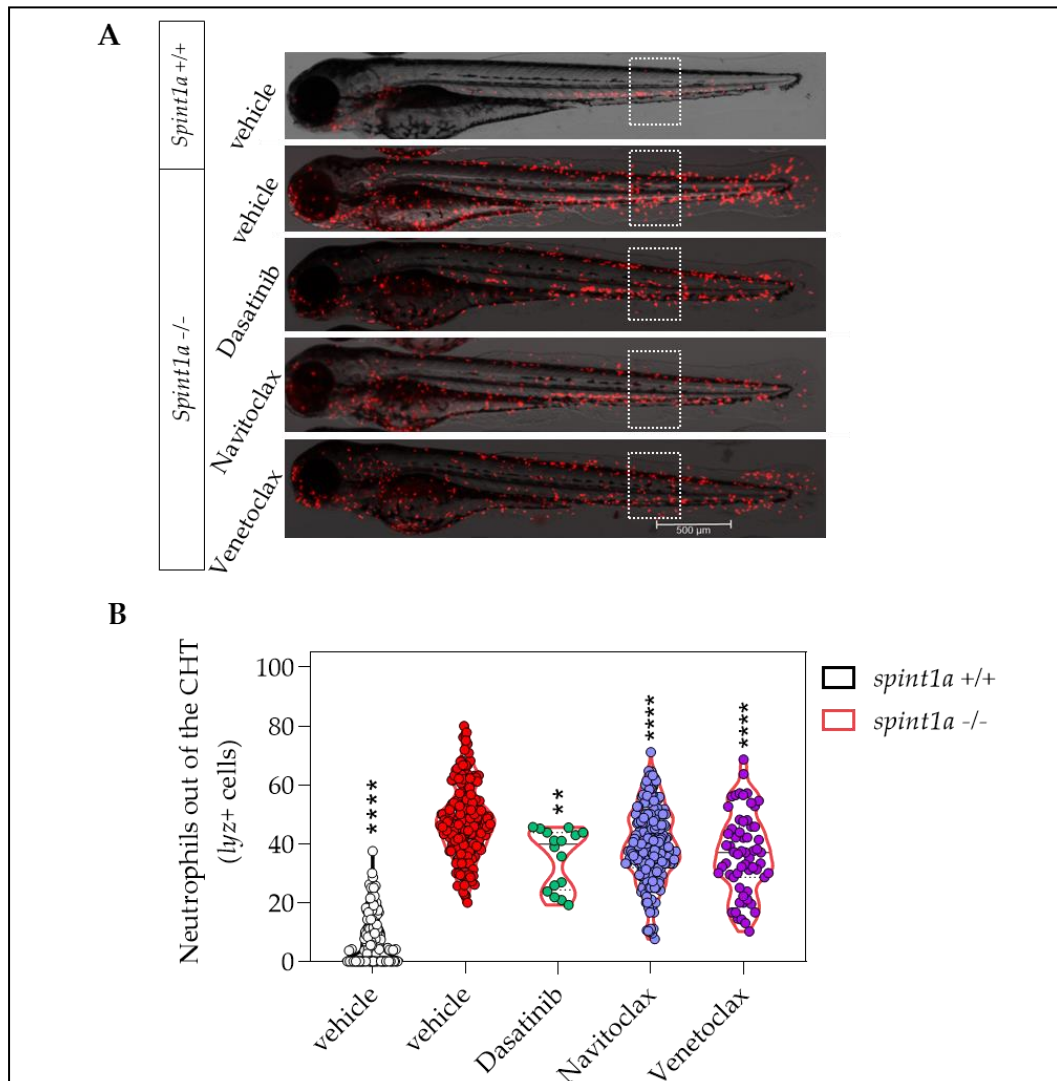


Figure 65. Senolytics ameliorate the skin inflammation phenotype of *Spint1a*-deficient larvae. **A)** Representative images of neutrophil phenotype of 3 dpf larvae with neutrophils labeled in red (*lyz:DsRED2*). Discontinuous white squares represent the ROI for quantification. **B)** Quantification of the number of neutrophils out of the CHT of 3 dpf larvae with neutrophils labeled in red (*lyz:DsRED2*). The violin plots with the median shown as a horizontal line show the distribution of *lyz*+ cells, and are overlaid with the raw data, where each dot represents an individual. The graph shows the accumulation of 3 independent experiments (N=3). ** $p < 0.01$; **** $p < 0.0001$ according to Kruskal-Wallis followed by uncorrected Dunn's multiple comparison test. ROI: region of interest. CHT: caudal hematopoietic tissue. Scale bar: 500 μ M.

The same effect was observed in the number of keratinocyte aggregates, although dasatinib was less potent than navitoclax and venetoclax (**Fig. 66**).

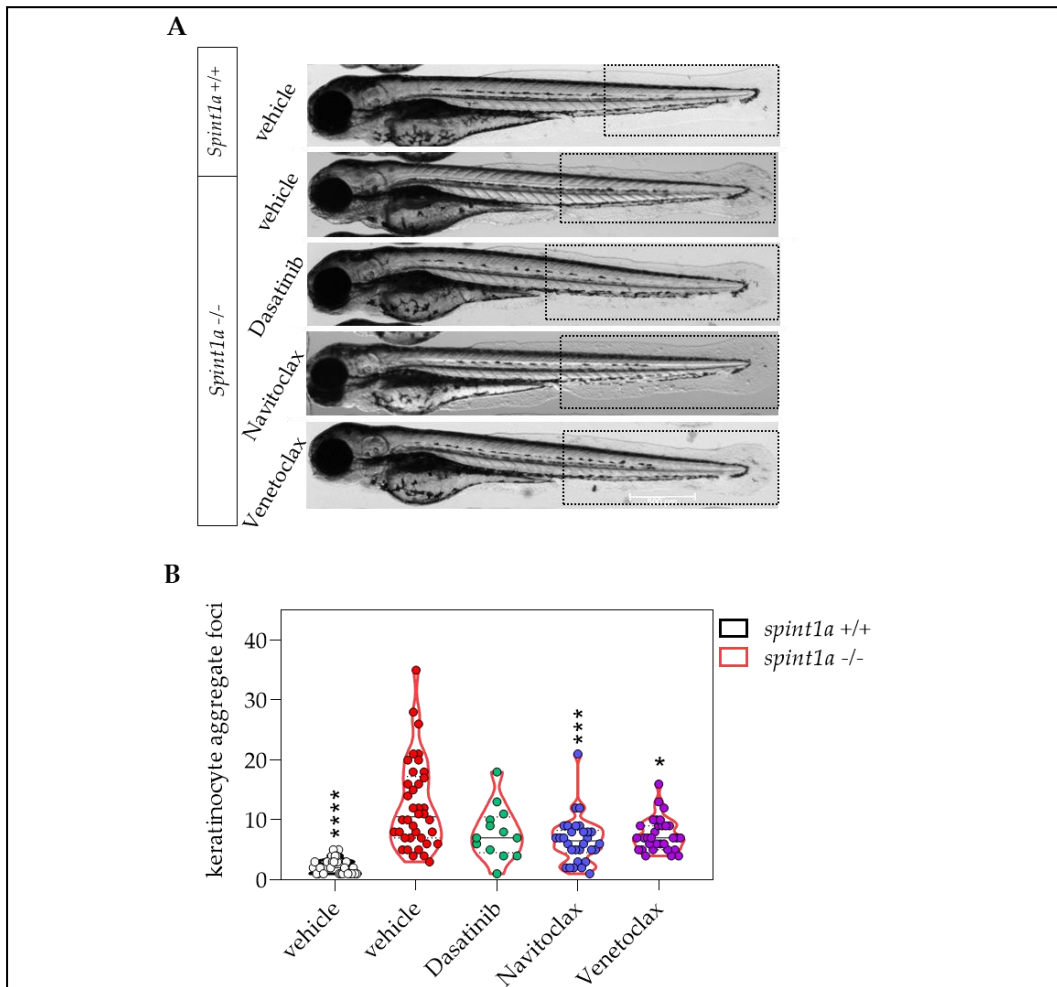


Figure 66. Senolytics ameliorate the skin inflammation phenotype of *Spint1a*-deficient larvae. **A)** Representative images of skin phenotype of 3 dpf larvae. Discontinuous black squares represent the ROI for quantification. **B)** Quantification of the keratinocyte aggregate foci at the skin of 3 dpf larvae. The violin plots with the median shown as a horizontal line show the distribution of keratinocyte aggregate foci, and are overlaid with the raw data, where each dot represents an individual. The graph shows the accumulation of 3 independent experiments (N=3). * $p < 0.05$; **** $p < 0.0001$ according to Kruskal-Wallis followed by uncorrected Dunn's multiple comparison test. ROI: region of interest. Scale bar: 500 μ M.

These results were further supported by the robust reduction of the mRNA levels of the genes encoding pro-inflammatory interleukin-1 (*Il1 β*), tumor necrosis factor alpha (*Tnf- α*), and chemokine (C-X-C motif) ligand 8b, duplicate 1 (*Cxcl8b.1*) by all senolytics, except for *tnf- α* by navitoclax (**Fig. 67**).

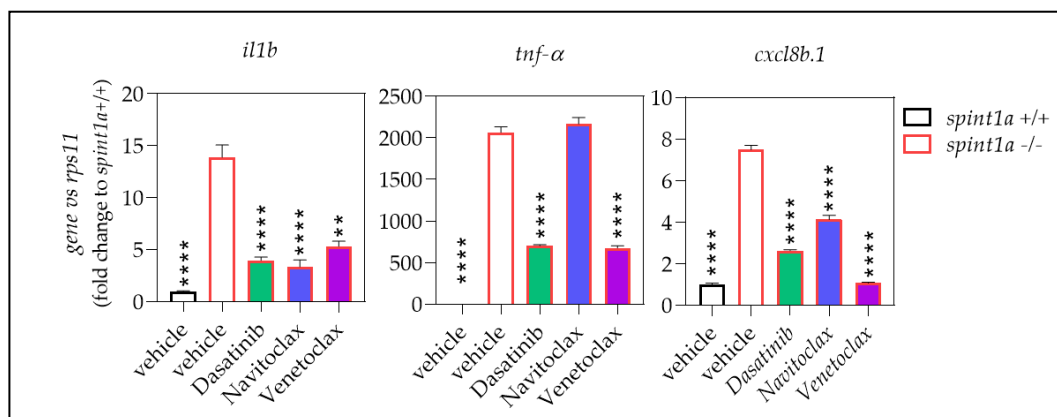


Figure 67. Senolytics ameliorate genes related to inflammation phenotype of *Spint1a*-deficient larvae. The mRNA level of *il1b*, *tnfa*, *cxcl8b.1* was determined by RT-qPCR and normalized against *rps11* in fin folds. The bars show the mean \pm SEM of 20 pooled larvae (n=20) and triplicate samples from 2 independent experiments (N=2). ** $p < 0.01$; **** $p < 0.0001$ according to Kruskal-Wallis followed by uncorrected Dunn's multiple comparison test.

Our results point to a new anti-inflammatory potential of dasatinib, navitoclax, and venetoclax in the context of chronic skin inflammation.

VI. DISCUSSION

VI – DISCUSSION

Advances in both public health and medicine have made it possible to increase life expectancy, but also the predisposition to many diseases associated with aging (Calvin B. et al., 1990). Currently, there is great interest in understanding the basic mechanisms that drive aging and the relationship between aging and age-related chronic diseases to slow or delay their onset, thus increasing healthy life expectancy (Kennedy et al., 2014). The main mechanism responsible for aging is the progressive telomere shortening that occurs through the process of replicative senescence (Blasco, 2005; López-Otín et al., 2013). At this point, cells enter a state of cellular senescence (*view section I.2*). As the immune system requires a high rate of cell proliferation and renewal to perform its functions correctly, telomere shortening is greatly affecting, leading to an immune-specific aging process known as immunosenescence (Goronzy et al., 2015; Pawelec, 2012; Wherry & Kurachi, 2015).

On the other hand, in older organisms it has been observed a chronic pro-inflammatory state, presents a low-grade inflammation with chronic activation of the innate immune system, which is called inflammation (Franceschi et al., 2000). This process has been cataloged as another molecular mechanism influencing aging along with telomere shortening. The processes of immunosenescence and chronic inflammation reflect a decrease in the capacity of the immune system to eliminate senescent cells (Antonangeli et al., 2019; Prata et al., 2018), thus leading to their accumulation in different tissues, which results in the appearance of many aging-related diseases (Childs et al., 2015; Bernardes de Jesus & Blasco, 2012).

Animal models are essential for aging research, both to study diseases at the organism level and, but not least, for drug development and repurposing. Nowadays, mammalian models are the most widely used due to the availability of a huge variety of preclinical models of human diseases (Hayden, 2014). During

clinical trials, many compounds have failed, the attrition rate reaches 96%, due to unfavorable ADMET (Administration, Distribution, Metabolism and Excretion), or because the research model is not well characterized (Lin et al., 2003). This fact triggers a large consumption of time, money, and human resources, which finally results in a lack of improvement in the health of patients. Therefore, the aim of this Thesis has been to make a synergy between *in silico* and *in vivo* research to help make the development of anti-aging drugs faster.

VI.1 In vivo zebrafish models of premature aging.

Due to its characteristics, the zebrafish is an excellent model to study aging, since the different molecular mechanisms associated with aging are highly conserved (Carneiro, de Castro, et al., 2016). As in aged humans, both telomere shortening and accumulation of senescent cells in different tissues occur in aged zebrafish (Carneiro et al., 2016; Dimri et al., 1995; Kishi et al., 2003). Since the study of aging is a long process, obtaining models of premature aging at short ages would be of great interest. For this reason, we have generated a model of shortened telomere-induced premature aging, termed as ST2 model, which is an improved version of the emblematic telomerase-deficient model (**Fig. 20C**). ST2 zebrafish larvae showed the main characteristics of shortened telomere-induced premature aging: i) reduced telomerase gene (*tert*) expression; ii) decreased telomerase activity; and iii) telomere attrition (**Fig. 20A, B**). Because of telomere shortening, we also observed an accumulation of senescent cells and an increase in oxidative stress levels in ST2 larvae compared to its wild-type (wt) counterpart. Associated with the above, ST2 model showed a greater cellular death, determined by both the DNA fragmentation level and the quantification of mRNA levels of different genes related to cell cycle arrest such as *p53* and *p21*, or related to cell survival like *bcl-2* (**Fig. 23**). As a result of these signs of premature aging, the ST2 line died

prematurely during the larval stage (**Fig. 24**), which is a great advantage for studying aging. Altogether, these results validate the ST2 model as an excellent model of premature aging in larvae that can be very useful for the rapid evaluation of the anti-aging effect of molecules through drug screening by using as read out, for instance, telomere length or survival.

On the other hand, it has been observed that child cancer survivors develop premature aging and show a shortened life expectancy (Armenian et al., 2019; Guida et al., 2021). Because of the genotoxic effect of chemotherapeutic drugs, the DNA is damaged, which induces aging (Ness & Wogksch, 2020). Therefore, until Science finds a better alternative than chemotherapy to treat cancer, it is necessary to identify new adjuvant molecules that help alleviate the toxic effects on healthy cells (Lin et al., 2019). To address aging from the point of view of DNA damage by an external agent, we generated a chemotherapy-induced DNA damage model, the QiDD model, by treating wild-type zebrafish larvae with different chemotherapeutic agents. As suspected, two cycles of chemotherapy in 3- and 5-pdf larvae were sufficient to trigger a significant telomere shortening that presumably caused a notable reduction in half-life and limited survival (**Fig. 27**), although we cannot rule out that this effect is a side effect of the treatment itself. This model can be very useful for the rapid evaluation and identification of new molecules that can be used as adjuvants to alleviate the aging effects of chemotherapy.

Aging can also be addressed from the context of chronic inflammation. In this sense, we used 2 different approaches.

The first one is in the context of metabolic inflammation, as it is known that nutrient excess is the main stimulus that triggers inflammaging (Franceschi et al., 2018; Gregor & Hotamisligil, 2011). We used a zebrafish larvae model of meta-inflammation induced by a high-cholesterol diet (HCD), originally described

as a non-alcoholic fatty liver disease/non-alcoholic steatohepatitis (NAFLD/NASH) zebrafish model, where the HCD promotes non-resolving inflammation in the liver and enhances cancer progression (de Oliveira et al., 2019). Although this state of metabolic inflammation was not sufficient to induce premature aging in larvae, as they did not exhibit telomere shortening (**Fig. 30**), the model allows a search for preventive treatments.

The second model is a chronic skin inflammation model, the *Spint1a*-deficient model. During the first week of life, larvae show characteristics of the inflammation process such as neutrophil infiltration in the skin, keratinocyte aggregate foci, epithelial integrity disruption, and high cell death levels (Carney et al., 2007; Mathias et al., 2007) through parthanatos cell death as a consequence of hyperactivation of PARP1 in response to ROS-induced DNA damage (Martínez-Morcillo et al., 2021). Again, this state of chronic skin inflammation was not sufficient to induce premature aging in larvae, as they did not exhibit telomere shortening or increased cellular senescence (**Fig. 31**), so we cannot say *Spint1a*-deficient larvae is a model of inflammaging, at least at the time assayed, but a model of chronic inflammation in a stage prior the induction of senescence. So, with this model we can search new anti-inflammatory drugs.

VI.2 Evaluation of the anti-aging potential of resveratrol and navitoclax in the ST2 model. A proof of concept.

The search for molecules with a potential anti-aging effect is necessary to reduce the burden of age-related diseases and disabilities to increase healthy life expectancy (Kennedy et al., 2014). As a starting point, we decided to evaluate the effects of two reference molecules, resveratrol, and navitoclax, in our ST2 premature aging model. Resveratrol and navitoclax represent polyphenols and senolytics, respectively, which have been widely studied and proposed to treat

aging (Gutlapalli et al., 2020; Li et al., 2018). As expected, navitoclax was able to reduce the senescence-associated β -gal positive area compared to untreated ST2 control (**Fig. 35**). Regarding telomere biology, the treatment with resveratrol increased both the mRNA level of *tert* and telomerase activity and the telomere length. However, the induction of *tert* expression produced by treatment with navitoclax, had no repercussion on telomerase activity or telomere length (**Fig. 16**). As a response to the effect of resveratrol on telomere length, we observed a significant reduction in the DNA fragmentation level (**Fig. 18**), which ultimately translated into an increased half-life of ST2 larvae by 12.5% and survival by 6.25% (**Fig. 19**). At this point, we considered using resveratrol and navitoclax as references to carry out an *in silico* scrutiny and discover molecules derived from them.

VI.3 *In silico* discovery of new drugs with anti-aging potential.

Virtual Screening (VS) is the main technique used for *in silico* discovery of new drugs. VS can be performed in a fast and low-cost manner, as there are several docking programs and other tools that are free for academic use. VS not only significantly increases the identification of potential drugs but also reduces the number of molecules screened significantly, from millions to tens. As resveratrol is a natural antioxidant approved by the FDA to reduce cellular damage and prolong the healthspan, as has also been confirmed in the ST2 model of premature aging, we used it as a reference to look for other natural antioxidants by VS.

After several VS calculations based on the similarity of both the structure and pharmacophoric properties compared to resveratrol, we obtained a list of 10 natural antioxidant compounds with anti-aging potential out of a total of 10000 (**Fig. 21**). These compounds would have also the ability to bind to TERT (**Fig. 22**), favoring its biological function and, therefore, were candidates for screening in aging models of zebrafish. Another molecule that is a firm candidate to fight

against aging is navitoclax, which has senolytic properties (Mohamad Anuar et al., 2020). We performed the same *in silico* screening process with navitoclax as the reference molecule. However, due to the high structural and pharmacophoric complexity of the molecule, we could not find any molecule with enough structural or pharmacophoric characteristics in common with navitoclax (**Fig. 23**). At this point, we decided to try another reference senolytic called dasatinib (Breccia & Alimena, 2011; Chan et al., 2012; Montero et al., 2011) but, again, the complexity of the molecule did not allow us to get positive results (**Fig. 25**).

Zebrafish is a promising and unique model in that it offers the opportunity of screening quickly and cost-effectively under *in vivo* conditions, bridging the gap between *in vitro* and rodent studies. The in tandem work of VS and zebrafish aging models allows the testing of selected compounds with anti-aging potential in the context of an *in vivo* organism, making it possible to advance candidate molecules to clinical trials in a shorter time frame.

VI.4 *In vivo* validation of candidates with anti-aging potential in different aging zebrafish models for repurposing.

The next step was the *in vivo* evaluation of the anti-aging effect of VS candidate natural antioxidant molecules in the different zebrafish models described above. The candidates have been already cataloged as anti-aging and anti-inflammatory compounds (Jiang et al., 2016). Naringenin participates in the regulation of INS/IGF-1, a pathway that influences the life expectancy of different organisms including humans. In addition, both naringenin and apigenin act by producing a decrease of ROS and oxidative stress level (Lim & Kim, 2018; Qin et al., 2016). On the other hand, quercetin participates in pathways directly related to aging (Jiang et al., 2016). Genestein and sakuranetin, are also related to the reduction of oxidative stress (Charles et al., 2014). Hesperetin protects neurons

against H₂O₂-induced apoptosis and reduces oxidative damage (Pan et al., 2012). Liquiritigenin and tricetin have anti-inflammatory properties (Majidinia et al., 2020).

Once assessed the toxicity, isoliquiritigenin and kaempferol were discarded, so we evaluated the anti-aging effects of the rest of candidates in the ST2 premature aging model. Unfortunately, none of the molecules behaved like resveratrol. However, some of them caught our attention: apigenin, despite good VS results, did not affect neither telomerase activity, nor telomere length; hesperetin and naringenin had conflicting effects on telomerase activity and telomere length, and both sakuranetin and tricetin induced telomerase activity, but without affecting telomere length (**Fig. 28**). Then, we selected apigenin, naringenin, sakuranetin, and resveratrol to check their effect on ST2 life expectancy. Hesperetin and tricetin were not available for a while and we decided to continue the study without them. The results on survival were consistent with telomere length, except in the case of apigenin, which was able to increase half-life by 12.5% despite not lengthening telomeres (**Fig. 29**)

Nowadays, chemotherapy is the most common cancer treatment despite chemotherapeutic drugs are genotoxic (Ness & Wogksch, 2020) agents and their effectiveness are limited. Moreover, cancer survivors, and especially childhood cancer survivors, show premature aging and their life expectancy is reduced because of the DNA damage produced by these drugs. Therefore, it is necessary to search for new anti-aging adjuvant compounds for the treatment of cancer (Abaza et al., 2015). Therefore, we performed the treatment of the chemotherapy-induced DNA damage-induced premature aging (QiDD) larvae with five different chemotherapeutic agents in combination with the candidates apigenin, naringenin, resveratrol and sakuranetin. We evaluated the anti-aging adjuvant effects on larval survival compared to chemotherapeutics alone. The results showed a clear and

beneficial effect on survival when naringenin was co-treated with all chemotherapeutic compounds but methotrexate. However, the effects of apigenin, resveratrol, and sakuranetin were not as robust, but dependent on the chemotherapeutic agent they combined with (**Table IV**). These results are in line with other studies. Naringenin has been reported to present many protective effects, such as anti-inflammatory, antioxidant, anti-atherogenic, anti-cancer, and neuroprotective, and significantly reduces the DNA damage induced by chemotherapy (Ganaie et al., 2019). The use of naringenin and metformin in combination the chemotherapeutic agent doxorubicin results in an improved tumor activity compared to doxorubicin alone (Pateliya et al., 2021). On the other hand, the use of apigenin and resveratrol as chemoprotective agents has also been recently reported (Xiao et al., 2019). Regarding sakuranetin, several studies have shown not only its protective role against chemotherapy, but also its anti-cancer role, through induction of cancer cell death by apoptosis both *in vitro* and *in vivo* experiments (Stompor, 2020).

We also had the chance to assess the effect of some candidates in the context of chronic inflammation. First, by using the zebrafish model of metainflammation induced by a high cholesterol diet (HCD), we showed a reduction of both neutrophils and macrophages after apigenin, naringenin and sakuranetin treatment, confirming their anti-inflammatory properties. This result led us to evaluate the anti-inflammatory effect of natural antioxidants on the chronic skin inflammation of Spint1a-deficient model. We identified apigenin, naringenin, sakuranetin and tricetin as the molecules with the greatest effect on reducing neutrophil infiltration in the skin (**Fig. 42**). Contrary to resveratrol, genestein, naringenin and sakuranetin were also able to decrease the keratinocyte aggregates (**Fig. 43**). Again, apigenin and genestein were effective in reducing oxidative stress (**Fig. 44**). The list of successful candidates increased by 50% with the measurement

of cell death level, being apigenin, genestein and hesperetin those who reduced it the most (**Fig. 45**). In general, all these results highlight the anti-inflammatory effect of most natural antioxidants in the context of chronic inflammation, their preventive use to avoid the possible development of chronic inflammation-induced aging could be assessed. Finally, despite the little success of the *in silico* screening using navitoclax and dasatinib as a reference, we did not want to miss the opportunity to test the effect of navitoclax in the context of metainflammation. Surprisingly, navitoclax dampened emergency myelopoiesis by reversing neutrophilia and monocytosis (**Fig. 39**), but without reversing the inflammation-related genes *il1b*, *tnfa*, and *cxcl8b.1* (**Fig. 40**). These results are not fully unexpected, since navitoclax has been shown to effectively remove senescent bone marrow hematopoietic stem cells (HSCs) in aged mice, mitigating premature aging of the hematopoietic system (Chang et al., 2016). Therefore, our results pave the way for future studies aimed at investigating whether emergency hematopoiesis promotes the senescence of HSCs or navitoclax can regulate hematopoiesis by a senolytic-independent mechanism.

These results prompted us to assess the effect of not only navitoclax, but dasatinib and venetoclax in the *Spint1a*-deficient zebrafish chronic skin inflammation model. Accordingly, two days of treatment with the senolytics dasatinib, navitoclax, and venetoclax was sufficient to ameliorate the phenotype of skin inflammation in terms of neutrophil skin infiltration, keratinocyte aggregate foci, and the mRNA levels of genes encoding major proinflammatory cytokines (**Fig. 47-49**). To date, dasatinib, navitoclax, and venetoclax are well documented as drugs with senolytic activity, inducing apoptosis, specifically in senescent cells (Montero et al., 2011; Souers et al., 2013; Tse et al., 2008). Although their senolytic activity usually ameliorates inflammation by reducing the senescence-associated secretory phenotype (SASP), which is associated with inflammation, senolytic-

independent anti-inflammatory activities have not been reported to date. However, it is not uncommon for a molecule to have different properties. In fact, the senolytic potential of curcumin on senescent intervertebral disc cells by reducing the SASP and back pain by modulating the Nrf2 and NF- κ B pathways has been recently reported (Cherif et al., 2019; Mantzorou et al., 2018). In addition, curcumin has also been demonstrated to be effective as adjuvant therapy for psoriasis, reducing skin inflammation and serum IL-22 levels (Antiga et al., 2015), these effects being independent of its senolytic activity. Something similar occurs with quercetin, which has been shown to reduce the inflammatory response in patients undergoing coronary artery bypass surgery following an acute coronary syndrome and improves endothelial function by eliminating senescent vascular endothelial cells (Dagher et al., 2021). The multipurpose properties of these nutraceuticals support our results, which point to an anti-inflammatory effect of dasatinib, navitoclax, and venetoclax, acting even before the cell surrounded by a chronic inflammatory microenvironment becomes senescent. Although the mechanism for this new anti-inflammatory effect is not yet sufficiently detailed and more experiments are needed, these drugs could be repurposed as anti-inflammatory agents to treat chronic inflammatory disorders.

VII. CONCLUSIONS

CONCLUSIONS

The result obtained in this work lead to the following conclusions:

1. Zebrafish models with telomeric shortening, either due to telomerase deficiency or to exposure to chemotherapeutic agents, constitute an ideal model for anti-aging drugs screening. The ST2 larvae model has demonstrated its validity for screening by means of a pilot trial with antioxidant (resveratrol) and senolytic (navitoclax) reference molecules.
2. Spint1a-deficient zebrafish model and larvae fed with a high cholesterol diet (HCD) model do not show cellular senescence or premature aging. Therefore, they are not models of chronic inflammation-induced aging, at least up to the short times observed.
3. A list of natural antioxidant compounds has been identified by virtual screening techniques using resveratrol as reference molecule.
4. Polyphenols do not show a clear role in the rescue of aging markers in ST2 models.
5. In models of premature aging due to exposure to chemotherapy, a protective effect of polyphenols was observed on co-treatment. The effect of each polyphenol depends on the therapeutic agent. In general, we can say that narigenin is the polyphenol with the best protection against most of the chemotherapeutic tested.
6. Apigenin and sakuranetin show anti-inflammatory activity in models of chronic inflammation, improving the phenotypes in both cases.
7. Dasatinib, navitoclax and venetoclax show anti-inflammatory effects independent of their senolytic activity. Thus, they can reduce chronic inflammation in zebrafish models that do not.

VIII. LIMITACIONES Y FUTURAS LINEAS DE INVESTIGACIÓN

Limitaciones:

La limitación principal del estudio del envejecimiento es que se trata de un proceso lento que consume tiempo. Por tanto, la obtención de resultados también lleva tiempo ya que se precisa que los modelos animales envejezcan. Para resolver ese problema, uno de los objetivos de esta Tesis Doctoral fue generar modelos que mostraran los síntomas de envejecimiento precozmente. En concreto buscábamos un envejecimiento prematuro en las primeras semanas de vida de las larvas, lo que no sólo permite ver antes los fenotipos de envejecimiento, sino que además facilitaba su utilización en escrutinios de manera rápida y sencilla.

Otra limitación de la Tesis es la correcta elección de los compuestos de referencia "rejuvenecedores" para hacer un cribado virtual y posteriormente un cribado *in vivo*. Muchas son las moléculas que se han descrito que tienen un efecto beneficioso en el organismo, entre ellas los polifenoles y los senolíticos. En un escrutinio siempre está el riesgo de no tener éxito. Con el fin de aumentar la probabilidad de encontrar moléculas rejuvenecedoras se eligieron dos senolíticos y un polifenol como moléculas de referencia, y además se establecieron hasta 4 modelos de envejecimiento prematuro (2 por acortamiento telomérico y 2 por inflamación crónica)

A pesar de que los tiempos de envejecimiento de las larvas se redujeron a dos semanas, la reversión de los fenotipos por los tratamientos es compleja. No se conoce la dosis correcta de los compuestos, todos los experimentos son *in vivo* y requieren de ensayos complejos que además necesitan de análisis de imagen. Se precisa cruces constantes de las distintas líneas modificadas para la obtención de gran cantidad de larvas lo que a veces no se consigue semanalmente.

Futuras líneas de investigación:

En vista de los resultados, se abren nuevas líneas de investigación.

Se precisa una mejor caracterización de otros procesos, entre ellos las capacidades cognitivas, ya que uno de los síntomas de envejecimiento es la pérdida progresiva de las mismas.

Se estudiará el mecanismo molecular por el que los compuestos ejercen su función protectora sobre los diferentes modelos de envejecimiento prematuro. Posiblemente el más interesante sea el efecto protector de los compuestos antioxidantes cuando se co-trata con quimioterapéuticos. Los supervivientes de cáncer, especialmente los pediátricos, después de conseguir vencer a esta temible enfermedad, ven acortada la esperanza de vida y la calidad debido a los efectos severos de los tratamientos oncológicos. Por tanto, es de especial importancia entender cómo ejerce esa función y poder disponer de ellos para estos pacientes.

Una vez conocido el mecanismo molecular podría revelar nuevas dianas terapéuticas, que podrían ser objeto de escrutinios *in silico* y revelar nuevos compuestos a ensayar *in vivo*.

Por último, sería deseable proponer el mejor candidato para un ensayo clínico, donde se puedan evaluar los efectos beneficiosos en la salud de las personas.

IX. REFERENCES

IX-References

- Abad, J. P., de Pablos, B., Agudo, M., Molina, I., Giovinazzo, G., Martín-Gallardo, A., & Villasante, A. (2004). Genomic and cytological analysis of the Y chromosome of *Drosophila melanogaster*: Telomere-derived sequences at internal regions. *Chromosoma*, *113*(6), 295–304. <https://doi.org/10.1007/s00412-004-0318-0>
- Abaza, M. S. I., Orabi, K. Y., Al-Quattan, E., & Al-Attiyah, R. J. (2015). Growth inhibitory and chemo-sensitization effects of naringenin, a natural flavanone purified from *Thymus vulgaris*, on human breast and colorectal cancer. *Cancer Cell International*, *15*(1). <https://doi.org/10.1186/s12935-015-0194-0>
- Albuquerque-gonzález, B., Bernabé-garcía, Á., Bernabé-garcía, M., Ruiz-sanz, J., López-calderón, F. F., Gonnelli, L., Banci, L., Peña-garcía, J., Luque, I., Nicolás, F. J., Cayuela-fuentes, M. L., Luchinat, E., Pérez-sánchez, H., Montoro-garcía, S., & Conesa-zamora, P. (2021). The fda-approved antiviral raltegravir inhibits fascin1-dependent invasion of colorectal tumor cells in vitro and in vivo. *Cancers*, *13*(4), 1–22. <https://doi.org/10.3390/cancers13040861>
- Albuquerque-González, B., Bernabé-García, M., Montoro-García, S., Bernabé-García, Á., Rodrigues, P. C., Ruiz Sanz, J., López-Calderón, F. F., Luque, I., Nicolas, F. J., Cayuela, M. L., Salo, T., Pérez-Sánchez, H., & Conesa-Zamora, P. (2020). New role of the antidepressant imipramine as a Fascin1 inhibitor in colorectal cancer cells. *Experimental and Molecular Medicine*, *52*(2), 281–292. <https://doi.org/10.1038/s12276-020-0389-x>
- Algire, C., Moiseeva, O., Deschênes-Simard, X., Amrein, L., Petruccelli, L., Birman, E., Viollet, B., Ferbeyre, G., & Pollak, M. N. (2012). Metformin reduces endogenous reactive oxygen species and associated DNA damage. *Cancer Prevention Research*, *5*(4), 536–543. <https://doi.org/10.1158/1940-6207.CAPR-11-0536>
- Aloufi, B. H., Snoussi, M., & Sulieman, A. M. E. (2022). Antiviral Efficacy of Selected Natural Phytochemicals against SARS-CoV-2 Spike Glycoprotein Using Structure-Based Drug Designing. *Molecules*, *27*(8), 2401. <https://doi.org/10.3390/molecules27082401>
- Alshinnawy, A. S., El-Sayed, W. M., Sayed, A. A. A., Salem, A. M., & Taha, A. S. M. (2021). Telomerase activator-65 and pomegranate peel improved the health status of the liver in aged rats; Multi-targets involved. *Iranian Journal of Basic Medical Sciences*, *24*(6), 842–850. <https://doi.org/10.22038/ijbms.2021.56670.12655>

- Anchelin, M., Alcaraz-Pérez, F., Martínez, C. M., Bernabé-García, M., Mulero, V., & Cayuela, M. L. (2013). Premature aging in telomerase-deficient zebrafish. *DMM Disease Models and Mechanisms*, 6(5), 1101–1112. <https://doi.org/10.1242/dmm.011635>
- Anchelin, M., Murcia, L., Alcaraz-Pérez, F., García-Navarro, E. M., & Cayuela, M. L. (2011). Behaviour of telomere and telomerase during aging and regeneration in zebrafish. *PLoS ONE*, 6(2). <https://doi.org/10.1371/journal.pone.0016955>
- Angarola, B. L., & Anczuków, O. (2021). Splicing alterations in healthy aging and disease. In *Wiley Interdisciplinary Reviews: RNA* (Vol. 12, Issue 4). Blackwell Publishing Ltd. <https://doi.org/10.1002/wrna.1643>
- Antiga, E., Bonciolini, V., Volpi, W., del Bianco, E., & Caproni, M. (2015). Oral curcumin (meriva) is effective as an adjuvant treatment and is able to reduce IL-22 serum levels in patients with psoriasis vulgaris. *BioMed Research International*, 2015. <https://doi.org/10.1155/2015/283634>
- Antonangeli, F., Zingoni, A., Soriani, A., & Santoni, A. (2019). Senescent cells: Living or dying is a matter of NK cells. In *Journal of Leukocyte Biology* (Vol. 105, Issue 6, pp. 1275–1283). John Wiley and Sons Inc. <https://doi.org/10.1002/JLB.MR0718-299R>
- Armenian, S. H., Gibson, C. J., Rockne, R. C., & Ness, K. K. (2019). Premature aging in young cancer survivors. In *Journal of the National Cancer Institute* (Vol. 111, Issue 3, pp. 226–232). Oxford University Press. <https://doi.org/10.1093/jnci/djy229>
- Arriola Apelo, S. I., & Lamming, D. W. (2016). Rapamycin: An InhibiTOR of aging emerges from the soil of Easter island. In *Journals of Gerontology - Series A Biological Sciences and Medical Sciences* (Vol. 71, Issue 7, pp. 841–849). Oxford University Press. <https://doi.org/10.1093/gerona/glw090>
- Barzilai, N., Crandall, J. P., Kritchevsky, S. B., & Espeland, M. A. (2016). Metformin as a Tool to Target Aging. In *Cell Metabolism* (Vol. 23, Issue 6, pp. 1060–1065). Cell Press. <https://doi.org/10.1016/j.cmet.2016.05.011>
- Bassing, C. H., Swat, W., & Alt, F. W. (2002). The Mechanism and Regulation of Chromosomal V(D)J Recombination cessibility control, for example as related to transcrip-tion, replication, and repair, is a broadly relevant biologi-cal process. Herein, we review our current understanding. In *Cell* (Vol. 109).
- Batandier, C., Guigas, B., Detaille, D., El-Mir, M., Fontaine, E., Rigoulet, M., & Leverve, X. M. (2006). The ROS production induced by a reverse-electron flux at respiratory-chain complex 1 is hampered by metformin. *Journal of Bioenergetics and Biomembranes*, 38(1), 33–42. <https://doi.org/10.1007/s10863-006-9003-8>

- Batool, M., Ahmad, B., & Choi, S. (2019). A structure-based drug discovery paradigm. In *International Journal of Molecular Sciences* (Vol. 20, Issue 11). MDPI AG. <https://doi.org/10.3390/ijms20112783>
- Bauer, B., Mally, A., & Liedtke, D. (2021). Zebrafish embryos and larvae as alternative animal models for toxicity testing. In *International Journal of Molecular Sciences* (Vol. 22, Issue 24). MDPI. <https://doi.org/10.3390/ijms222413417>
- Bender, B. J., Gahbauer, S., Luttens, A., Lyu, J., Webb, C. M., Stein, R. M., Fink, E. A., Balius, T. E., Carlsson, J., Irwin, J. J., & Shoichet, B. K. (2021). A practical guide to large-scale docking. In *Nature Protocols* (Vol. 16, Issue 10, pp. 4799–4832). Nature Research. <https://doi.org/10.1038/s41596-021-00597-z>
- Berman, H. M., Westbrook, J., Feng, Z., Gilliland, G., Bhat, T. N., Weissig, H., Shindyalov, I. N., & Bourne, P. E. (2000). The Protein Data Bank. In *Nucleic Acids Research* (Vol. 28, Issue 1). <http://www.rcsb.org/pdb/status.html>
- Billard, C. (2013). BH3 mimetics: Status of the field and new developments. In *Molecular Cancer Therapeutics* (Vol. 12, Issue 9, pp. 1691–1700). <https://doi.org/10.1158/1535-7163.MCT-13-0058>
- Bitto, A., Ito, T. K., Pineda, V. v, LeTexier, N. J., Huang, H. Z., Sutlief, E., Tung, H., Vizzini, N., Chen, B., Smith, K., Meza, D., Yajima, M., Beyer, R. P., Kerr, K. F., Davis, D. J., Gillespie, C. H., Snyder, J. M., Treuting, P. M., & Kaeberlein, M. (2016). *Transient rapamycin treatment can increase lifespan and healthspan in middle-aged mice*. <https://doi.org/10.7554/eLife.16351.001>
- Blackburn, E. H. (2005). Telomeres and telomerase: Their mechanisms of action and the effects of altering their functions. *FEBS Letters*, 579(4 SPEC. ISS.), 859–862. <https://doi.org/10.1016/j.febslet.2004.11.036>
- Blasco, M. A. (2005). Telomeres and human disease: Ageing, cancer and beyond. In *Nature Reviews Genetics* (Vol. 6, Issue 8, pp. 611–622). <https://doi.org/10.1038/nrg1656>
- Bouz, G., & al Hasawi, N. (2018). The zebrafish model of tuberculosis - no lungs needed. In *Critical Reviews in Microbiology* (Vol. 44, Issue 6, pp. 779–792). Taylor and Francis Ltd. <https://doi.org/10.1080/1040841X.2018.1523132>
- Breccia, M., & Alimena, G. (2011). *Activity and Safety of Dasatinib as Second-Line Treatment or in Newly Diagnosed Chronic Phase Chronic Myeloid Leukemia Patients*.

- Brink, T. ten, & Exner, T. E. (2009). Influence of protonation, tautomeric, and stereoisomeric states on protein-ligand docking results. *Journal of Chemical Information and Modeling*, 49(6), 1535–1546. <https://doi.org/10.1021/ci800420z>
- Cabreiro, F., Au, C., Leung, K. Y., Vergara-Irigaray, N., Cochemé, H. M., Noori, T., Weinkove, D., Schuster, E., Greene, N. D. E., & Gems, D. (2013). Metformin retards aging in *C. elegans* by altering microbial folate and methionine metabolism. *Cell*, 153(1), 228–239. <https://doi.org/10.1016/j.cell.2013.02.035>
- Calado, R. T., & Dumitriu, B. (2013). Telomere dynamics in mice and humans. *Seminars in Hematology*, 50(2), 165–174. <https://doi.org/10.1053/j.seminhematol.2013.03.030>
- Calcinotto, A., Kohli, J., Zagato, E., Pellegrini, L., Demaria, M., & Alimonti, A. (2019). Cellular Senescence: Aging, Cancer, and Injury. *Physiol Rev*, 99, 1047–1078. <https://doi.org/10.1152/physrev.00020.2018.-Cellular>
- Calvin B., Harley A., Bruce Futcher, & Carol W. Greider. (1990). Telomeres shorten during ageing of human fibroblasts. *Nature*, 458–460.
- Candel, S., de Oliveira, S., López-Muñoz, A., García-Moreno, D., Espín-Palazón, R., Tyrkalska, S. D., Cayuela, M. L., Renshaw, S. A., Corbalán-Vélez, R., Vidal-Abarca, I., Tsai, H. J., Meseguer, J., Sepulcre, M. P., & Mulero, V. (2014). Tnfa Signaling Through Tnfr2 Protects Skin Against Oxidative Stress-Induced Inflammation. *PLoS Biology*, 12(5). <https://doi.org/10.1371/journal.pbio.1001855>
- Cao, W., Dou, Y., & Li, A. (2018). Resveratrol Boosts Cognitive Function by Targeting SIRT1. In *Neurochemical Research* (Vol. 43, Issue 9, pp. 1705–1713). Springer New York LLC. <https://doi.org/10.1007/s11064-018-2586-8>
- Carneiro, M. C., de Castro, I. P., & Ferreira, M. G. (2016). Telomeres in aging and disease: Lessons from zebrafish. In *DMM Disease Models and Mechanisms* (Vol. 9, Issue 7, pp. 737–748). Company of Biologists Ltd. <https://doi.org/10.1242/dmm.025130>
- Carneiro, M. C., Henriques, C. M., Nabais, J., Ferreira, T., Carvalho, T., & Ferreira, M. G. (2016). Short Telomeres in Key Tissues Initiate Local and Systemic Aging in Zebrafish. *PLoS Genetics*, 12(1). <https://doi.org/10.1371/journal.pgen.1005798>
- Carney, T. J., von der Hardt, S., Sonntag, C., Amsterdam, A., Topczewski, J., Hopkins, N., & Hammerschmidt, M. (2007). Inactivation of serine protease Matriptase1a by its inhibitor Hai1 is required for epithelial integrity of the zebrafish epidermis. *Development*, 134(19), 3461–3471. <https://doi.org/10.1242/dev.004556>

- Carosi, J. M., & Sargeant, T. J. (2019). Rapamycin and Alzheimer disease: a double-edged sword? In *Autophagy* (Vol. 15, Issue 8, pp. 1460–1462). Taylor and Francis Inc. <https://doi.org/10.1080/15548627.2019.1615823>
- Carpenter, K. A., Cohen, D. S., Jarrell, J. T., & Huang, X. (2018). Deep learning and virtual drug screening. In *Future Medicinal Chemistry* (Vol. 10, Issue 21, pp. 2557–2567). Future Medicine Ltd. <https://doi.org/10.4155/fmc-2018-0314>
- Carregal, A. P., Maciel, F. v., Carregal, J. B., dos Reis Santos, B., da Silva, A. M., & Taranto, A. G. (2017). Docking-based virtual screening of Brazilian natural compounds using the OOMT as the pharmacological target database. *Journal of Molecular Modeling*, 23(4). <https://doi.org/10.1007/s00894-017-3253-8>
- Cayuela, M. L., Claes, K. B. M., Ferreira, M. G., Henriques, C. M., van Eeden, F., Varga, M., Vierstraete, J., & Mione, M. C. (2019). The Zebrafish as an Emerging Model to Study DNA Damage in Aging, Cancer and Other Diseases. *Frontiers in Cell and Developmental Biology*, 6. <https://doi.org/10.3389/fcell.2018.00178>
- Chan, C. M., Jing, X., Pike, L. A., Zhou, Q., Lim, D. J., Sams, S. B., Lund, G. S., Sharma, V., Haugen, B. R., & Schweppe, R. E. (2012). Targeted inhibition of Src kinase with dasatinib blocks thyroid cancer growth and metastasis. *Clinical Cancer Research*, 18(13), 3580–3591. <https://doi.org/10.1158/1078-0432.CCR-11-3359>
- Chang, J., Wang, Y., Shao, L., Laberge, R. M., Demaria, M., Campisi, J., Janakiraman, K., Sharpless, N. E., Ding, S., Feng, W., Luo, Y., Wang, X., Aykin-Burns, N., Krager, K., Ponnappan, U., Hauer-Jensen, M., Meng, A., & Zhou, D. (2016). Clearance of senescent cells by ABT263 rejuvenates aged hematopoietic stem cells in mice. *Nature Medicine*, 22(1), 78–83. <https://doi.org/10.1038/nm.4010>
- Charles, C., Nachtergaeel, A., Ouedraogo, M., Belayew, A., & Duez, P. (2014). Effects of chemopreventive natural products on non-homologous end-joining DNA double-strand break repair. *Mutation Research - Genetic Toxicology and Environmental Mutagenesis*, 768, 33–41. <https://doi.org/10.1016/j.mrgentox.2014.04.014>
- Check Hayden, E. (2014). Misleading mouse studies waste medical resources. *Nature*. <https://doi.org/10.1038/nature.2014.14938>
- Cheng, T., Li, Q., Zhou, Z., Wang, Y., & Bryant, S. H. (2012). Structure-based virtual screening for drug discovery: A problem-centric review. In *AAPS Journal* (Vol. 14, Issue 1, pp. 133–141). <https://doi.org/10.1208/s12248-012-9322-0>
- Cherif, H., Bisson, D. G., Jarzem, P., Weber, M., Ouellet, J. A., & Haglund, L. (2019). Curcumin and o-vanillin exhibit evidence of senolytic activity in human ivd cells in vitro. *Journal of Clinical Medicine*, 8(4). <https://doi.org/10.3390/jcm8040433>

- Childs, B. G., Durik, M., Baker, D. J., & van Deursen, J. M. (2015). Cellular senescence in aging and age-related disease: From mechanisms to therapy. In *Nature Medicine* (Vol. 21, Issue 12, pp. 1424–1435). Nature Publishing Group.
<https://doi.org/10.1038/nm.4000>
- Cho, K., Chung, J. Y., Cho, S. K., Shin, H. W., Jang, I. J., Park, J. W., Yu, K. S., & Cho, J. Y. (2015). Antihyperglycemic mechanism of metformin occurs via the AMPK/LXR α /POMC pathway. *Scientific Reports*, 5.
<https://doi.org/10.1038/srep08145>
- Chung, C. L., Lawrence, I., Hoffman, M., Elgindi, D., Nadhan, K., Potnis, M., Jin, A., Sershon, C., Binnebose, R., Lorenzini, A., & Sell, C. (2019). Topical rapamycin reduces markers of senescence and aging in human skin: an exploratory, prospective, randomized trial. *GeroScience*, 41(6), 861–869.
<https://doi.org/10.1007/s11357-019-00113-y>
- Chung, H. Y., Lee, E. K., Choi, Y. J., Kim, J. M., Kim, D. H., Zou, Y., Kim, C. H., Lee, J., Kim, H. S., Kim, N. D., Jung, J. H., & Yu, B. P. (2011). Molecular inflammation as an underlying mechanism of the aging process and age-related diseases. In *Journal of Dental Research* (Vol. 90, Issue 7, pp. 830–840).
<https://doi.org/10.1177/0022034510387794>
- Clemens A. Schmitt, Jordan S. Fridman, Meng Yang, Soyoung Lee, Eugene Baranov, Robert M. Hoffman, & Scott W. Lowe. (2002). *A Senescence Program Controlled by p53 and p16INK4a Contributes to the Outcome of Cancer Therapy*. <http://www.cell.com>
- Cournia, Z., Allen, B. K., Beuming, T., Pearlman, D. A., Radak, B. K., & Sherman, W. (2020). Rigorous free energy simulations in virtual screening. In *Journal of Chemical Information and Modeling* (Vol. 60, Issue 9, pp. 4153–4169). American Chemical Society. <https://doi.org/10.1021/acs.jcim.0c00116>
- Cox, L. S., & Mason, P. A. (2010). Prospects for rejuvenation of aged tissue by telomerase reactivation. *Rejuvenation Research*, 13(6), 749–754.
<https://doi.org/10.1089/rej.2010.1140>
- Dagher, O., Mury, P., Noly, P.-E., Fortier, A., Lettre, G., Thorin, E., & Carrier, M. (2021). Design of a Randomized Placebo-Controlled Trial to Evaluate the Anti-inflammatory and Senolytic Effects of Quercetin in Patients Undergoing Coronary Artery Bypass Graft Surgery. *Frontiers in Cardiovascular Medicine*, 8.
<https://doi.org/10.3389/fcvm.2021.741542>

- de Cabo, R., & Mattson, M. P. (2019). Effects of Intermittent Fasting on Health, Aging, and Disease. *New England Journal of Medicine*, 381(26), 2541–2551. <https://doi.org/10.1056/nejmra1905136>
- de Jesus, B. B., & Blasco, M. A. (2012a). Assessing cell and organ senescence biomarkers. In *Circulation research* (Vol. 111, Issue 1, pp. 97–109). <https://doi.org/10.1161/CIRCRESAHA.111.247866>
- de Jesus, B. B., & Blasco, M. A. (2012b). Potential of telomerase activation in extending health span and longevity. In *Current Opinion in Cell Biology* (Vol. 24, Issue 6, pp. 739–743). <https://doi.org/10.1016/j.ceb.2012.09.004>
- de Jesus, B. B., Schneeberger, K., Vera, E., Tejera, A., Harley, C. B., & Blasco, M. A. (2011). The telomerase activator TA-65 elongates short telomeres and increases health span of adult/old mice without increasing cancer incidence. *Aging Cell*, 10(4), 604–621. <https://doi.org/10.1111/j.1474-9726.2011.00700.x>
- de Magalhães, J. P., & Passos, J. F. (2018). Stress, cell senescence and organismal ageing. In *Mechanisms of Ageing and Development* (Vol. 170, pp. 2–9). Elsevier Ireland Ltd. <https://doi.org/10.1016/j.mad.2017.07.001>
- de Oliveira, S., Boudinot, P., Calado, Â., & Mulero, V. (2015). Duox1-Derived H₂O₂ Modulates Cxcl8 Expression and Neutrophil Recruitment via JNK/c-JUN/AP-1 Signaling and Chromatin Modifications. *The Journal of Immunology*, 194(4), 1523–1533. <https://doi.org/10.4049/jimmunol.1402386>
- de Oliveira, S., Houseright, R. A., Graves, A. L., Golenberg, N., Korte, B. G., Miskolci, V., & Huttenlocher, A. (2019). Metformin modulates innate immune-mediated inflammation and early progression of NAFLD-associated hepatocellular carcinoma in zebrafish. *Journal of Hepatology*, 70(4), 710–721. <https://doi.org/10.1016/j.jhep.2018.11.034>
- Debnath, S., Debnath, T., Bhaumik, S., Majumdar, S., Kalle, A. M., & Aparna, V. (2019). Discovery of novel potential selective HDAC8 inhibitors by combine ligand-based, structure-based virtual screening and in-vitro biological evaluation. *Scientific Reports*, 9(1). <https://doi.org/10.1038/s41598-019-53376-y>
- DeCensi, A., Puntoni, M., Goodwin, P., Cazzaniga, M., Gennari, A., Bonanni, B., & Gandini, S. (2010). Metformin and cancer risk in diabetic patients: A systematic review and meta-analysis. *Cancer Prevention Research*, 3(11), 1451–1461. <https://doi.org/10.1158/1940-6207.CAPR-10-0157>
- Demaria, M., Ohtani, N., Youssef, S. A., Rodier, F., Toussaint, W., Mitchell, J. R., Laberge, R. M., Vijg, J., VanSteeg, H., Dollé, M. E. T., Hoeijmakers, J. H. J., deBruin, A., Hara,

- E., & Campisi, J. (2014). An essential role for senescent cells in optimal wound healing through secretion of PDGF-AA. *Developmental Cell*, 31(6), 722–733. <https://doi.org/10.1016/j.devcel.2014.11.012>
- Devi, R. V., Sathya, S. S., & Coumar, M. S. (2015). Evolutionary algorithms for de novo drug design - A survey. *Applied Soft Computing Journal*, 27, 543–552. <https://doi.org/10.1016/j.asoc.2014.09.042>
- Dimri, G. P., Lee, X., Basile, G., Acosta, M., Scott, G., Roskelley, C., Medrano, E. E., Linskens, M., Rubelj, I., Pereira-Smith, O., Peacocke, M., & Campisi, J. (1995). A Biomarker that Identifies Senescent Human Cells in Culture and in Aging Skin in vivo. In *Source* (Vol. 92, Issue 20). <http://www.jstor.orgURL:http://www.jstor.org/stable/2368471>
- Dimri, G. P., Leet, X., Basile, G., Acosta, M., Scorrt, G., Roskelley, C., Medrano, E. E., Linskensi, M., Rubeljii, I., Pereira-Smithii, O., Peacocket, M., Campisi, J., & Pardee, B. (1995). A biomarker that identifies senescent human cells in culture and in aging skin in vivo (replicative senescence/tumor suppression/18-galactosidase) Communicated by Arthur. In *Cell Bioiogy* (Vol. 92).
- Dow, C. T., & Harley, C. B. (2016). Evaluation of an oral telomerase activator for early age-related macular degeneration - A pilot study. *Clinical Ophthalmology*, 10, 243–249. <https://doi.org/10.2147/OPHTH.S100042>
- Duan, J., Dixon, S. L., Lowrie, J. F., & Sherman, W. (2010). Analysis and comparison of 2D fingerprints: Insights into database screening performance using eight fingerprint methods. *Journal of Molecular Graphics and Modelling*, 29(2), 157–170. <https://doi.org/10.1016/j.jmgm.2010.05.008>
- Dutkiewicz, Z., & Mikstacka, R. (2018). Structure-Based Drug Design for Cytochrome P450 Family 1 Inhibitors. In *Bioinorganic Chemistry and Applications* (Vol. 2018). Hindawi Limited. <https://doi.org/10.1155/2018/3924608>
- Eimon, P. M., & Rubinstein, A. L. (2009). The use of in vivo zebrafish assays in drug toxicity screening. In *Expert Opinion on Drug Metabolism and Toxicology* (Vol. 5, Issue 4, pp. 393–401). <https://doi.org/10.1517/17425250902882128>
- Ellett, F., Pase, L., Hayman, J. W., Andrianopoulos, A., & Lieschke, G. J. (2011). *mpeg1 promoter transgenes direct macrophage-lineage expression in zebrafish*. <https://doi.org/10.1182/blood-2010-10>
- Franceschi, C., Bonafè, M., Valensin, S., Olivieri, F., Luca, M. de, Ottaviani, E., & Benedictis, G. de. (2000). *Inflamm-aging An Evolutionary Perspective on Immunosenescence INTRODUCTION: THE NETWORK HYPOTHESIS OF AGING*.

- Franceschi, C., Garagnani, P., Parini, P., Giuliani, C., & Santoro, A. (2018). Inflammaging: a new immune–metabolic viewpoint for age-related diseases. In *Nature Reviews Endocrinology* (Vol. 14, Issue 10, pp. 576–590). Nature Publishing Group. <https://doi.org/10.1038/s41574-018-0059-4>
- Friesner, R. A., Banks, J. L., Murphy, R. B., Halgren, T. A., Klicic, J. J., Mainz, D. T., Repasky, M. P., Knoll, E. H., Shelley, M., Perry, J. K., Shaw, D. E., Francis, P., & Shenkin, P. S. (2004). Glide: A New Approach for Rapid, Accurate Docking and Scoring. 1. Method and Assessment of Docking Accuracy. *Journal of Medicinal Chemistry*, 47(7), 1739–1749. <https://doi.org/10.1021/jm0306430>
- Gad, S. C. (2008). *PRECLINICAL DEVELOPMENT HANDBOOK ADME and Biopharmaceutical Properties*.
- Galiniak, S., Aebisher, D., & Bartusik-Aebisher, D. (2019). Health benefits of resveratrol administration. In *Acta Biochimica Polonica* (Vol. 66, Issue 1, pp. 13–21). Acta Biochimica Polonica. https://doi.org/10.18388/abp.2018_2749
- Galloza, J., Castillo, B., & Micheo, W. (2017). Benefits of Exercise in the Older Population. In *Physical Medicine and Rehabilitation Clinics of North America* (Vol. 28, Issue 4, pp. 659–669). W.B. Saunders. <https://doi.org/10.1016/j.pmr.2017.06.001>
- Ganaie, M. A., Jan, B. L., Khan, T. H., Alharthy, K. M., & Sheikh, I. A. (2019). The Protective Effect of Naringenin on Oxaliplatin-Induced Genotoxicity in Mice. In *Chem. Pharm. Bull* (Vol. 67, Issue 5).
- García-Valtanan, P., Martínez-López, A., López-Muñoz, A., Bello-Perez, M., Medina-Gali, R. M., Ortega-Villaizán, M. del M., Varela, M., Figueras, A., Mulero, V., Novoa, B., Estepa, A., & Coll, J. (2017). Zebra fish lacking adaptive immunity acquire an antiviral alert state characterized by upregulated gene expression of apoptosis, multigene families, and interferon-related genes. *Frontiers in Immunology*, 8(FEB). <https://doi.org/10.3389/fimmu.2017.00121>
- Gerhart-Hines, Z., Rodgers, J. T., Bare, O., Lerin, C., Kim, S. H., Mostoslavsky, R., Alt, F. W., Wu, Z., & Puigserver, P. (2007). Metabolic control of muscle mitochondrial function and fatty acid oxidation through SIRT1/PGC-1 α . *EMBO Journal*, 26(7), 1913–1923. <https://doi.org/10.1038/sj.emboj.7601633>
- González-Suárez, E., Geserick, C., Flores, J. M., & Blasco, M. A. (2005). Antagonistic effects of telomerase on cancer and aging in K5-mTert transgenic mice. *Oncogene*, 24(13), 2256–2270. <https://doi.org/10.1038/sj.onc.1208413>
- Gorgulla, C., Boeszoermenyi, A., Wang, Z. F., Fischer, P. D., Coote, P. W., Padmanabha Das, K. M., Malets, Y. S., Radchenko, D. S., Moroz, Y. S., Scott, D. A., Fackeldey, K.,

- Hoffmann, M., Iavniuk, I., Wagner, G., & Arthanari, H. (2020). An open-source drug discovery platform enables ultra-large virtual screens. *Nature*, *580*(7805), 663–668. <https://doi.org/10.1038/s41586-020-2117-z>
- Goronzy, J. J., Fang, F., Cavanagh, M. M., Qi, Q., & Weyand, C. M. (2015). Naive T Cell Maintenance and Function in Human Aging. *The Journal of Immunology*, *194*(9), 4073–4080. <https://doi.org/10.4049/jimmunol.1500046>
- Gregor, M. F., & Hotamisligil, G. S. (2011). Inflammatory mechanisms in obesity. *Annual Review of Immunology*, *29*, 415–445. <https://doi.org/10.1146/annurev-immunol-031210-101322>
- Guida, J. L., Agurs-Collins, T., Ahles, T. A., Campisi, J., Dale, W., Demark-Wahnefried, W., Dietrich, J., Fuldner, R., Gallicchio, L., Green, P. A., Hurria, A., Janelsins, M. C., Jhappan, C., Kirkland, J. L., Kohanski, R., Longo, V., Meydani, S., Mohile, S., Niedernhofer, L. J., ... Ness, K. K. (2021). Strategies to Prevent or Remediate Cancer and Treatment-Related Aging. In *Journal of the National Cancer Institute* (Vol. 113, Issue 2, pp. 112–122). Oxford University Press. <https://doi.org/10.1093/jnci/djaa060>
- Gutlapalli, S. D., Kondapaneni, V., Toulassi, I. A., Poudel, S., Zeb, M., Choudhari, J., & Cancarevic, I. (2020). The Effects of Resveratrol on Telomeres and Post Myocardial Infarction Remodeling. *Cureus*. <https://doi.org/10.7759/cureus.11482>
- Hakami, A. R., Bakheit, A. H., Almehezia, A. A., & Ghazwani, M. Y. (2022). Selection of SARS-CoV-2 main protease inhibitor using structure-based virtual screening. *Future Medicinal Chemistry*, *14*(2), 61–79. <https://doi.org/10.4155/fmc-2020-0380>
- Hall, C., Flores, M., Storm, T., Crosier, K., & Crosier, P. (2007). The zebrafish lysozyme C promoter drives myeloid-specific expression in transgenic fish. *BMC Developmental Biology*, *7*. <https://doi.org/10.1186/1471-213X-7-42>
- Henriques, C. M., Carneiro, M. C., Tenente, I. M., Jacinto, A., & Ferreira, M. G. (2013). Telomerase Is Required for Zebrafish Lifespan. *PLoS Genetics*, *9*(1). <https://doi.org/10.1371/journal.pgen.1003214>
- Henriques, C. M., & Ferreira, M. G. (2012). Consequences of telomere shortening during lifespan. In *Current Opinion in Cell Biology* (Vol. 24, Issue 6, pp. 804–808). <https://doi.org/10.1016/j.ceb.2012.09.007>
- Herbert, B. S., Hochreiter, A. E., Wright, W. E., & Shay, J. W. (2006). Nonradioactive detection of telomerase activity using the telomeric repeat amplification protocol. *Nature Protocols*, *1*(3), 1583–1590. <https://doi.org/10.1038/nprot.2006.239>

- Horrillo, D., Sierra, J., Arribas, C., García-San Frutos, M., Carrascosa, J. M., Lauzurica, N., Fernández-Agulló, T., & Ros, M. (2011). Age-associated development of inflammation in Wistar rats: Effects of caloric restriction. *Archives of Physiology and Biochemistry*, 117(3), 140–150. <https://doi.org/10.3109/13813455.2011.577435>
- Horvath, D. (1997). *A Virtual Screening Approach Applied to the Search for Trypanothione Reductase Inhibitors*. <https://pubs.acs.org/sharingguidelines>
- Howe, K., Clark, M. D., Torroja, C. F., Torrance, J., Berthelot, C., Muffato, M., Collins, J. E., Humphray, S., McLaren, K., Matthews, L., McLaren, S., Sealy, I., Caccamo, M., Churcher, C., Scott, C., Barrett, J. C., Koch, R., Rauch, G. J., White, S., ... Stemple, D. L. (2013). The zebrafish reference genome sequence and its relationship to the human genome. *Nature*, 496(7446), 498–503. <https://doi.org/10.1038/nature12111>
- Huang, N., Shoichet, B. K., & Irwin, J. J. (2006). Benchmarking sets for molecular docking. *Journal of Medicinal Chemistry*, 49(23), 6789–6801. <https://doi.org/10.1021/jm0608356>
- Huang, S. Y., Grinter, S. Z., & Zou, X. (2010). Scoring functions and their evaluation methods for protein-ligand docking: Recent advances and future directions. *Physical Chemistry Chemical Physics*, 12(40), 12899–12908. <https://doi.org/10.1039/c0cp00151a>
- Hwangbo, D. S., Lee, H. Y., Abozaid, L. S., & Min, K. J. (2020). Mechanisms of lifespan regulation by calorie restriction and intermittent fasting in model organisms. In *Nutrients* (Vol. 12, Issue 4). MDPI AG. <https://doi.org/10.3390/nu12041194>
- Imai, S. I., & Guarente, L. (2010). Ten years of NAD-dependent SIR2 family deacetylases: Implications for metabolic diseases. In *Trends in Pharmacological Sciences* (Vol. 31, Issue 5, pp. 212–220). <https://doi.org/10.1016/j.tips.2010.02.003>
- Ivanciuc, O., Taraviras, S. L., & Cabrol-Bass, D. (2000). Quasi-orthogonal Basis Sets of Molecular Graph Descriptors as a Chemical Diversity Measure. *Journal of Chemical Information and Computer Sciences*, 40(1), 126–134. <https://doi.org/10.1021/ci990064x>
- Jian-Guo Jiang, C., Zhu, W., Shen, C.-Y., Jiang, J.-G., Yang, L., & Wang, D.-W. (2016). *Anti-ageing active ingredients from herbs and nutraceuticals used in traditional Chinese medicine: pharmacological mechanisms and implications for drug discovery*. <https://doi.org/10.1111/bph.v174.11/issuetoc>

- Jørgensen, A. M. M., & Pedersen, J. T. (2001). Structural diversity of small molecule libraries. *Journal of Chemical Information and Computer Sciences*, 41(2), 338–345. <https://doi.org/10.1021/ci000111h>
- Kennedy, B. K., Berger, S. L., Brunet, A., Campisi, J., Cuervo, A. M., Epel, E. S., Franceschi, C., Lithgow, G. J., Morimoto, R. I., Pessin, J. E., Rando, T. A., Richardson, A., Schadt, E. E., Wyss-Coray, T., & Sierra, F. (2014). Geroscience: Linking aging to chronic disease. In *Cell* (Vol. 159, Issue 4, pp. 709–713). Cell Press. <https://doi.org/10.1016/j.cell.2014.10.039>
- Khaw, S. L., Mérino, D., Anderson, M. A., Glaser, S. P., Bouillet, P., Roberts, A. W., & Huang, D. C. S. (2014). Both leukaemic and normal peripheral B lymphoid cells are highly sensitive to the selective pharmacological inhibition of prosurvival Bcl-2 with ABT-199. *Leukemia*, 28(6), 1207–1215. <https://doi.org/10.1038/leu.2014.1>
- Kim, E. C., & Kim, J. R. (2019). Senotherapeutics: Emerging strategy for healthy aging and age-related disease. In *BMB Reports* (Vol. 52, Issue 1, pp. 47–55). The Biochemical Society of the Republic of Korea. <https://doi.org/10.5483/BMBRep.2019.52.1.293>
- Kirkland, J. L., & Tchkonina, T. (2020). Senolytic drugs: from discovery to translation. In *Journal of Internal Medicine* (Vol. 288, Issue 5, pp. 518–536). Blackwell Publishing Ltd. <https://doi.org/10.1111/joim.13141>
- Kishi, S., Uchiyama, J., Baughman, A. M., Goto, T., Lin, M. C., & Tsai, S. B. (2003). The zebrafish as a vertebrate model of functional aging and very gradual senescence. *Experimental Gerontology*, 38(7), 777–786. [https://doi.org/10.1016/S0531-5565\(03\)00108-6](https://doi.org/10.1016/S0531-5565(03)00108-6)
- Kraus, A., Huertas, M., Ellis, L., Boudinot, P., Levraud, J. P., & Salinas, I. (2022). Intranasal delivery of SARS-CoV-2 spike protein is sufficient to cause olfactory damage, inflammation and olfactory dysfunction in zebrafish. *Brain, Behavior, and Immunity*, 102, 341–359. <https://doi.org/10.1016/j.bbi.2022.03.006>
- Kumari, R., & Jat, P. (2021). Mechanisms of Cellular Senescence: Cell Cycle Arrest and Senescence Associated Secretory Phenotype. In *Frontiers in Cell and Developmental Biology* (Vol. 9). Frontiers Media S.A. <https://doi.org/10.3389/fcell.2021.645593>
- Laghi, V., Rezelj, V., Boucontet, L., Frétaud, M., da Costa, B., Boudinot, P., Salinas, I., Lutfalla, G., Vignuzzi, M., & Levraud, J. P. (2022). Exploring Zebrafish Larvae as a COVID-19 Model: Probable Abortive SARS-CoV-2 Replication in the Swim Bladder. *Frontiers in Cellular and Infection Microbiology*, 12. <https://doi.org/10.3389/fcimb.2022.790851>

- Lau, L. M. S., Dagg, R. A., Henson, J. D., Au, A. Y. M., Royds, J. A., & Reddel, R. R. (2013). Detection of alternative lengthening of telomeres by telomere quantitative PCR. *Nucleic Acids Research*, 41(2). <https://doi.org/10.1093/nar/gks781>
- Lavecchia, A., & di Giovanni, C. (2013). *Virtual Screening Strategies in Drug Discovery: A Critical Review*. <http://www.enamine.net/>
- Leach, A. R., Gillet, V. J., Lewis, R. A., & Taylor, R. (2010). Three-dimensional pharmacophore methods in drug discovery. In *Journal of Medicinal Chemistry* (Vol. 53, Issue 2, pp. 539–558). <https://doi.org/10.1021/jm900817u>
- Leelananda, S. P., & Lindert, S. (2016). Computational methods in drug discovery. In *Beilstein Journal of Organic Chemistry* (Vol. 12, pp. 2694–2718). Beilstein-Institut Zur Forderung der Chemischen Wissenschaften. <https://doi.org/10.3762/bjoc.12.267>
- Li, Y. R., Li, S., & Lin, C. C. (2018). Effect of resveratrol and pterostilbene on aging and longevity. In *BioFactors* (Vol. 44, Issue 1, pp. 69–82). Blackwell Publishing Inc. <https://doi.org/10.1002/biof.1400>
- Lim, K. H., & Kim, G. R. (2018). Inhibitory effect of naringenin on LPS-induced skin senescence by SIRT1 regulation in HDFs. *Biomedical Dermatology*, 2(1). <https://doi.org/10.1186/s41702-018-0035-6>
- Lin, J., Sahakian, D. C., F de Morais, S. M., Xu, J. J., Polzer, R. J., & Winter, S. M. (2003). The Role of Absorption, Distribution, Metabolism, Excretion and Toxicity in Drug Discovery. In *Current Topics in Medicinal Chemistry* (Vol. 3).
- Lin, S.-R., Chang, C.-H., Hsu, C.-F., Tsai, M.-J., Cheng, H., Leong, M. K., Sung, P.-J., Chen, J.-C., & Weng, C.-F. (2019). *Natural compounds as potential adjuvants to cancer therapy: Preclinical evidence*. <https://doi.org/10.1111/bph.v177.6/issuetoc>
- Lindqvist, D., Epel, E. S., Mellon, S. H., Penninx, B. W., Révész, D., Verhoeven, J. E., Reus, V. I., Lin, J., Mahan, L., Hough, C. M., Rosser, R., Bersani, F. S., Blackburn, E. H., & Wolkowitz, O. M. (2015). Psychiatric disorders and leukocyte telomere length: Underlying mechanisms linking mental illness with cellular aging. In *Neuroscience and Biobehavioral Reviews* (Vol. 55, pp. 333–364). Elsevier Ltd. <https://doi.org/10.1016/j.neubiorev.2015.05.007>
- Lionta, E., Spyrou, G., Vassilatis, D. K., & Cournia, Z. (2014). Send Orders for Reprints to reprints@benthamscience.net Structure-Based Virtual Screening for Drug Discovery: Principles, Applications and Recent Advances. In *Current Topics in Medicinal Chemistry* (Vol. 14).

- Liu, B., Fan, Z., Edgerton, S. M., Yang, X., Lind, S. E., & Thor, A. D. (2011). Potent anti-proliferative effects of metformin on trastuzumab-resistant breast cancer cells via inhibition of ErbB2/IGF-1 receptor interactions. *Cell Cycle*, *10*(17), 2959–2966. <https://doi.org/10.4161/cc.10.17.16359>
- López-Otín, C., Blasco, M. A., Partridge, L., Serrano, M., & Kroemer, G. (2013). The hallmarks of aging. In *Cell* (Vol. 153, Issue 6, p. 1194). Elsevier B.V. <https://doi.org/10.1016/j.cell.2013.05.039>
- Ma, X. H., Jia, J., Zhu, F., Xue, Y., Li, Z. R., & Chen, Y. Z. (2009). Comparative Analysis of Machine Learning Methods in Ligand-Based Virtual Screening of Large Compound Libraries. In *Combinatorial Chemistry & High Throughput Screening* (Vol. 12). <http://www.vanguardsw.com/decisionpro/jdtree.htm>
- MacRae, C. A., & Peterson, R. T. (2015). Zebrafish as tools for drug discovery. In *Nature Reviews Drug Discovery* (Vol. 14, Issue 10, pp. 721–731). Nature Publishing Group. <https://doi.org/10.1038/nrd4627>
- Maduro, A. T., Luís, C., & Soares, R. (2021). Ageing, cellular senescence and the impact of diet: an overview. *Porto Biomedical Journal*, *6*(1), e120. <https://doi.org/10.1097/j.pbj.0000000000000120>
- Maia, E. H. B., Assis, L. C., de Oliveira, T. A., da Silva, A. M., & Taranto, A. G. (2020). Structure-Based Virtual Screening: From Classical to Artificial Intelligence. In *Frontiers in Chemistry* (Vol. 8). Frontiers Media S.A. <https://doi.org/10.3389/fchem.2020.00343>
- Maia, E. H. B., Campos, V. A., dos Reis Santos, B., Costa, M. S., Lima, I. G., Greco, S. J., Ribeiro, R. I. M. A., Munayer, F. M., da Silva, A. M., & Taranto, A. G. (2017). Octopus: a platform for the virtual high-throughput screening of a pool of compounds against a set of molecular targets. *Journal of Molecular Modeling*, *23*(1). <https://doi.org/10.1007/s00894-016-3184-9>
- Majidinia, M., Karimian, A., Alemi, F., Yousefi, B., & Safa, A. (2020). Targeting miRNAs by polyphenols: Novel therapeutic strategy for aging. In *Biochemical Pharmacology* (Vol. 173). Elsevier Inc. <https://doi.org/10.1016/j.bcp.2019.113688>
- Mannick, J. B., Giudice, G. del, Lattanzi, M., Valiante, N. M., Praestgaard, J., Huang, B., Lonetto, M. A., Maecker, H. T., Kovarik, J., Carson, S., Glass, D. J., & Klickstein, L. B. (2014). *mTOR inhibition improves immune function in the elderly*. www.ScienceTranslationalMedicine.org
- Mantzorou, M., Pavlidou, E., Vasios, G., Tsagalioti, E., & Giaginis, C. (2018). Effects of curcumin consumption on human chronic diseases: A narrative review of the most

- recent clinical data. In *Phytotherapy Research* (Vol. 32, Issue 6, pp. 957–975). John Wiley and Sons Ltd. <https://doi.org/10.1002/ptr.6037>
- Martínez-Morcillo, F. J., Cantón-Sandoval, J., Martínez-Navarro, F. J., Cabas, I., Martínez-Vicente, I., Armistead, J., Hatzold, J., López-Muñoz, A., Martínez-Menchón, T., Corbalán-Vélez, R., Lacal, J., Hammerschmidt, M., García-Borrón, J. C., García-Ayala, A., Cayuela, M. L., Pérez-Oliva, A. B., García-Moreno, D., & Mulero, V. (2021). NAMPT-derived NAD+fuels PARP1 to promote skin inflammation through parthanatos cell death. *PLoS Biology*, *19*(11). <https://doi.org/10.1371/journal.pbio.3001455>
- Mathias, J. R., Dodd, M. E., Walters, K. B., Rhodes, J., Kanki, J. P., Look, A. T., & Huttenlocher, A. (2007). Live imaging of chronic inflammation caused by mutation of zebrafish Hai1. *Journal of Cell Science*, *120*(19), 3372–3383. <https://doi.org/10.1242/jcs.009159>
- Matsuda, H. (2018). Zebrafish as a model for studying functional pancreatic β cells development and regeneration. In *Development Growth and Differentiation* (Vol. 60, Issue 6, pp. 393–399). Blackwell Publishing. <https://doi.org/10.1111/dgd.12565>
- Matthew P. Repasky, Mee Shelley, & Richard A. Friesner. (2007). *Flexible Ligand Docking with Glide*.
- McGann, M. (2012). FRED and HYBRID docking performance on standardized datasets. *Journal of Computer-Aided Molecular Design*, *26*(8), 897–906. <https://doi.org/10.1007/s10822-012-9584-8>
- McGrath, C., Sankaran, J. S., Misaghian-Xanthos, N., Sen, B., Xie, Z., Styner, M. A., Zong, X., Rubin, J., & Styner, M. (2020). Exercise Degrades Bone in Caloric Restriction, Despite Suppression of Marrow Adipose Tissue (MAT). *Journal of Bone and Mineral Research*, *35*(1), 106–115. <https://doi.org/10.1002/jbmr.3872>
- McHugh, D., & Gil, J. (2018). Senescence and aging: Causes, consequences, and therapeutic avenues. In *Journal of Cell Biology* (Vol. 217, Issue 1, pp. 65–77). Rockefeller University Press. <https://doi.org/10.1083/jcb.201708092>
- Meijer, A. H. (2016). Protection and pathology in TB: learning from the zebrafish model. In *Seminars in Immunopathology* (Vol. 38, Issue 2, pp. 261–273). Springer Verlag. <https://doi.org/10.1007/s00281-015-0522-4>
- Melzer, D., Pilling, L. C., & Ferrucci, L. (2020). The genetics of human ageing. In *Nature Reviews Genetics* (Vol. 21, Issue 2, pp. 88–101). Nature Research. <https://doi.org/10.1038/s41576-019-0183-6>

- Miles, J. A., & Ross, B. P. (2021). Recent Advances in Virtual Screening for Cholinesterase Inhibitors. In *ACS Chemical Neuroscience* (Vol. 12, Issue 1, pp. 30–41). American Chemical Society. <https://doi.org/10.1021/acscchemneuro.0c00627>
- Mohamad Anuar, N. N., Nor Hisam, N. S., Liew, S. L., & Ugusman, A. (2020). Clinical Review: Navitoclax as a Pro-Apoptotic and Anti-Fibrotic Agent. In *Frontiers in Pharmacology* (Vol. 11). Frontiers Media S.A. <https://doi.org/10.3389/fphar.2020.564108>
- Molgora, B., Bateman, R., Sweeney, G., Finger, D., Dimler, T., Effros, R. B., & Valenzuela, H. F. (2013). Functional assessment of pharmacological telomerase activators in human T cells. *Cells*, 2(1), 57–63. <https://doi.org/10.3390/cells2010057>
- Montero, J. C., Seoane, S., Ocaña, A., & Pandiella, A. (2011). Inhibition of Src family kinases and receptor tyrosine kinases by dasatinib: Possible combinations in solid tumors. In *Clinical Cancer Research* (Vol. 17, Issue 17, pp. 5546–5552). <https://doi.org/10.1158/1078-0432.CCR-10-2616>
- Morris, G. M., Goodsell, D. S., Halliday, R. S., Huey, R., Hart, W. E., Belew, R. K., & Olson, A. J. (1639). Automated Docking Using a Lamarckian Genetic Algorithm and an Empirical Binding Free Energy Function. *Journal of Computational Chemistry*, 19(14), 1639–1662.
- Most, J., Gilmore, L. A., Smith, S. R., Han, H., Ravussin, E., & Redman, L. M. (2018). Significant improvement in cardiometabolic health in healthy nonobese individuals during caloric restriction-induced weight loss and weight loss maintenance. *Am J Physiol Endocrinol Metab*, 314, 396–405. <https://doi.org/10.1152/ajpendo.00261.2017.-Calorie>
- Mosteiro, L., Pantoja, C., Alcazar, N., Marión, R. M., Chondronasiou, D., Rovira, M., Fernandez-Marcos, P. J., Muñoz-Martin, M., Blanco-Aparicio, C., Pastor, J., Gómez-López, G., de Martino, A., Blasco, M. A., Abad, M., & Serrano, M. (2016). Tissue damage and senescence provide critical signals for cellular reprogramming in vivo. *Science*, 354(6315). <https://doi.org/10.1126/science.aaf4445>
- Mugumbate, G., Mendes, V., Blaszczyk, M., Sabbah, M., Papadatos, G., Lelievre, J., Ballell, L., Barros, D., Abell, C., Blundell, T. L., & Overington, J. P. (2017). Target identification of Mycobacterium tuberculosis phenotypic hits using a concerted chemogenomic, biophysical, and structural approach. *Frontiers in Pharmacology*, 8(SEP). <https://doi.org/10.3389/fphar.2017.00681>
- Muñoz-Espín, D., Cañamero, M., Maraver, A., Gómez-López, G., Contreras, J., Murillo-Cuesta, S., Rodríguez-Baeza, A., Varela-Nieto, I., Ruberte, J., Collado, M., & Serrano,

- M. (2013). Programmed cell senescence during mammalian embryonic development. *Cell*, *155*(5), 1104. <https://doi.org/10.1016/j.cell.2013.10.019>
- Nair, V., Sreevalsan, S., Basha, R., Abdelrahm, M., Abudayyeh, A., Hoffman, A. R., & Safe, S. (2014). Mechanism of metformin-dependent inhibition of mammalian target of rapamycin (mTOR) and Ras activity in pancreatic cancer. *Journal of Biological Chemistry*, *289*(40), 27692–27701. <https://doi.org/10.1074/jbc.M114.592576>
- Neff, F., Flores-Dominguez, D., Ryan, D. P., Horsch, M., Schröder, S., Adler, T., Afonso, L. C., Aguilar-Pimentel, J. A., Becker, L., Garrett, L., Hans, W., Hettich, M. M., Holtmeier, R., Hölter, S. M., Moreth, K., Prehn, C., Puk, O., Rácz, I., Rathkolb, B., ... Ehninger, D. (2013). Rapamycin extends murine lifespan but has limited effects on aging. *Journal of Clinical Investigation*, *123*(8), 3272–3291. <https://doi.org/10.1172/JCI67674>
- Ness, K. K., & Wogksch, M. D. (2020). Frailty and aging in cancer survivors. In *Translational Research* (Vol. 221, pp. 65–82). Mosby Inc. <https://doi.org/10.1016/j.trsl.2020.03.013>
- Ng, T. P., Feng, L., Yap, K. B., Lee, T. S., Tan, C. H., & Winblad, B. (2014). Long-term metformin usage and cognitive function among older adults with diabetes. *Journal of Alzheimer's Disease*, *41*(1), 61–68. <https://doi.org/10.3233/JAD-131901>
- Niedernhofer, L. J., & Robbins, P. D. (2018). Senotherapeutics for healthy ageing. In *Nature Reviews Drug Discovery* (Vol. 17, Issue 5, p. 377). Nature Publishing Group. <https://doi.org/10.1038/nrd.2018.44>
- Novoa, B., Pereiro, P., López-Muñoz, A., Varela, M., Forn-Cuní, G., Anchelin, M., Dios, S., Romero, A., Martínez-López, A., Medina-Gali, R. M., Collado, M., Coll, J., Estepa, A., Cayuela, M. L., Mulero, V., & Figueras, A. (2019). Rag1 immunodeficiency-induced early aging and senescence in zebrafish are dependent on chronic inflammation and oxidative stress. *Aging Cell*, *18*(5). <https://doi.org/10.1111/accel.13020>
- Nunes, R. R., da Fonseca, A. L., Pinto, A. C. D. S., Maia, E. H. B., da Silva, A. M., Varotti, F. D. P., & Taranto, A. G. (2019). Brazilian malaria molecular targets (BraMMT): Selected receptors for virtual high-throughput screening experiments. *Memorias Do Instituto Oswaldo Cruz*, *114*(2). <https://doi.org/10.1590/0074-02760180465>
- Ott, E., Wendik, B., Srivastava, M., Pacho, F., Töchterle, S., Salvenmoser, W., & Meyer, D. (2016). Pronephric tubule morphogenesis in zebrafish depends on Mnx mediated repression of *irx1b* within the intermediate mesoderm. *Developmental Biology*, *411*(1), 101–114. <https://doi.org/10.1016/j.ydbio.2015.10.014>

- Palacio-Rodríguez, K., Lans, I., Cavasotto, C. N., & Cossio, P. (2019). Exponential consensus ranking improves the outcome in docking and receptor ensemble docking. *Scientific Reports*, *9*(1). <https://doi.org/10.1038/s41598-019-41594-3>
- Palmer, S. C., Mavridis, D., Nicolucci, A., Johnson, D. W., Tonelli, M., Craig, J. C., Maggo, J., Gray, V., de Berardis, G., Ruospo, M., Natale, P., Saglimbene, V., Badve, S. v., Cho, Y., Nadeau-Fredette, A. C., Burke, M., Faruque, L., Lloyd, A., Ahmad, N., ... Strippoli, G. F. M. (2016). Comparison of clinical outcomes and adverse events associated with glucose-lowering drugs in patients with type 2 diabetes a meta-analysis. *JAMA - Journal of the American Medical Association*, *316*(3), 313–324. <https://doi.org/10.1001/jama.2016.9400>
- Pan, M. H., Lai, C. S., Tsai, M. L., Wu, J. C., & Ho, C. T. (2012). Molecular mechanisms for anti-aging by natural dietary compounds. In *Molecular Nutrition and Food Research* (Vol. 56, Issue 1, pp. 88–115). <https://doi.org/10.1002/mnfr.201100509>
- Pan, R., Hogdal, L. J., Benito, J. M., Bucci, D., Han, L., Borthakur, G., Cortes, J., Deangelo, D. J., Debose, L., Mu, H., Döhner, H., Gaidzik, V. I., Galinsky, I., Golfman, L. S., Haferlach, T., Harutyunyan, K. G., Hu, J., Levenson, J. D., Marcucci, G., ... Letai, A. G. (2014). Selective BCL-2 inhibition by ABT-199 causes on-target cell death in acute myeloid Leukemia. *Cancer Discovery*, *4*(3), 362–675. <https://doi.org/10.1158/2159-8290.CD-13-0609>
- Park, D. W., Kim, J. S., Chin, B. R., & Baek, S. H. (2012). Resveratrol inhibits inflammation induced by heat-killed listeria monocytogenes. *Journal of Medicinal Food*, *15*(9), 788–794. <https://doi.org/10.1089/jmf.2012.2194>
- Pateliya, B., Burade, V., & Goswami, S. (2021). Enhanced antitumor activity of doxorubicin by naringenin and metformin in breast carcinoma: an experimental study. *Naunyn-Schmiedeberg's Archives of Pharmacology*, *394*(9), 1949–1961. <https://doi.org/10.1007/s00210-021-02104-3>
- Pawelec, G. (2012). Hallmarks of human “immunosenesescence” : Adaptation or dysregulation? In *Immunity and Ageing* (Vol. 9). <https://doi.org/10.1186/1742-4933-9-15>
- Peirs, S., Matthijssens, F., Goossens, S., van de Walle, I., Ruggero, K., de Bock, C. E., Degryse, S., Canté, K., Canté-Barrett, C., Briot, D., Clappier, E., Lammens, T., de Moerloose, B., Benoit, Y., Poppe, B., Meijerink, J. P., Cools, J., Soulier, J., Rabbitts, T. H., ... van Vlierberghe, P. (2014). ABT-199 mediated inhibition of BCL-2 as a novel therapeutic strategy in T-cell acute lymphoblastic leukemia. *BLOOD*, *124*, 3738–3747. <https://doi.org/10.1182/blood-2014-05>

- Pérez-Revuelta, B. I., Hettich, M. M., Ciociaro, A., Rotermond, C., Kahle, P. J., Krauss, S., & di Monte, D. A. (2014). Metformin lowers Ser-129 phosphorylated α -synuclein levels via mTOR-dependent protein phosphatase 2A activation. *Cell Death and Disease*, 5(5). <https://doi.org/10.1038/cddis.2014.175>
- Picca, A., Pesce, V., & Lezza, A. M. S. (2017). Does eating less make you live longer and better? An update on calorie restriction. In *Clinical Interventions in Aging* (Vol. 12, pp. 1887–1902). Dove Medical Press Ltd. <https://doi.org/10.2147/CIA.S126458>
- Pifferi, F., & Aujard, F. (2019). Caloric restriction, longevity and aging: Recent contributions from human and non-human primate studies. In *Progress in Neuro-Psychopharmacology and Biological Psychiatry* (Vol. 95). Elsevier Inc. <https://doi.org/10.1016/j.pnpbp.2019.109702>
- Prata, L. G. P. L., Ovsyannikova, I. G., Tchkonja, T., & Kirkland, J. L. (2018). Senescent cell clearance by the immune system: Emerging therapeutic opportunities. In *Seminars in Immunology* (Vol. 40). Academic Press. <https://doi.org/10.1016/j.smim.2019.04.003>
- Price, N. L., Gomes, A. P., Ling, A. J. Y., Duarte, F. v., Martin-Montalvo, A., North, B. J., Agarwal, B., Ye, L., Ramadori, G., Teodoro, J. S., Hubbard, B. P., Varela, A. T., Davis, J. G., Varamini, B., Hafner, A., Moaddel, R., Rolo, A. P., Coppari, R., Palmeira, C. M., ... Sinclair, D. A. (2012). SIRT1 is required for AMPK activation and the beneficial effects of resveratrol on mitochondrial function. *Cell Metabolism*, 15(5), 675–690. <https://doi.org/10.1016/j.cmet.2012.04.003>
- Pryor, R., & Cabreiro, F. (2015). Repurposing metformin: An old drug with new tricks in its binding pockets. In *Biochemical Journal* (Vol. 471, Issue 3, pp. 307–322). Portland Press Ltd. <https://doi.org/10.1042/BJ20150497>
- Puertas-Martín, S., Banegas-Luna, A. J., Paredes-Ramos, M., Redondo, J. L., Ortigosa, P. M., Brovarets', O. O., & Pérez-Sánchez, H. (2020). Is high performance computing a requirement for novel drug discovery and how will this impact academic efforts? In *Expert Opinion on Drug Discovery* (Vol. 15, Issue 9, pp. 981–986). Taylor and Francis Ltd. <https://doi.org/10.1080/17460441.2020.1758664>
- Qin, W., Ren, B., Wang, S., Liang, S., He, B., Shi, X., Wang, L., Liang, J., & Wu, F. (2016). Apigenin and naringenin ameliorate PKC β II-associated endothelial dysfunction via regulating ROS/caspase-3 and NO pathway in endothelial cells exposed to high glucose. *Vascular Pharmacology*, 85, 39–49. <https://doi.org/10.1016/j.vph.2016.07.006>

- Raldúa, D., & Piña, B. (2014). In vivo zebrafish assays for analyzing drug toxicity. In *Expert Opinion on Drug Metabolism and Toxicology* (Vol. 10, Issue 5, pp. 685–697). Informa Healthcare. <https://doi.org/10.1517/17425255.2014.896339>
- Rattan, S. I. S. (2014). Aging is not a disease: Implications for intervention. In *Aging and Disease* (Vol. 5, Issue 3, pp. 196–202). International Society on Aging and Disease. <https://doi.org/10.14336/AD.2014.0500196>
- Redman, L. M., Smith, S. R., Burton, J. H., Martin, C. K., Il'yasova, D., & Ravussin, E. (2018). Metabolic Slowing and Reduced Oxidative Damage with Sustained Caloric Restriction Support the Rate of Living and Oxidative Damage Theories of Aging. *Cell Metabolism*, 27(4), 805-815.e4. <https://doi.org/10.1016/j.cmet.2018.02.019>
- Robertson, A. L., Avagyan, S., Gansner, J. M., & Zon, L. I. (2016). Understanding the regulation of vertebrate hematopoiesis and blood disorders – big lessons from a small fish. In *FEBS Letters* (Vol. 590, Issue 22, pp. 4016–4033). Wiley Blackwell. <https://doi.org/10.1002/1873-3468.12415>
- Rödel, C. J., & Abdelilah-Seyfried, S. (2021). A zebrafish toolbox for biomechanical signaling in cardiovascular development and disease. *Current Opinion in Hematology*, 28(3), 198–207. <https://doi.org/10.1097/MOH.0000000000000648>
- Rodríguez-Rodero, S., Luis Fernández-Morera, J., Menéndez-Torre, E., Calvanese, V., Fernández, A. F., Fraga, M. F., & Clavería, J. (2011). Aging Genetics and Aging. In *Gene and Aging Aging and Disease* • (Vol. 2, Issue 3).
- Rojas, W. M., Oviedo, K. N., Oliveroverbel, J., Rojas, M., Noguera Oviedo, K., & Olivero, J. (2012). *ACOPLAMIENTO INVERSO Y MAPEO DE FARMACÓFORO COMO HERRAMIENTAS PARA ENCONTRAR NUEVOS BLANCOS FARMACOLÓGICOS DE COMPUESTOS NATURALES*. <http://www.pdb.org/pdb/home/home.do>
- Rollinger, J. M., Stuppner, H., & Langer, T. (2008). Virtual screening for the discovery of bioactive natural products. In *Progress in Drug Research* (Vol. 65).
- Sahin, E., Colla, S., Liesa, M., Moslehi, J., Müller, F. L., Guo, M., Cooper, M., Kotton, D., Fabian, A. J., Walkey, C., Maser, R. S., Tonon, G., Foerster, F., Xiong, R., Wang, Y. A., Shukla, S. A., Jaskelioff, M., Martin, E. S., Heffernan, T. P., ... DePinho, R. A. (2011). Telomere dysfunction induces metabolic and mitochondrial compromise. *Nature*, 470(7334), 359–365. <https://doi.org/10.1038/nature09787>
- Salvestrini, V., Sell, C., & Lorenzini, A. (2019). Obesity may accelerate the aging process. In *Frontiers in Endocrinology* (Vol. 10, Issue MAY). Frontiers Media S.A. <https://doi.org/10.3389/fendo.2019.00266>

- Sanders, M. P. A., McGuire, R., Roumen, L., de Esch, I. J. P., de Vlieg, J., Klomp, J. P. G., & de Graaf, C. (2012). From the protein's perspective: The benefits and challenges of protein structure-based pharmacophore modeling. *MedChemComm*, 3(1), 28–38. <https://doi.org/10.1039/c1md00210d>
- Saraiva, L. R., Ahuja, G., Ivandic, I., Syed, A. S., Marioni, J. C., Korsching, S. I., & Logan, D. W. (2015). Molecular and neuronal homology between the olfactory systems of zebrafish and mouse. *Scientific Reports*, 5. <https://doi.org/10.1038/srep11487>
- Sawda, C., Moussa, C., & Turner, R. S. (2017). Resveratrol for alzheimer's disease. In *Annals of the New York Academy of Sciences* (Vol. 1403, Issue 1, pp. 142–149). Blackwell Publishing Inc. <https://doi.org/10.1111/nyas.13431>
- Saxton, R. A., & Sabatini, D. M. (2017). mTOR Signaling in Growth, Metabolism, and Disease. In *Cell* (Vol. 168, Issue 6, pp. 960–976). Cell Press. <https://doi.org/10.1016/j.cell.2017.02.004>
- Scapin, G. (2006). Structural Biology and Drug Discovery. In *Current Pharmaceutical Design* (Vol. 12).
- Schlender, L., Martinez, Y. v., Adeniji, C., Reeves, D., Faller, B., Sommerauer, C., al Qur'An, T., Woodham, A., Kunnamo, I., Sönnichsen, A., & Renom-Guiteras, A. (2017). Efficacy and safety of metformin in the management of type 2 diabetes mellitus in older adults: A systematic review for the development of recommendations to reduce potentially inappropriate prescribing. In *BMC Geriatrics* (Vol. 17). BioMed Central Ltd. <https://doi.org/10.1186/s12877-017-0574-5>
- Schuster, D. (2010). 3D pharmacophores as tools for activity profiling. In *Drug Discovery Today: Technologies* (Vol. 7, Issue 4). Elsevier Ltd. <https://doi.org/10.1016/j.ddtec.2010.11.006>
- Shen, J., Xu, X., Cheng, F., Liu, H., Luo, X., Shen, J., Chen, K., Zhao, W., Shen, X., & Jiang, H. (2003). Virtual Screening on Natural Products for Discovering Active Compounds and Target Information. In *Current Medicinal Chemistry* (Vol. 10). <http://www.rcsb.org/pdb/index.html>
- Simin N.Meydani, Sai K. Das, Carl F. Pieper, Michael R. Lewis, Sam Klein, Vishwa D.Dixit, Alok K. Gupta, Dennis T. Villareal, Manjushri Bhapkar, Megan Huang, Paul J. Fuss, Susan B. Roberts, John O. Holloszy, & Luigi Fontana. (2016). Long-term moderate calorie restriction inhibits inflammation without. *AGING*, 8(7).
- Simon, M., Hosen, I., Gousias, K., Rachakonda, S., Heidenreich, B., Gessi, M., Schramm, J., Hemminki, K., Waha, A., & Kumar, R. (2015). TERT promoter mutations: A novel

- independent prognostic factor in primary glioblastomas. *Neuro-Oncology*, 17(1), 45–52. <https://doi.org/10.1093/neuonc/nou158>
- Sliwoski, G., Kothiwale, S., Meiler, J., & Lowe, E. W. (2014). Computational methods in drug discovery. In *Pharmacological Reviews* (Vol. 66, Issue 1, pp. 334–395). <https://doi.org/10.1124/pr.112.007336>
- Smith, E. M., Pendlebury, D. F., & Nandakumar, J. (2020). Structural biology of telomeres and telomerase. In *Cellular and Molecular Life Sciences* (Vol. 77, Issue 1, pp. 61–79). Springer. <https://doi.org/10.1007/s00018-019-03369-x>
- Souers, A. J., Levenson, J. D., Boghaert, E. R., Ackler, S. L., Catron, N. D., Chen, J., Dayton, B. D., Ding, H., Enschede, S. H., Fairbrother, W. J., Huang, D. C. S., Hymowitz, S. G., Jin, S., Khaw, S. L., Kovar, P. J., Lam, L. T., Lee, J., Maecker, H. L., Marsh, K. C., ... Elmore, S. W. (2013). ABT-199, a potent and selective BCL-2 inhibitor, achieves antitumor activity while sparing platelets. *Nature Medicine*, 19(2), 202–208. <https://doi.org/10.1038/nm.3048>
- Spadaro, A., Negri, M., Marchais-Oberwinkler, S., Bey, E., & Frotscher, M. (2012). Hydroxybenzothiazoles as new nonsteroidal inhibitors of 17 β -hydroxysteroid dehydrogenase type 1 (17 β -HSD1). *PLoS ONE*, 7(1). <https://doi.org/10.1371/journal.pone.0029252>
- Spence, R., Gerlach, G., Lawrence, C., & Smith, C. (2008). The behaviour and ecology of the zebrafish, *Danio rerio*. In *Biological Reviews* (Vol. 83, Issue 1, pp. 13–34). <https://doi.org/10.1111/j.1469-185X.2007.00030.x>
- Srinivas, N., Rachakonda, S., & Kumar, R. (2020). Telomeres and telomere length: A general overview. In *Cancers* (Vol. 12, Issue 3). MDPI AG. <https://doi.org/10.3390/cancers12030558>
- Stillman, Bruce., Stewart, D. J. (David J., & Cold Spring Harbor Laboratory. (2005). *Molecular approaches to controlling cancer*. Cold Spring Harbor Laboratory Press.
- Stompor, M. (2020). A review on sources and pharmacological aspects of sakuranetin. In *Nutrients* (Vol. 12, Issue 2). MDPI AG. <https://doi.org/10.3390/nu12020513>
- Stroganov, O. v., Novikov, F. N., Stroylov, V. S., Kulkov, V., & Chilov, G. G. (2008). Lead finder: An approach to improve accuracy of protein-ligand docking, binding energy estimation, and virtual screening. *Journal of Chemical Information and Modeling*, 48(12), 2371–2385. <https://doi.org/10.1021/ci800166p>
- Stynen, B., Abd-Rabbo, D., Kowarzyk, J., Miller-Fleming, L., Aulakh, S. K., Garneau, P., Ralsler, M., & Michnick, S. W. (2018). Changes of Cell Biochemical States Are

- Revealed in Protein Homomeric Complex Dynamics. *Cell*, 175(5), 1418-1429.e9.
<https://doi.org/10.1016/j.cell.2018.09.050>
- Sukardi, H., Chng, H. T., Chan, E. C. Y., Gong, Z., & Lam, S. H. (2011). Zebrafish for drug toxicity screening: Bridging the in vitro cell-based models and in vivo mammalian models. In *Expert Opinion on Drug Metabolism and Toxicology* (Vol. 7, Issue 5, pp. 579–589). <https://doi.org/10.1517/17425255.2011.562197>
- Surabhi, S., & Singh, B. (2018). COMPUTER AIDED DRUG DESIGN: AN OVERVIEW. *Journal of Drug Delivery and Therapeutics*, 8(5), 504–509.
<https://doi.org/10.22270/jddt.v8i5.1894>
- Svensson, F., Karlén, A., & Sköld, C. (2012). Virtual screening data fusion using both structure-and ligand-based methods. *Journal of Chemical Information and Modeling*, 52(1), 225–232. <https://doi.org/10.1021/ci2004835>
- Talele, T. T., Khedkar, S. A., & Rigby, A. C. (2010). Successful Applications of Computer Aided Drug Discovery: Moving Drugs from Concept to the Clinic. In *Current Topics in Medicinal Chemistry* (Vol. 10).
- Targowska-Duda KM, Maj M, Drączkowski P, Budzyńska B, Boguszewska-Czubara A, Wróbel TM, Laitinen T, Kaczmar P, Poso A, & Kaczor AA. (2022). WaterMap-Guided Structure-Based Virtual Screening for Acetylcholinesterase Inhibitors. *ChemMedChem*.
- Tomás-Loba, A., Flores, I., Fernández-Marcos, P. J., Cayuela, M. L., Maraver, A., Tejera, A., Borrás, C., Matheu, A., Klatt, P., Flores, J. M., Viña, J., Serrano, M., & Blasco, M. A. (2008). Telomerase Reverse Transcriptase Delays Aging in Cancer-Resistant Mice. *Cell*, 135(4), 609–622. <https://doi.org/10.1016/j.cell.2008.09.034>
- Trott, O., & Olson, A. J. (2009). AutoDock Vina: Improving the speed and accuracy of docking with a new scoring function, efficient optimization, and multithreading. *Journal of Computational Chemistry*, NA-NA. <https://doi.org/10.1002/jcc.21334>
- Tsai, C. F., Wang, K. T., Chen, L. G., Lee, C. J., Tseng, S. H., & Wang, C. C. (2014). Anti-inflammatory effects of vitis thunbergii var. taiwaniana on knee damage associated with arthritis. *Journal of Medicinal Food*, 17(4), 479–486.
<https://doi.org/10.1089/jmf.2013.2914>
- Tse, C., Shoemaker, A. R., Adickes, J., Anderson, M. G., Chen, J., Jin, S., Johnson, E. F., Marsh, K. C., Mitten, M. J., Nimmer, P., Roberts, L., Tahir, S. K., Xiao, Y., Yang, X., Zhang, H., Fesik, S., Rosenberg, S. H., & Elmore, S. W. (2008). ABT-263: A potent and orally bioavailable Bcl-2 family inhibitor. *Cancer Research*, 68(9), 3421–3428.
<https://doi.org/10.1158/0008-5472.CAN-07-5836>

- Tsoukalas, D., Fragkiadaki, P., Docea, A. O., Alegakis, A. K., Sarandi, E., Thanasoula, M., Spandidos, D. A., Tsatsakis, A., Razgonova, M. P., & Calina, D. (2019). Discovery of potent telomerase activators: Unfolding new therapeutic and anti-aging perspectives. *Molecular Medicine Reports*, *20*(4), 3701–3708. <https://doi.org/10.3892/mmr.2019.10614>
- Tümpel, S., & Rudolph, K. L. (2012). The role of telomere shortening in somatic stem cells and tissue aging: Lessons from telomerase model systems. *Annals of the New York Academy of Sciences*, *1266*(1), 28–39. <https://doi.org/10.1111/j.1749-6632.2012.06547.x>
- Ulaner, G. A., & Giudice, L. C. (1997). Developmental regulation of telomerase activity in human fetal tissues during gestation. In *Molecular Human Reproduction* (Vol. 3, Issue 9).
- Vandenberg, C. J., & Cory, S. (2013). *ABT-199, a new Bcl-2-specific BH3 mimetic, has in vivo efficacy against aggressive Myc-driven mouse lymphomas without provoking thrombocytopenia*. <https://doi.org/10.1182/blood>
- Vázquez, J., López, M., Gibert, E., Herrero, E., & Javier Luque, F. (2020). Merging ligand-based and structure-based methods in drug discovery: an overview of combined virtual screening approaches. In *Molecules* (Vol. 25, Issue 20). MDPI AG. <https://doi.org/10.3390/molecules25204723>
- Ventura Fernandes, B. H., Feitosa, N. M., Barbosa, A. P., Bomfim, C. G., Garnique, A. M. B., Rosa, I. F., Rodrigues, M. S., Doretto, L. B., Costa, D. F., Camargo-dos-Santos, B., Franco, G. A., Neto, J. F., Lunardi, J. S., Bellot, M. S., Alves, N. P. C., Costa, C. C., Aracati, M. F., Rodrigues, L. F., Costa, C. C., ... Charlie-Silva, I. (2022). Toxicity of spike fragments SARS-CoV-2 S protein for zebrafish: A tool to study its hazardous for human health? *Science of The Total Environment*, *813*, 152345. <https://doi.org/10.1016/j.scitotenv.2021.152345>
- Vera, E., Bernardes de Jesus, B., Foronda, M., Flores, J. M., & Blasco, M. A. (2013). Telomerase Reverse Transcriptase Synergizes with Calorie Restriction to Increase Health Span and Extend Mouse Longevity. *PLoS ONE*, *8*(1). <https://doi.org/10.1371/journal.pone.0053760>
- Villareal, D. T., Fontana, L., Das, S. K., Redman, L., Smith, S. R., Saltzman, E., Bales, C., Rochon, J., Pieper, C., Huang, M., Lewis, M., & Schwartz, A. v. (2016). Effect of Two-Year Caloric Restriction on Bone Metabolism and Bone Mineral Density in Non-Obese Younger Adults: A Randomized Clinical Trial. *Journal of Bone and Mineral Research*, *31*(1), 40–51. <https://doi.org/10.1002/jbmr.2701>

- Vogler, M., Dinsdale, D., Dyer, M. J. S., & Cohen, G. M. (2013). ABT-199 selectively inhibits BCL2 but not BCL2L1 and efficiently induces apoptosis of chronic lymphocytic leukaemic cells but not platelets. In *British Journal of Haematology* (Vol. 163, Issue 1, pp. 139–142). <https://doi.org/10.1111/bjh.12457>
- Wang, X., Ma, S., Meng, N., Yao, N., Zhang, K., Li, Q., Zhang, Y., Xing, Q., Han, K., Song, J., Yang, B., & Guan, F. (2016). Resveratrol exerts dosage-dependent effects on the self-renewal and neural differentiation of hUC-MSCs. *Molecules and Cells*, 39(5), 418–425. <https://doi.org/10.14348/molcells.2016.2345>
- Wanner, E., Thoppil, H., & Riabowol, K. (2021). Senescence and Apoptosis: Architects of Mammalian Development. In *Frontiers in Cell and Developmental Biology* (Vol. 8). Frontiers Media S.A. <https://doi.org/10.3389/fcell.2020.620089>
- Weichhart, T. (2018). MTOR as Regulator of Lifespan, Aging, and Cellular Senescence: A Mini-Review. In *Gerontology* (Vol. 64, Issue 2, pp. 127–134). S. Karger AG. <https://doi.org/10.1159/000484629>
- Wendt, M. D. (2008). Case History Discovery of ABT-263, a Bcl-family protein inhibitor: observations on targeting a large protein-protein interaction. *Expert Opin. Drug Discov*, 3(9), 1123–1143. <https://doi.org/10.1517/17460440802332151>
- Wherry, E. J., & Kurachi, M. (2015). Molecular and cellular insights into T cell exhaustion. In *Nature Reviews Immunology* (Vol. 15, Issue 8, pp. 486–499). Nature Publishing Group. <https://doi.org/10.1038/nri3862>
- Widrick, J. J., Gibbs, D. E., Sanchez, B., Gupta, V. A., Pakula, A., Lawrence, C., Beggs, A. H., & Kunkel, L. M. (2018). An open source microcontroller based flume for evaluating swimming performance of larval, juvenile, and adult zebrafish. *PLoS ONE*, 13(6). <https://doi.org/10.1371/journal.pone.0199712>
- Wienholds, E., Schulte-Merker, S., Walderich, B., & Plasterk, R. H. A. (2002). Target-selected inactivation of the zebrafish rag1 gene. *Science*, 297(5578), 99–102. <https://doi.org/10.1126/science.1071762>
- Wójcikowski, M., Ballester, P. J., & Siedlecki, P. (2017). Performance of machine-learning scoring functions in structure-based virtual screening. *Scientific Reports*, 7. <https://doi.org/10.1038/srep46710>
- Wolber, G., & Langer, T. (2005). LigandScout: 3-D pharmacophores derived from protein-bound ligands and their use as virtual screening filters. *Journal of Chemical Information and Modeling*, 45(1), 160–169. <https://doi.org/10.1021/ci049885e>

- Xia, N., Förstermann, U., & Li, H. (2017). Effects of resveratrol on eNOS in the endothelium and the perivascular adipose tissue. In *Annals of the New York Academy of Sciences* (Vol. 1403, Issue 1, pp. 132–141). Blackwell Publishing Inc. <https://doi.org/10.1111/nyas.13397>
- Xiao, Q., Zhu, W., Feng, W., Lee, S. S., Leung, A. W., Shen, J., Gao, L., & Xu, C. (2019). A review of resveratrol as a potent chemoprotective and synergistic agent in cancer chemotherapy. In *Frontiers in Pharmacology* (Vol. 9, Issue JAN). Frontiers Media S.A. <https://doi.org/10.3389/fphar.2018.01534>
- Xie, M., Mosig, A., Qi, X., Li, Y., Stadler, P. F., & Chen, J. J. L. (2008). Structure and function of the smallest vertebrate telomerase RNA from teleost fish. *Journal of Biological Chemistry*, 283(4), 2049–2059. <https://doi.org/10.1074/jbc.M708032200>
- Xie, Y., Meijer, A. H., & Schaaf, M. J. M. (2021). Modeling Inflammation in Zebrafish for the Development of Anti-inflammatory Drugs. In *Frontiers in Cell and Developmental Biology* (Vol. 8). Frontiers Media S.A. <https://doi.org/10.3389/fcell.2020.620984>
- Xue W, Zender L, & Miething C. (2007). *Senescence and tumour clearance is triggered by p53 restoration in mu-rine liver carcinomas.*
- Yamamoto, K. Z., Yasuo, N., & Sekijima, M. (2022). Screening for Inhibitors of Main Protease in SARS-CoV-2: In Silico and In Vitro Approach Avoiding Peptidyl Secondary Amides. *Journal of Chemical Information and Modeling*, 62(2), 350–358. <https://doi.org/10.1021/acs.jcim.1c01087>
- Zhu, X., Yang, J., Zhu, W., Yin, X., Yang, B., Wei, Y., & Guo, X. (2018). Combination of berberine with resveratrol improves the lipid-lowering efficacy. *International Journal of Molecular Sciences*, 19(12). <https://doi.org/10.3390/ijms19123903>
- Zhu, Y., Liu, X., Ding, X., Wang, F., & Geng, X. (2019). Telomere and its role in the aging pathways: telomere shortening, cell senescence and mitochondria dysfunction. In *Biogerontology* (Vol. 20, Issue 1). Springer Netherlands. <https://doi.org/10.1007/s10522-018-9769-1>

X. ANEXOS

X.1 ANEXO: CALIDAD DE LAS PUBLICACIONES.

Esta Tesis Doctoral ha dado lugar a la publicación de un primer artículo científico y un artículo de revisión (revisado y pendiente de aceptación), ambos en revistas de alto nivel situadas en el primer cuartil (Q1) según el índice JCR y con un factor de impacto igual o superior a 3. Actualmente, otros dos artículos científicos están en proceso de redacción y serán enviados próximamente.

Los datos relativos a la calidad de las revistas se detallan en los siguientes apartados.

X.1.1. Senescence-Independent Anti-Inflammatory Activity of the Senolytic Drugs Dasatinib, Navitoclax, and Venetoclax in Zebrafish Models of Chronic Inflammation.

El artículo científico *Senescence-Independent Anti-Inflammatory Activity of the Senolytic Drugs Dasatinib, Navitoclax, and Venetoclax in Zebrafish Models of Chronic Inflammation* (<https://doi.org/10.3390/ijms231810468>) ha sido publicado en la revista *International Journal of Molecular Sciences*. A continuación, se muestran los datos relativos a la calidad de dicha revista:

ISSN: 1422-0067

Impact Factor (2021): 6.208

5-year Impact Factor: 6.628

JCR category rank: Q1, Biochemistry & Molecular Biology.

Q2, Chemistry, Multidisciplinary

X.1.2 Virtual and zebrafish screening models in tandem, for drug discovery and development.

El artículo de revisión (por invitación) *Virtual and zebrafish screening models in tandem, for drug repurposing, discovery and development* está depositado en la plataforma *Preprints* (ID: preprints-63000). Ha sido revisado y está pendiente de aceptación en la revista *Expert Opinion on Drug Discovery*. A continuación, se muestran los datos relativos a la calidad de dicha revista:

ISSN: 1746-0441

Impact Factor (2021): 7.050

5-year Impact Factor: 6.466

JCR category rank: Q1, Pharmacology & Pharmacy.

X.2 ANEXO: PATENTES.

El desarrollo de esta Tesis Doctoral ha dado lugar al depósito de una patente:

Número de solicitud: 202230840

Cayuela Fuentes, María Luisa; Alcaraz Pérez, Francisca; Hernández Silva, David; Pérez Sánchez, Horacio; Mulero Méndez, Victoriano; Cantón Sandoval, Joaquín. *Compuestos antienvjecimiento*. P202230840 (2022).

X.3 ANEXO: OTRAS COMUNICACIONES

El desarrollo de esta tesis ha dado lugar a una serie de publicaciones en congresos, jornadas y seminarios adicionales a los artículos:

1. Título: **Anti-inflammatory property of senolytics in skin inflammation and metaflammation.**

- Autores: **David Hernández Silva**; Joaquín Cantón Sandoval, Francisco Juan Martínez Navarro, Elena Naranjo Sánchez, Horacio Pérez Sánchez, Sofia de Oliveira, Victoriano Mulero, Francisca Alcaraz-Pérez, María L Cayuela.
- Tipo de comunicación: Escrita (póster).
Nombre del Congreso: ZDM15
Fecha de celebración: 5/09/2022 - 9/09/2022.
Ciudad de celebración: Sheffield, Inglaterra.
2. Título: *In silico* and *in vivo* strategies for the development of molecules with antiaging effects.
Autores: **David Hernández Silva**; Miriam Roca Martínez; María Dolores López Abellán; Jorge De la Peña García; María Mulero; Miriam Fernández Lajarín; Elena Martínez Balsalobre; Elena Naranjo Sánchez; Elena Gómez Abenza; María Concepción López Maya; Ruth Conde Garrosa; Victoriano Mulero Méndez; Horacio Emilio Pérez Sánchez; Francisca Alcaraz Pérez; María L. Cayuela Fuentes.
Tipo de comunicación: Escrita (póster).
Nombre de la Jornada: V Jornadas Científicas del IMIB-Arrixaca.
Fecha de celebración: 23/11/2020 - 24/11/2020.
Ciudad de celebración: Murcia, España.
3. Título: Efecto de las relaciones intergeneracionales en las capacidades cognitivas del pez cebra.
Autores: Miriam Roca Martínez; **David Hernández Silva**; Isadora Marqués Paiva; Miriam Fernández Lajarín; Elena Naranjo Sánchez; Elena Martínez Balsalobre; Jesús García Castillo; Cynthia María Cabello Villalba; Francisca Alcaraz Pérez; María L. Cayuela Fuentes.
Tipo de comunicación: Escrita (póster).
Nombre de la Jornada: V Jornadas Científicas del IMIB-Arrixaca.
Fecha de celebración: 23/11/2020 - 24/11/2020.
Ciudad de celebración: Murcia, España.
4. Título: Función del componente de ARN de la telomerasa en la modulación de la inflamación crónica en piel.
Autores: Elena Naranjo Sánchez; Joaquín Cantón Sandoval; Jesús García Castillo; Elena Martínez Balsalobre; Miriam Fernández Lajarín; **David**

Hernández Silva; Francisca Alcaraz Pérez; Victoriano Mulero Méndez; María L. Cayuela Fuentes.

Tipo de comunicación: Escrita (póster).

Nombre de la Jornada: V Jornadas Científicas del IMIB-Arrixaca.

Fecha de celebración: 23/11/2020 - 24/11/2020.

Ciudad de celebración: Murcia, España.

5. Título: *In silico* and *in vivo* strategies for the development of molecules with antiaging effects.

Autores: **David Hernández Silva;** Miriam Roca Martínez; María Dolores López Abellán; Jorge De la Peña García; María Mulero; Miriam Fernández Lajarín; Elena Martínez Balsalobre; Elena Naranjo Sánchez; Elena Gómez Abenza; María Concepción López Maya; Ruth Conde Garrosa; Victoriano Mulero Méndez; Horacio Emilio Pérez Sánchez; Francisca Alcaraz Pérez; María L. Cayuela Fuentes.

Tipo de comunicación: Escrita (póster).

Nombre de la Jornada: IV Jornadas Científicas del IMIB-Arrixaca.

Fecha de celebración: 11/11/2019 - 11/11/2019.

Ciudad de celebración: Murcia, España.

6. Título: Predicción *in-silico* y caracterización *in vivo* de compuestos con actividad telomerasa mejorada.

Autores: **David Hernández Silva;** Francisca Alcaraz Pérez; María L Cayuela Fuentes; Jorge Peña García; Horacio Emilio Pérez Sánchez.

Tipo de comunicación: Oral.

Nombre del Congreso: Ciencia sin fronteras.

Fecha de celebración: 31/05/2019 - 31/05/2019.

Ciudad de celebración: Murcia, España.

7. Título: Telomerase contributes to tumor aggressiveness through a non-canonical mechanism of direct regulation of microRNAs.

Autores: Manuel Bernabé García; Elena Martínez Balsalobre; Diana García Moreno; Beatriz C. Revilla Nuin; Jesús García Castillo; Miriam Fernández Lajarín; **David Hernández Silva;** Elena Naranjo Sánchez; María C. López Maya; Victoriano Mulero Méndez; Francisca Alcaraz Pérez; María L. Cayuela Fuentes.

Tipo de comunicación: Escrita (póster).

Nombre de la Jornada: III Jornadas Científicas del IMIB-Arrixaca.

Fecha de celebración: 19/11/2019 - 20/11/2019.

Ciudad de celebración: Murcia, España.

8. Título: Zebrafish is the first animal model to study alternative lengthening of telomeres mechanism.

Autores: Elena Martínez Balsalobre; Monique Anchin; Jesús García Castillo; Manuel Bernabé García; Francisca Alcaraz Pérez; Miriam Fernández Lajarín; Elena Naranjo Sánchez; **David Hernández Silva**; Victoriano Mulero Méndez; María L. Cayuela Fuentes.

Tipo de comunicación: Oral

Nombre de la Jornada: III Jornadas Científicas del IMIB-Arrixaca.

Fecha de celebración: 19/11/2019 - 20/11/2019.

Ciudad de celebración: Murcia, España.

9. Título: Telomerase lncRNA recruits RNA polymerase II to target genes to promote myelopoiesis.

Autores: Jesús García Castillo; Francisca Alcaraz Pérez; Diana García Moreno; Elena Martínez Balsalobre; Manuel Bernabé García; Miriam Fernández Lajarín; **David Hernández Silva**; Elena Naranjo; Marlies Rossman; Isaac Adatto; Leonard I Zon; Victoriano Mulero; María L Cayuela Fuentes.

Tipo de comunicación: Oral

Nombre del Congreso: 11th Annual Zebrafish Disease Models Conference.

Fecha de celebración: 10/07/2018 - 13/07/2018.

Ciudad de celebración: Leiden, Holanda.

10. Título: Zebrafish as a new model to study telomerase-independent telomere maintenance mechanism: regeneration and cancer.

Autores: Elena Martínez Balsalobre; Monique Anchin; Jesús García Castillo; Manuel Bernabé García; Francisca Alcaraz Pérez; Miriam Fernández Lajarín; Elena Naranjo; **David Hernández Silva**; Victoriano Mulero; María L Cayuela.

Tipo de comunicación: Oral

Nombre del Congreso: 11th Annual Zebrafish Disease Models Conference.

Fecha de celebración: 10/07/2018 - 13/07/2018.

Ciudad de celebración: Leiden, Holanda.

11. Título: Telomerase RNA component: A lncRNA which recruits RNA polymerase II to target genes to promote myelopoiesis.

Autores: Jesús García Castillo; Francisca Alcaraz Pérez; Diana García Moreno; Elena Martínez Balsalobre; Manuel Bernabé García; Miriam Fernández Lajarín; **David Hernández Silva**; Elena Naranjo; Leonard I Zon; Victoriano Mulero; María L Cayuela.

Tipo de comunicación: Oral

Nombre del Congreso: Telomere biology in health and human disease.

Fecha de celebración: 01/05/2018 - 06/05/2018.

Ciudad de celebración: Tróia, Portugal.